POLYMER COATINGS TO IMPROVE HOST RESPONSE TO IMPLANTED NEURAL ELECTRODES

A Dissertation
Presented to
The Academic Faculty

by

Stacie Marie Gutowski

In Partial Fulfillment
of the Requirements for the Degree
Doctor of Philosophy in the
Department of Biomedical Engineering

Georgia Institute of Technology
August 2014

POLYMER COATINGS TO IMPROVE HOST RESPONSE TO IMPLANTED NEURAL ELECTRODES

Approved by:

Dr. Andrés García, Ph.D., Advisor
George W. Woodruff School of Mechanical Engineering
Georgia Institute of Technology

Dr. Andrew Lyon, Ph.D.
School of Chemistry and Biochemistry
Georgia Institute of Technology

Dr. Ravi Bellamkonda, Ph.D.
Wallace H. Coulter Department of Biomedical Engineering
Georgia Institute of Technology and Emory University

Dr. Robert Gross, M.D., Ph.D.
Departments of Neurosurgery and Neurology
Emory University

Dr. Garrett Stanley, Ph.D.
Wallace H. Coulter Department of Biomedical Engineering
Georgia Institute of Technology and Emory University

Date Approved: May 30, 2014

To my parents, for all of their love, support, and sacrifice.

ACKNOWLEDGEMENTS

There is a saying that it takes a village to raise a child, and I think the same analogy can be applied to a person obtaining a Ph.D. It is a lengthy and challenging yet rewarding journey starting as a fresh-faced, naïve first year that wants to save the world, only to figure out that you will only contribute a small amount of information to the entirety of human knowledge. But the fun part is that you DO contribute something new and different to the greater scientific community with the hopes that it might one day lead to an important breakthrough.

First, I want to thank all of the faculty and staff who have played a role in my grad school experience over the years. I have had some great professors on my thesis committee, as teachers of grad classes, and as mentors during my time at Tech. There are a lot of unique and fascinating things going on at GT all the time and the faculty play a major role in making GT what it is today. There are also the unsung heroes, the people who do all the grunt work in the background with little recognition. Meg, Colly, Floyd, and the other IBB staff have been fantastic to work with over the years, especially through my involvement in various leadership positions in BBUGS. The BME department staff, especially Shannon and Sally, has been extremely helpful with so many things from administrative questions to trying to find a job. IBB support staff keeps our core facilities running, take care of problems, and make sure everything runs smoothly in the building. The PRL staff has been great as well, taking care of our animals and making sure we have everything we need to succeed with our *in vivo* experiments. There are so

many people that help to keep everything running, and I am grateful that we have such a great support system on campus.

I also have to thank my many collaborators over the years. I was first trained by members of the Bellamkonda lab in surgical procedures and I still ask them questions all the time about brain stuff. Isaac, George, Jessica, Akhil, Tarun, Lohitash, and others have been very helpful in answering my many questions over the years. My first paper was published with a polymer developed in the Lyon lab with Toni South who was a great mentor when I was a new grad student trying to figure out all this new chemistry. Jeff Gaulding, Emily Herman, and Grant Hendrickson have also been a great help during my thesis. My work with the Collard lab has been interesting, starting with developing a new coating method with Katelyn. Although that project didn't end up working out, I made some great friends in Katelyn and Guillermo. The Stanley lab was also very helpful when I was exploring the recording aspect of electrodes. Doug, Qi, and Daniel were all very patient as I tried to learn more about the recording system and I thank them for all of their help. Finally, JT in the LaPlaca lab has been extremely helpful over the years. He harvested all of the primary cells for my *in vitro* studies and was always there to share his expertise when I had a question, and there were many questions during my time here. I am immensely grateful for all of the help I have received from these people throughout my thesis.

Next, I would like to thank two of the people who set me on this journey. My senior project advisers at WPI, George Pins and Glenn Gaudette, were instrumental in my decision to go to grad school when I was weighing my post-graduation options as an undergrad. I wasn't really sure if grad school was what I wanted to do with the next five

(six) years of my life, and it was a difficult decision. After being immersed in research with these two professors and after several soul-searching conversations, I was on the path to the Ph.D. I can't thank them enough for their advice over 6 years ago.

Of course no grad student experience would be complete without other the other grad students in the program. I have had the opportunity to meet so many people while pursuing my PhD at Georgia Tech through BME, BioE, IBB, BBUGS, ORGT and other organizations. There are too many to list here, but each person I have met along the way has played some role, great or small, in my journey. There are a few people in particular that I would like to mention. Morris, I've had a great time climbing and kayaking with you. We've had some fun times through ORGT and on our own trips and I will miss the adventures. Hopefully I can come back to Atlanta to visit and we can go explore the outdoors together again! Patricia and Kristin – I've had many a great meal at your apartment, and you guys are a ton of fun. I wish you all the best with finishing your theses and as you move on in life. Tanu has been a good friend over the years, always good for a laugh whenever we brought up cats or kids. Simone and Nina brought the European perspective during their short time in the Garcia lab and we had a great time exploring Atlanta together.

Alice, Si, Shu, and Tiffany, and Gen. We have spent the better part of five years together, and I wouldn't change a minute of it. Together we've been through the good, the bad, and the ugly. We've complained about our advisers, our failed experiments, and our frustration with science. We've seen each other through hard times, but also celebrated some wonderful accomplishments. Passing quals, presenting successful proposals and dissertations, birthdays, best papers, and so many other things have filled

our lives. I knew I could always count on your guys to be there for me. We've explored Atlanta and its many food options, and you have expanded my palette in ways I never imagined before coming here. All those nights of tofu soup or Vietnamese or dumplings followed by hours spent talking over bubble tea – these were the best. I have never known a better group of friends and I hope we keep in touch as we all move on to bigger and better things.

Of course no acknowledgements section is complete without the lab. Andres, you've been a great adviser. There were times I wanted to run away screaming from this project and you always managed to keep me grounded. I have learned that negative results aren't necessarily bad results; it's just how science works (or doesn't work). Thank you for being supportive and for teaching me how to conduct real, thorough scientific research and think through things critically. I have learned so much in my time here and I hope I can contribute big things to science in the future. To the rest of the García lab, I'll miss you. Some days were difficult, others were great. We've seen each other through quals, proposal, defenses, days with good data, days with nothing but failure, and many productive (or not) days in the lair. I can honestly say each person I have met during my time in the lab has taught me something, and I look forward to seeing where we all end up in several years as we move on to bigger and better things.

Kellie and Susan, you two get a section all to yourselves. You two have been so important in my life over the years, and I can't thank you enough for all of your support. Our daily lunch sessions were therapeutic and made me realize that I wasn't the only person who was frustrated with science and lab. You've each taught me a lot over the last

few years, different things in different ways. I hope we keep in touch as we all go our separate ways and I wish you all the best.

Last but not least, I have to thank my parents for all of their love and support over the years. Mom and Dad, you have been my rock through everything since I was a little girl. You two worked extra jobs so to pay for music lessons and school supplies and so I could participate in marching band. I always had everything I needed to succeed in school and life because of all your hard work. I'm not just referring to school supplies and money for field trips, but all the support and discipline you gave while I was growing up. Even though my math and science questions became too difficult by the time I reached high school, you never stopped pushing me to do my best, no matter what. I always knew I could count on you to be my cheerleaders, especially in the hard times when I needed it the most. I would not have made it here without you, and I am eternally grateful for all the sacrifices you have made over the years to allow me all the opportunities I had to get where I am today. Thank you so very much, and I love you.

TABLE OF CONTENTS

LIST OF TABLES

LIST OF FIGURES

LIST OF SYMBOLS AND ABBREVIATIONS

AFM	atomic force microscopy
BBB	blood brain barrier
BMI	brain-machine interface
CNS	central nervous system
DMSO	dimethyl sulfoxide
ELISA	enzyme-linked immunosorbent assay
EtOH	ethanol
GAG	glycosaminoglycan
GM-CSF	granulocyte macrophage colony stimulating factor
IF	immunofluorescence
IL-1	Interleukin-1
IL-1Ra	Interleukin-1 receptor antagonist
MMP	matrix metalloproteinase
PBS	phosphate-buffered saline
PEG	poly(ethylene glycol)
PEG-mal	PEG-maleimide
qRT-PCR	quantitative real-time polymerase chain reaction
Si	silicon
SPM	silane-PEG-maleimide
XPS	X-ray photoelectron spectroscopy

SUMMARY

Neural electrodes are an important part of brain-machine interface devices that can restore functionality to patients with sensory and movement impairments including spinal cord injury and limb loss. Currently, chronically implanted neural electrodes induce an unfavorable tissue response which includes inflammation, scar formation, and neuronal cell death, eventually causing loss of electrode functionality in the long term. The objective of this research was to develop a coating to improve the tissue response to implanted neural electrodes. The hypothesis was that coating the surface of neural electrodes with a non-fouling, anti-inflammatory coating would cause reduced inflammation and a better tissue response to the implanted electrode. We developed a polymer coating with non-fouling characteristics, incorporated an anti-inflammatory agent, and engineered a stimulus-responsive degradable portion for on-demand release of the anti-inflammatory agent in response to inflammatory stimuli. We characterized the coating using XPS and ellipsometry, and analyzed cell adhesion, cell spreading, and cytokine release *in vitro*. We analyzed the *in vivo* tissue response using immunohistochemistry and microarray qRT-PCR. Although no differences were observed among the samples for inflammatory cell markers, lower IgG penetration into the tissue around PEG + IL-1Ra coated electrodes suggests an improvement in BBB integrity. Gene expression analysis showed higher expression of IL-6 and MMP-2 around PEG + IL-1Ra samples, as well as an increase in CNTF expression, an important marker for neuronal survival. An important finding from this research is the increased neuronal

survival around coated electrodes compared to uncoated controls, which is a significant finding as neuronal survival near the implant interface is an essential part of maintaining electrode functionality.

CHAPTER 1

INTRODUCTION

Specific Aims

Neural electrodes are an essential part of brain-machine interfaces that can restore functionality to patients with spinal cord injury and limb loss. However, current tissue responses to implanted neural electrodes comprise inflammation, scar formation, and neuronal cell death. These adverse reactions severely reduce the ability of the electrode to receive electrical signals from surrounding neurons, thereby affecting long-term electrode functionality.

The objective of this project is to improve the tissue response to implanted neural electrodes. My central hypothesis is that coating implantable neural electrodes with a non-fouling coating will reduce cell adhesion and scar formation around the electrode. Additionally, by incorporating an anti-inflammatory agent we can modulate inflammation in the tissue at the electrode interface.

Specific Aim 1: Analyze host response to microgel coatings on neural electrodes implanted in the brain.

We hypothesized that coating neural electrodes with a thermally-responsive poly(ethylene glycol) – N(isopropylacrylamide) – acrylic acid (PEG-NIPAm-acrylic acid) microgel coating would yield a biocompatible coating that would reduce scar formation and inflammation in the brain. We showed that the microgel coating is successfully applied to the surface and also that the coating does reduce cell adhesion *in vitro.* However, results from long-term *in vivo* implantation studies in the rat brain indicate that the coating alone is not sufficient to reduce scar formation and inflammation in this rat model.

Specific Aim 2: Engineer protease-degradable PEG-maleimide coatings with on-demand release of an anti-inflammatory agent (IL-1Ra) to improve tissue response to implanted neural electrodes.

We hypothesized that an engineered protease-degradable PEG-maleimide coating with incorporated anti-inflammatory agent (IL-1Ra) would improve tissue response to implanted electrodes in the brain. We successfully coated the electrode surface with the PEG-maleimide coating which showed reduced cell adhesion and cytokine secretion *in vitro*. Additionally, results from an *in vivo* study indicate neuroprotective effects of the IL-1Ra. Gene expression results indicate higher levels of IL-6 and MMP-2 in PEG + IL-1Ra samples, as well as higher CNTF expression, which is an important marker for neuronal survival.

Project Significance

The research completed for this thesis is significant because it contributes to the development of coatings for neural implants for enhanced tissue integration. We have shown that cell adhesion-resistant polymer coatings alone are not sufficient to reduce scar formation and/or inflammation in the brain. However, by adding an anti-inflammatory agent we enhanced neuronal survival in the vicinity of the implant. This is an important finding because survival of the neurons at the implant interface is necessary for the neurons to send signals and maintain electrode functionality. Collectively, these results contribute to a better understanding of the coatings used to improve neural electrode technology.

CHAPTER 2

LITERATURE REVIEW

Introduction

Neural electrodes are important devices for use in systems that can monitor brain activity and provide a route of communication between the brain and the rest of the body for patients with various medical conditions that limit communication with the nervous system. Electrodes are an essential point of contact as they provide the interface between the brain and advanced systems known as brain-machine interfaces [2-4]. These brain-machine interfaces can be used to restore functionality to patients with a variety of brain-to-body communication issues, including spinal cord injury and control of prosthetic limbs [5-9]. In the United States alone, there are an estimated 12,400 new cases of spinal cord injury every year [10] as well as 2 million patients currently affected by limb loss [11]. These statistics indicate a need to develop new technologies to help improve the quality of life for patients experiencing limb loss and spinal cord injury. Neural electrodes are implanted in the brain tissue to receive signals from surrounding neurons. However, the recording ability of the majority of electrodes fails within days or weeks after implantation, rendering the current technology inconsistent and unstable. While many modifications have been made to improve long-term neural electrode functionality, there are still many issues that persist including inflammation, scar formation, and death of neurons surrounding the electrode [1, 12]. Current research aims to find solutions for these major problems with electrode technology so that we can improve long-term electrode functionality.

Brain Response to Implanted Materials – Chronic Persistence of Electrode

Implantation of a foreign material into the body will evoke an immediate response by the surrounding tissue which has been well characterized and includes an acute inflammatory response, chronic inflammatory response, and formation of granulation tissue over time [13]. This foreign body reaction is noted in other types of biosensors as well, such as implantable glucose monitoring sensors [14]. Implantation of materials, including electrodes, into the brain will elicit a similar response that has been characterized in multiple studies and includes acute and chronic inflammation, recruitment of microglia and astrocytes, astrocytic scar formation, and death of neurons at the implant interface [15-17].

Upon implantation of an electrode, a cascade of events begins in response to the implant. Implantation procedures generally try to avoid large vasculature when inserting the electrode, but it is inevitable that some microvasculature will be broken and the blood brain barrier (BBB) will be breached. The severity of BBB breach is an important determinant in the long-term tissue response to implanted devices, with BBB breach causing increased inflammation and neuronal death as well as decreased electrode recording functionality [18]. The inflammatory cascade begins with recruitment of microglia to the insertion location. Microglia are the macrophages of the brain, and they normally exist throughout the brain in a resting state with morphology that resembles a star. Upon initiation of the inflammatory cascade, the microglia are sent into an active state which causes their morphology to change to a more compact and rounded form [15, 19, 20]. Both resident and activated microglia are recruited to the site of injury. As the electrode persists, the inflammatory cascade continues with further macrophage

recruitment as well as astrocyte recruitment [21]. This response is similar to the response observed in the rest of the body when monocytes and macrophages are recruited to the implant / injury site [13, 22], with the main difference being that microglia, or brain specific macrophages, are recruited to the electrode surface. Astrocytes that are recruited to the implant surface then form a physical barrier around the device [23-25], similar to the fibrotic capsule the forms around implanted materials in the rest of the body [26]. This physical barrier formed by the astrocytes is problematic because it prevents electrical signals, sent by surrounding neurons, from reaching the implant surface. If the electrical signals cannot reach the electrode surface, the electrode cannot then receive and transmit those signals to an external signal processor, essentially rendering the implant useless. The inflammatory cascade continues with further macrophage recruitment and cytokine release in the surrounding tissue. Figure 2.1 demonstrates the tissue response to chronically implanted electrodes as illustrated by Szarowski et al [1].

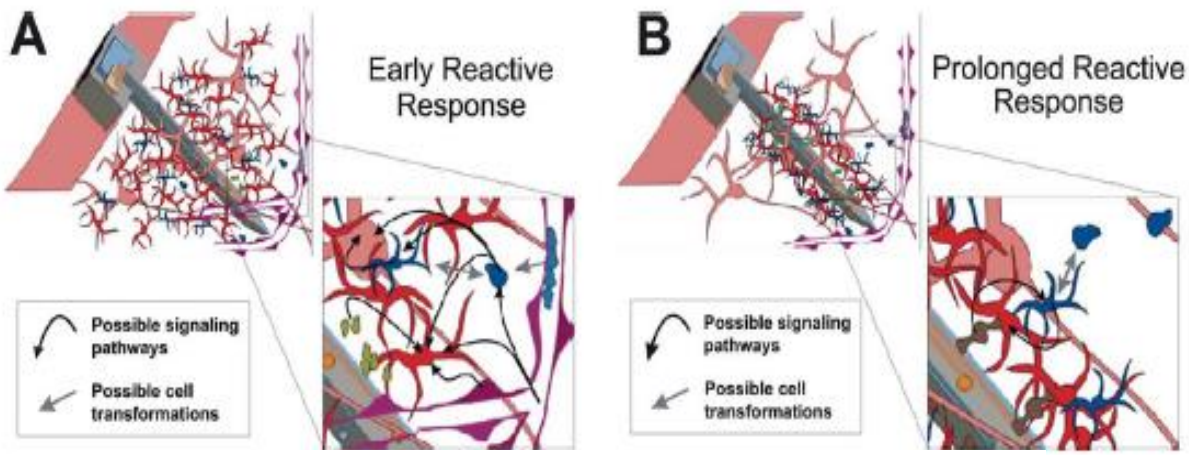

Figure 2.1: Tissue Response to Chronically Implanted Neural Electrodes [1].

Finally, there is neuronal death around the implant itself. The degeneration and death of neurons are known side effects of electrode implantation, however the mechanisms for neuronal death are not well understood. Cytokines released as a result of

inflammation can lead to downstream neuronal death or survival depending on the combination and levels of cytokines that are present [19, 27]. There is also evidence to indicate that reducing reactive oxygen species can modulate neurodegeneration [28]. It is likely that neuronal death and degeneration are due to a combination of the presence of the astrocytic scar, activation of microglia, and the inflammatory cytokines that are present in the tissue [29].

There are several interesting aspects to the tissue response as it relates to implanted neural electrodes. First, the electrode must persist in the tissue in order for the inflammatory response to persist. If the electrode is inserted and removed, the tissue will eventually mostly heal. Another intriguing observation is the multi-phasic nature of the inflammatory response to electrode implantation with persistent placement of electrodes as well as stab wounds in the brain. When the electrode is implanted, there is an initial inflammatory response that will peak around 2 weeks, decrease, and then increase again between 8-16 weeks [30], indicating that the inflammatory response changes over time. Finally, there are some differences in the time course when comparing tissue response between rat and mouse models with regards to electrode implantation [31], which is an important finding as it indicates differences in brain tissue response between species.

Review of Electrode Technology

The tissue response to implanted neural electrodes is similar to the way the body responds to various implanted materials, but with unique aspects that are specific to the brain. As with all implanted devices, the tissue response to implanted electrodes is complex. Many groups have tried to modulate this response through a wide range of approaches including designing different electrode geometries, modifying insertion

techniques, and applying various coatings to improve the tissue response with varying levels of success [16] as described in the following sections.

Recording Lifetime

One of the most significant problems with existing electrode technology is the failure of electrode recording over time. In some cases, the cause of the failure is known such as broken components within the electrode itself. However, often it is hard to pinpoint the exact cause of electrode recording failure. It is believed to be caused by some combination of the three major factors discussed previously: glial scar formation, inflammation, and neuronal cell death. It is also important to note that electrode failure is highly variable. This variability can be due to the type of electrode being used, but it is also observed in different animals implanted with the same type of electrode, indicating high variability from subject to subject. The recording time line varies among studies, with some groups able to record for a year, while other studies show electrode failure within a few weeks [32-36]. It is also interesting that some electrodes seem to "recover" functionality after initial loss within the first few days or weeks of a study. Occasionally electrodes will receive signals for a short time, cease functioning, and regain function later. The period of functionality for the second time also varies from study to study. The cause of this behavior is unknown but it is possible that the variable inflammatory profile plays a role [18, 33]. After initial implantation, the electrode can record for a time until inflammation increases. Once the injury reaches a state of stability, the inflammation may subside enough to allow for further recordings using the electrode.

Electrode Design and Insertion Techniques

Many electrode designs have been developed over the last several decades. These include Michigan electrodes, Utah arrays, microwires, and polymer electrodes. Examples of some of these electrodes can be seen in Figure 2.2 [37, 38].

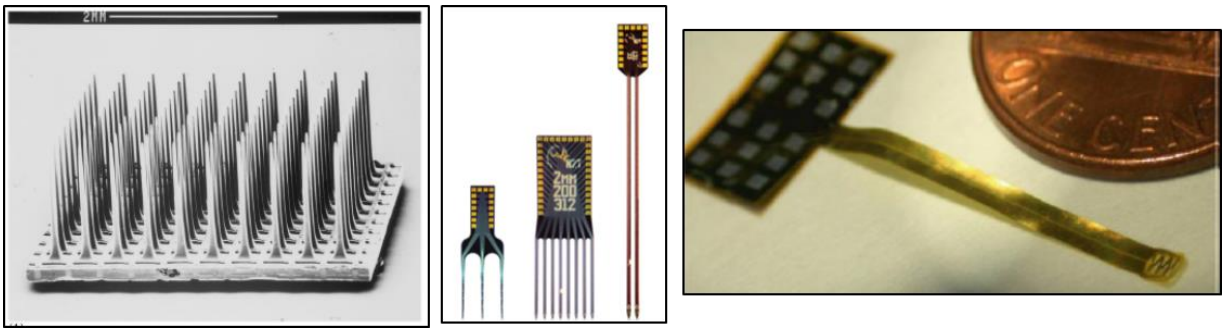

Figure 2.2: Examples of Neural Electrode Designs. Left: Utah array; middle: Michigan arrays; right: flexible polyimide array

There have been many attempts to improve electrode performance by modifying the design or insertion techniques of electrodes to improve one or more aspects of their geometry and/or tethering to the skull. First, geometry of the electrodes as well as the methods used to insert them can have an effect on the tissue response to the implant [16, 39]. Mechanical insertion using an assistive device yields better electrode functionality than manually inserted electrodes [40]. Bjornsson et al investigated different insertion speeds and electrode shapes and determined that the least amount of damage occurred with sharp electrodes, inserted at a fast speed, while avoiding all vasculature in the surrounding implant site [41]. Edell et al looked at different tip geometries and also found that sharp tips caused less tissue trauma upon insertion into the brain [42]. Another interesting aspect of electrode design is the geometry of the surface itself. Ereifej et al analyzed multiple surfaces and found that a nano-patterned electrode surface with specified geometry (3600 grooves/mm, 277 nm wide) had less protein adsorption, cell

adhesion, and cell proliferation than other surfaces tested [43]. As one might expect, smaller electrodes evoke a reduced inflammatory response compared to larger electrodes [34]. Kozai et al. showed the effectiveness of a microthread electrode to maintain recording function while minimizing blood-brain-barrier disruption as well as reducing tissue response compared to silicon electrodes, with reduced astrocyte and microglial recruitment [34].

Another important aspect of electrode design involves whether or not the electrode is tethered to the skull [33, 44]. After implantation, it is necessary to keep the electrode firmly implanted in the brain such that it does not move around or fall out of the brain as the animal moves. Some electrode designs utilize an "untethered" design meaning that the entire electrode apparatus is attached to the skull as one piece, usually with an acrylic material that hardens upon application. Other electrodes utilize a "floating" design where the implanted portion is placed in the brain similar to the untethered design, but the electrode itself contains an additional wire between the electrode and the external connector. This external connector is also attached to the skull with an acrylic headcap, but since the connector is not directly in line with the electrode, in has the ability to move freely from the electrode, minimizing micromotion that occurs as the animal moves.

One of the most complete studies to date by Karumbaiah et al. analyzed the differences between multiple electrode designs and tethered vs. untethered probes [33]. Comparing the histological response, cytokine release, and electrode recording performance among different electrode designs indicated that there is not one particular electrode design that solves all problems. While one electrode design might perform

better in one area, another design would outperform in another. An additional consideration of electrode design must be the potential blood-brain barrier breach. Saxena et al. conducted a thorough study of BBB breach and observed that electrodes causing a larger BBB breach also had an increased inflammatory response as well as a higher probability of electrode failure over time [18]. In addition, there was also variability among microwire electrodes with the same electrode design, indicating that electrode response is non-uniform even when using the same design. Collectively, these results indicate that electrode design alone may not be enough to mediate the tissue response and maintain long-term electrode functionality.

Electrode Materials and Coatings

Electrodes can be made of many materials including silicon, tungsten, other metals, ceramics, and a range of electrically active polymers like polyimide and parylene [16, 45, 46]. Silicon, tungsten, and ceramics are hard, non-compliant materials that possess a mechanical mismatch from the relatively soft tissue of the brain. New research with more compliant materials has shown improvements in tissue response surrounding the electrode [47]. Polymer microelectrode arrays that are less stiff than "traditional" electrode materials have shown mechanical compliance as well as necessary electrical performance [48]. A modified poly(vinyl acetate) electrode that more closely matches the mechanical stiffness of the brain showed promising results in being able to withstand the forces necessary to implant in the brain while also yielding increased neuronal survival around the implant [49, 50].

Research groups have applied various coatings to the surface of electrodes in an attempt to improve electrode performance as well as the *in vitro* and *in vivo* response to

electrodes. Conductive coatings are a widely-tested option as they can improve the electrical performance of the electrode. Combinations of poly(3,4-ethylenedioxythiophene) / poly(styrene sulfonate) (PEDOT/PSS) or polypyrrole (PPy) with a peptide-derivative from laminin have shown promising results to decrease impedance on the active sites of electrodes, making it easier for neuronal signals to reach the electrode surface [51-53]. However, there are concerns about long-term stability of such coatings *in vivo* as well as questions about the ability to effectively incorporate bioactive factors into these electrically active polymers [54].

In addition to electrically active polymers, others have tried passive polymer coatings to reduce protein adsorption and cell adhesion on the electrode surface. Azemi et al. coated silicon electrodes with a layer of laminin and seeded neural progenitor cells before implantation for a seven day study which showed reduced astrocytic scar formation compared to unmodified electrodes [55]. Polyaniline-coated platinum electrodes [56] and low-protein binding polymer films on silicon electrodes [57] showed reduced protein adsorption *in vitro* compared to unmodified controls. Poly(vinyl alcohol) /poly(acrylic acid) coatings also showed reduced protein adsorption and reduced astrocyte recruitment around the electrode site [58], while combination PEG/polyurethane coatings have shown reduced glial scarring and neuronal death around PEG/PU coated electrodes [59]. Conversely, a study with Parylene-C coated electrodes showed no difference in glial markers or neuronal survival compared to uncoated electrodes [60], indicating that non-fouling coatings alone may not provide enough intervention to solve the problems with chronically implanted neural electrodes.

Drug and Immunomodulatory Agent Delivery

Whereas polymer coatings may yield some improvements in tissue response, it may also be necessary to incorporate bioactive factors into neural electrode coatings. There have been multiple studies that have attempted to modify the tissue response using a range of drugs and immunomodulators as there is evidence to suggest that controlled release of anti-inflammatory agents can mediate the long-term tissue response to implanted biomaterials [61]. Bezuidenhout et al. demonstrated the effectiveness of loading dexamethasone into degradable and non-degradable PEG hydrogels to improve tissue response [62]. Further studies showed reduced inflammatory response and increased neuronal survival with dexamethasone-releasing coatings [63-67]. Tethering α-melanocyte stimulating hormone onto the surface of an electrode attenuated inflammatory cytokine release *in vitro* [68]. Incorporation of TGF-β on a laminin coating yielded reduced astrocytic recruitment on the electrode surface compared to laminin alone, indicating a potential target for reducing astrocytic scar formation [69]. Several groups have also investigated multi-function coating approaches that attempt to solve several problems simultaneously. Abidian and Martin demonstrated the ability to incorporate slow-release dexamethasone into an alginate hydrogel with PEDOT functionalization to improve electrical impedance with promising release characteristics *in vitro* [70], while Wadhwa et al. showed similar results with a polypyrrole coating and dex release *in vitro* [71]. Potter et al. utilized a poly(vinyl alcohol) material to improve the mechanical characteristics of the electrode to reduce mechanical mismatch while also incorporating curcumin to mediate the inflammatory response [72] with promising results at 4 weeks post-implantation, but all improvements were lost by 12 weeks.

In addition to drug therapeutics, it is also possible to target individual cytokines that are involved with inflammation in the brain. There are many cytokines involved in brain injury, disease, and inflammation. The cytokines responsible for modulating microglial activity and the inflammatory cascade in the brain include IL-1α, IL-1β, IL-1Ra, IL-4, IL-6, IL-10, IL-18, TNF-α, M-CSF, MIP-1α, MIP-1β, MIP-2 [19, 73-79]. With all of the cytokines that have been identified to have an effect on the inflammatory cascade in the brain, it is apparent that the tissue response to implanted electrodes is a complex problem that cannot be solved with polymer coatings alone, and an immunomodulator is likely necessary to improve the long-term functionality of implanted electrodes. Interleukin 1 (IL-1) is an important cytokine in the inflammatory cascade both in the brain and throughout the body, and presence of IL-1 can promote production of additional cytokines in the inflammatory cascade. IL-1 includes two agonists, IL-1α and IL-1β, both of which are 17 kDa molecules. These molecules are found in many inflammatory diseases and conditions within the body including inflammatory bowel disease, cancer, arthritis, arterial disease, kidney disease, and osteoporosis among others [73, 80]. Interleukin-1 receptor antagonist (IL-1Ra) is a 17 kDa protein that has been implicated as an important mediator of inflammation in diseases and conditions that contain IL-1 as part of the inflammatory cascade [73, 80]. IL-1Ra is the receptor antagonist for IL-1, meaning that the IL-1Ra molecule competes to bind IL-1 receptors in the cell. In the central nervous system, IL-1Ra has been shown to be effective in reducing inflammation in other CNS injury models such as the spinal cord, and it is also implicated in the recovery process after brain ischemia as well as stroke [73, 80]. IL-1Ra has also been shown to have neuroprotective effects when released by microglia [81]. Taub et al.

examined the effects of IL-1Ra integrated into a laminin coating on neural electrodes and noted moderate improvement of the astrocyte response to the IL-1Ra coated electrodes compared to uncoated controls, however no other cell types were analyzed [82]. Additionally, IL-1Ra is already approved for use in humans as a therapeutic for other inflammatory conditions such as arthritis [80]. Based on all this data, we hypothesized that IL-1Ra is a suitable candidate as an immunomodulator to improve the tissue response to implanted neural electrodes.

MMP-degradable Coatings

Matrix metalloproteinases (MMPs) are present in many tissues throughout the body and play an important role in tissue homeostasis and extracellular matrix remodeling. In addition to cell and tissue maintenance, MMPs are up-regulated in many disease states and conditions that cause increased inflammatory response [83, 84] including neurodegenerative diseases [85], central nervous system injury [86-88], and brain injury [89, 90]. MMPs are also necessary for mediation of inflammation, as MMP-9 deficiency has been shown to prolong the foreign body response in the brain [91]. With regards to electrode implantation, MMP-2 and MMP-9 have been implicated in the inflammatory cascade that occurs in response to neural electrodes [18, 76], indicating that the presence of MMPs in the injured brain does play a role in the chronic tissue response.

Since MMPs are up-regulated in the inflammatory cascade in the brain, it is possible to utilize MMPs that are already present in the inflamed tissue to serve as the stimuli to break down a material, such as a hydrogel, that contains MMP-degradable motifs. The use of MMP-degradable hydrogels has been demonstrated by several groups. These MMP-degradable hydrogels have been shown to be effective for a range of uses

including encapsulation of mesenchymal stem cells [92], fibroblasts [93, 94], vascular smooth muscle cells [95], drugs [96], and biomolecules such as RGD and VEGF [97-99]. The MMP-degradable nature of these hydrogels allows for the cells to remodel the gels, allowing for cell ingrowth as well as release of any incorporated bioactive factors. By incorporating anti-inflammatory drugs into these hydrogels, it is possible to take advantage of the inflammatory nature of an injury model, such as the implanted electrode, to utilize the existing MMPs in the tissue as the stimulus for cleaving the MMP-degradable motifs to release tethered anti-inflammatory molecules. An added benefit of this system is the on-demand release aspect as the MMP-degradable sequences are degraded in the presence of the MMPs that occur during inflammation. A system with this on-demand release of bioactive factors could be useful for mediating inflammatory response when used in conjunction with implanted biomaterials to improve implant biocompatibility.

Conclusion

Brain-machine interfaces have the potential to provide real change in improving the quality of life for patients with various life-altering conditions including limb loss and spinal cord injury. However, the electrodes that are used to interface with the brain still have limitations that must be addressed to maintain long-term electrode functionality. There has been much research into probe design, insertion techniques, tethering to the skull, in addition to a wide range of coatings to reduce cell adhesion, improve electrical impedance, improve neuronal survival, and reduce the inflammatory response. However, no single approach has been able to completely address all aspects of the tissue response to modulate inflammation, yield reduced cell recruitment and scarring, and maintain

neuronal survival near the implant interface. It is important to investigate other options that may provide a better solution for long-term electrode biocompatibility in the brain.

CHAPTER 3

HOST RESPONSE TO MICROGEL COATINGS ON NEURAL ELECTRODES IN THE BRAIN[1]

Summary

The performance of neural electrodes implanted in the brain is often limited by host response in the surrounding brain tissue, including astrocytic scar formation, neuronal cell death, and inflammation around the implant. We applied conformal microgel coatings to silicon neural electrodes and examined host responses to microgel-coated and uncoated electrodes following implantation in the rat brain. *In vitro* analyses demonstrated significantly reduced astrocyte and microglia adhesion to microgel-coated electrodes compared to uncoated controls. Microgel-coated and uncoated electrodes were implanted in the rat brain cortex and the extent of activated microglia and astrocytes as well as neuron density around the implant were evaluated at 1, 4, and 24 weeks post-implantation. Microgel coatings reduced astrocytic recruitment around the implant at later time points. However, microglial response indicated persistence of inflammation in the area around the electrode. Neuronal density around the implanted electrodes was also lower for both implant groups compared to the uninjured control. These results

---

[1] adapted from:
Stacie M. Gutowski, Kellie L. Templeman, Antoinette B. South, Jeffrey C. Gaulding, James T. Shoemaker, Michelle C. LaPlaca, Ravi V. Bellamkonda, L. Andrew Lyon, Andrés J. García. Host response to microgel coatings on neural electrodes implanted in the brain. *J Biomed Mater Res Part A*: 102A: 1486–1499, 2014.

demonstrate that microgel coatings do not significantly improve host responses to implanted neural electrodes and underscore the need for further improvements in implantable materials.

Introduction

Neuroprosthetic devices have the potential to restore functionality to patients affected by injuries and pathologies including sensory loss, neurological disorders, spinal cord injuries, and limb amputation [4-6, 8]. Devices that provide an interface between brain and machine require the use of neural electrodes that can receive and/or transmit electrical signals from neurons in the brain [4-6, 8]. A significant problem with current electrode technology is recording failure of electrodes over time. Devices implanted in the body provoke an inflammatory response from the surrounding tissue, which can lead to scar formation and failure of the implant over time [13]. Electrode failure involves host responses in the tissue surrounding the electrode including increased glial scar formation and a decrease in neurons due to cell death around the electrode [1, 25, 66]. Additionally, activation of microglia around implanted electrodes supports a role for inflammation in the tissue response around the implant [1]. Maintenance of recording ability varies from days to many months, however the time frame of electrode functionality is highly variable even between electrodes in the same array and many electrodes can fail within a matter of weeks after implantation [4]. In order to improve long-term electrode functionality, it is important to introduce a device that will elicit minimal reaction from the surrounding tissue [15]. By incorporating materials that reduce astrocytic and microglial cell adhesion, it may be possible to reduce scar formation around implanted materials.

To improve the tissue response to implanted neural electrodes, several groups have applied coatings to the electrode surface as a potential solution. Coatings with an incorporated peptide sequence derived from laminin promote neuronal cell adhesion and migration [51, 53, 55], as well as coatings containing brain-derived neurotrophic factor [100]. Whereas these coatings may increase neuronal cell numbers around the electrode, they may also promote adhesion of other cell types including astrocytes, one of the main cell types involved in scar formation. Recent work by Winslow et al. [60] demonstrated a lack of improved tissue response with cell adhesion resistant coatings, indicating the possible role of persistent inflammation in the long-term tissue response that results in electrode failure. Other studies have investigated releasing anti-inflammatory agents including α-melanocyte stimulating hormone [68] and dexamethasone [64, 65, 67] to attenuate the inflammatory response of surrounding tissue. While this research has introduced many improvements to the field, there has been limited success in improving long-term cellular response as a whole for time points longer than several weeks, and much work remains to mediate the problems involved with chronically implanted electrode failure.

In the present study, we engineered a conformal microgel coating to reduce cell adhesion on neural electrodes. This coating consists of multi-layers of cross-linked microgel particles composed mainly of poly(*N*-isopropylacrylamide) (pNIPAm), which is cross-linked with poly(ethylene glycol diacrylate) (PEG-DA). Under physiological conditions, the PEG chains decorate the surface of the pNIPAm microgels, serving as a non-fouling coating that has been shown to reduce protein adsorption and cell adhesion, as well as reduce inflammation *in vivo* [101-103]. The microgel coating is tethered to the

surface of silicon electrodes which are manufactured for neural recording applications [32]. We evaluated *in vitro* cell adhesion and host responses to microgel-coated and uncoated electrodes implanted in the rat brain. Our results in combination with previous studies indicate the need for materials that go beyond reducing cell adhesion alone but also incorporate improved attenuation of inflammation in the tissue surrounding the implanted electrode.

Materials and Methods

Microgel coating of electrodes

The electrode modifier used for this study is a thermo-responsive, micro-structured, hydrogel coating. This coating consists of multilayers of particles of copolymer poly(*N*-isopropylacrylamide) (pNIPAM) and acrylic acid (AAc) (pNIPAm-*co*AAc) cross-linked with poly(ethylene glycol) (PEG) chains. Particle size and composition were previously verified by dynamic light scattering and NMR, respectively [103]. Microgel coatings were applied to the surface of electrodes made of silicon and iridium. Electrodes were purchased from NeuroNexus Technologies (CM16 A4x4-4mm-200-200-1250). Each electrode is 4 mm long with 4 active sites on each of 4 prongs, and each active site has an area of 1,250 μm^2. Non-recording electrodes were used as they are significantly less expensive than functional electrodes.

Preliminary studies indicated variable application of coatings due to organic contaminants on the as-received electrode surface. Several cleaning protocols were evaluated by surface analyses and reproducible application of coating. An optimal cleaning procedure consisting of serial 5-minute incubations in trichloroethylene (Mallinckrodt/JT Baker), acetone (Sigma-Aldrich), and methanol (Sigma-Aldrich) was

used. Electrodes were then rinsed with absolute ethanol (Sigma-Aldrich). Following the cleaning procedure, electrodes were incubated in absolute ethanol for one hour. The surface was functionalized using a silane-based adhesion layer. Silicon has a natural oxide layer approximately 1 nm thick, and this layer was utilized for silanization of the surface. The electrodes were incubated for two hours with 1% 3-aminopropyl trimethoxysilane (APTMS, TCI America) in absolute ethanol. The substrate was then rinsed with ethanol and equilibrated in PBS. Anionic microgels were then added and Coulombic attraction between the cationic amine-modified silicon surface and anionic microgels resulted in the formation of a microgel monolayer. To further stabilize the initial layer, chemicals for carbodiimide coupling were used consisting of N-(3-dimethylaminopropyl)-N'-ethylcarbodiimide hydrochloride (EDC), N-hydroxysuccinimide (NHS), and hydroxylamine hydrochloride. Standard EDC/NHS coupling was used [104] to covalently attach the microgels to the silicon surface. Complete coverage of the surface with microgels was achieved by depositing four layers of microgels to coat the electrode surface. A cationic glue, polydiallyl dimethyl ammonium chloride (PDADMAC), was used between layers to promote multi-layer formation. Presence of the microgel coating was verified with atomic force microscopy (AFM) and X-ray photoelectron spectroscopy (XPS) (Fig.1). Upon completion of coating, or after cleaning for uncoated samples, electrodes were placed in PBS until experimentation, where further cleaning/sterilization was performed (as described below).

In Vitro Cell Adhesion

Either uncoated or microgel-coated electrodes were adhered to a glass coverslip using UV-cure adhesive (NOA 68, Norland Adhesives). A single coverslip with attached electrode sample was placed in an individual well of a 12-well plate (n=3, each group). The samples were washed twice with 70% ethanol followed by three washes with sterile PBS. Mixed astrocyte and microglial cells were added to each well at a density of 50,000 cells/cm^2 (~190,000 cells/well). The samples were cultured in DMEM/F12 (Invitrogen) + 10% FBS (Invitrogen) at 37 ºC and 5% CO_2 for 24 hours. Samples were stained with LIVE/DEAD stain (Invitrogen) and imaged with a 20X Apo Nikon objective (0.75 NA). Cell spread area on the electrode surface was measured using ImageJ software (NIH).

Electrode Implantation

NIH guidelines for the care and use of laboratory animals (NIH Publication #85-23 Rev. 1985) were observed. All surgical procedures were approved by the Institutional Animal Care and Use Committee at the Georgia Institute of Technology. The electrode implantation procedure is adapted from the protocol by McConnell et al. [17] Electrodes (uncoated, microgel-coated) were rinsed with ethanol for 24 hours then washed with sterile PBS prior to implantation in the brain cortex of a rat, one per animal (n=4 animals for all groups except n=3 for uncoated at 24 weeks, similar sample sizes were used in other studies [24, 30, 105]). Male Sprague-Dawley rats (Charles River Laboratories) were anesthetized with isoflurane. The surgical site was shaved, cleaned with chlorohexaderm, and rinsed with isopropyl alcohol before mounting the animal onto a stereotactic frame. Marcaine (0.15 mL of 0.5%) was injected subcutaneously at the site of incision. A midline incision 2-3 cm long was made in the scalp and the periosteum retracted to

expose the cranium. Five 1 mm-diameter pilot holes were made around the skull, four posterior to bregma, with two each on either side of the midline and one additional hole made anterior and right of bregma. A 4.7 mm stainless steel bone screw (Fine Science Tools 19010-00) was inserted into each of the pilot holes, with each screw penetrating the skull but leaving about 1-2 mm of each screw head remaining out of the skull to serve as an attachment point for the headcap. The craniotomy for electrode insertion was made anterior to and left of bregma using a 2.7 mm trephine bit (Fine Science Tools 18004-27). The electrode was held in the stereotactic frame above the 2.7 mm hole and slowly lowered into the cortex, careful to avoid any large vasculature in the surgical area. Agarose gel (1.5% w/v, SeaKem) was filled into the opening around the electrode and dental acrylic (OrthoJet, Inc.) was used to anchor the electrode assembly to the skull. The scalp incision was closed via wound clips and triple-antibiotic ointment was applied to the wound. Each animal was given an injection of 5 mL saline and allowed to recover from anesthesia before receiving a 0.03 mg/kg buprenorphine injection for pain relief. All animals were fully ambulatory post recovery.

At the designated time point (1, 4, and 24 weeks), the animal was anesthetized prior to transcardial perfusion with 200 mL 0.4% papaverine HCl in 0.9% NaCl, followed by 50 mL of 0.9% NaCl, and 200 mL of 4% paraformaldehyde in phosphate buffer. After perfusion, the skull was opened and the brain retrieved from the skull cavity. All samples were kept in 4% paraformaldehyde in phosphate buffer solution overnight then placed in 30% sucrose in PBS until the brain sank to the bottom of a 50 mL conical tube. Samples were embedded in OCT and frozen using isopentane in liquid nitrogen.

Histological Evaluation

Samples were sectioned in 16 μm-thick sections using a cryostat and stained for various cell markers as indicated in **Error! Reference source not found.**. All primary antibodies were visualized with AlexaFluor488-conjugated secondary antibody (Invitrogen) and counterstained with DAPI for cell nuclei recognition. Upon completion of staining, all slides were imaged using a 10X Nikon objective (0.30 NA) and SPOT Advanced software (Diagnostic Instruments, Inc.).

Table 3.1: Antibodies used for immunofluorescence analysis

Antibody	Supplier	Cell Type
Glial fibrillary acidic protein (GFAP)	Abcam ab7260	Astrocytes
NeuN	Millipore MAB377	Neuronal nuclei
OX42 / CD11b	Chemicon CBL1512	Resident microglia
ED1 / CD68	AbD Serotec MCA341R	Activated microglia

Data obtained from *in vivo* studies were analyzed using MATLAB software (Mathworks). A line was drawn manually along the edge of the injury caused by the electrode and the intensity values were gathered starting at the edge of the injury and moving 500 μm perpendicularly from the line (Fig. 3.3a) [12]. For GFAP, ED1, and OX42 staining, the average intensity was normalized to the intensity of the contralateral [background] image by utilizing point by point subtraction of the background staining (obtained from the corresponding contralateral uninjured hemisphere) from the injury image, taking into account the variation of field illumination. This method allows for subtracting the uninjured tissue staining of resident cells (GFAP and OX42), subtraction of the background (ED1), and accounting for the variation in field illumination in all samples. The normalized intensity per trajectory was plotted, yielding a curve indicating the intensity variation as a function of distance (x) from the edge of the implanted

electrode (Fig. 3.3a, right). Each curve was fit to equation 1 and a five-parameter fit applied to each curve.

Equation 1: normalized intensity $= intensity_1 * e^{-decay_1 x} + intensity_2 * e^{-decay_2 x} + f.$

This equation was chosen for the curve fit because there are two intensity and decay parameters in the equation corresponding to the initial steep decay in the intensity at distances corresponding to 0–100 μm (parameters: $intensity_1$ and $decay_1$) followed by a slower rate of decay at distances >100 μm from the edge of injury (parameters: $intensity_2$ and $decay_2$). Samples from each animal were used to generate independent intensity curves for each marker (GFAP, OX42/CD11b, ED1/CD68). The intensity curves for each individual animal were then combined and analyzed to obtain an inter-animal average per group for each marker at each time point. Analysis for NeuN staining utilized a similar methodology by analyzing cell staining starting at the scar and moving 500 μm away from the injury. However, staining is analyzed by counting NeuN+ cells [12] per 100 μm bin (Fig. 3b), as the staining for NeuN is either positive or negative for neuronal nuclei, with the number of positive cells indicating the number of neuronal nuclei in the analysis area. The number of NeuN+ cells is then plotted as a percentage of the corresponding uninjured control (contralateral hemisphere) (Fig 3b, bottom). Samples from each animal were combined to obtain an inter-animal average per group for NeuN at each time point.

Statistical Analysis

Data presented are mean +/- standard error. Statistical analyses for differences in the *in vitro* cell adhesion study were performed using a two-tailed t-test in JMP Pro10 (SAS Software). Mean and standard error for parameters of curve fits from non-linear regression ($intensity_1$, $intensity_2$, $decay_1$, $decay_2$) for GFAP, OX42, and ED1 for uncoated

and microgel-coated samples were obtained using the two-phase decay equation (Equation 1) in Graphpad Prism 6.0. Statistical analyses for differences between the two groups at a given time point were performed using a t-test. Analysis for differences in each parameter over time were performed using ANOVA with post-hoc analysis (Tukey) for comparison at different time points. Staining for NeuN+ cells was analyzed per 100 μm bin and compared between uncoated samples, microgel-coated samples, and contralateral uninjured controls using ANOVA in JMP Pro10 (SAS Software). Post-hoc testing consisted of Dunnett's method to test for differences between the contralateral (uninjured control) and experimental (uncoated and microgel-coated) samples, and Tukey-Kramer HSD test was used to test for differences between uncoated and microgel-coated samples in each bin per time point. A p-value of <0.05 was considered significant.

Results

Characterization of Microgel Coatings

Microgel coatings were characterized using atomic force microscopy (AFM) and X-ray photoelectron spectroscopy (XPS) to validate morphology and chemical composition. Figure 3.1a shows the molecular structure of the microgels consisting of N-isopropylacrylamide (NIPAm; 70.5 mol%), acrylic acid (AAc; 26 mol%), and the crosslinker poly(ethylene glycol) diacrylate (MW=575, PEGDA-575; 3.5 mol%). AFM analysis of electrodes that were cleaned, incubated with only APTMS and PDADMAC, and microgel-coated indicated a uniform conformal coating of microgels on the surface of the microgel-coated electrode (Figure 3.1b). The microgel coating covered both the silicon substrate as well as the iridium wire that is used for transmission of the electrical signal. As this study only utilized non-recording electrodes for the purposes of

histological evaluation, no tests were performed to observe changes in impedance at the electrode recording sites. However, because of the high water content of these films (~90%), we do not expect significant changes in the electrical impedance of the device. AFM analysis to determine wet thickness of the microgel coating was performed by introducing a scratch into the coating with a razor blade, exposing the bare substrate next to the microgel-coated area, and measuring the thickness of the coating in relation to the bare substrate. This analysis indicated microgel coating thickness of ~60 nm, which is consistent with previous studies [106]. Figure 3.1c indicates the change in chemical composition of the surface as analyzed by XPS. The presence of Si peaks is likely due to collapse of the microgel coating under vacuum within the penetration depth of the technique. Note the change in XPS spectra indicating increased carbon and nitrogen peaks on the microgel-coated electrodes corresponding to deposition of a coating on the electrode surface. Taken together, the AFM and XPS results demonstrate application of a uniform, conformal microgel coating on neural electrodes.

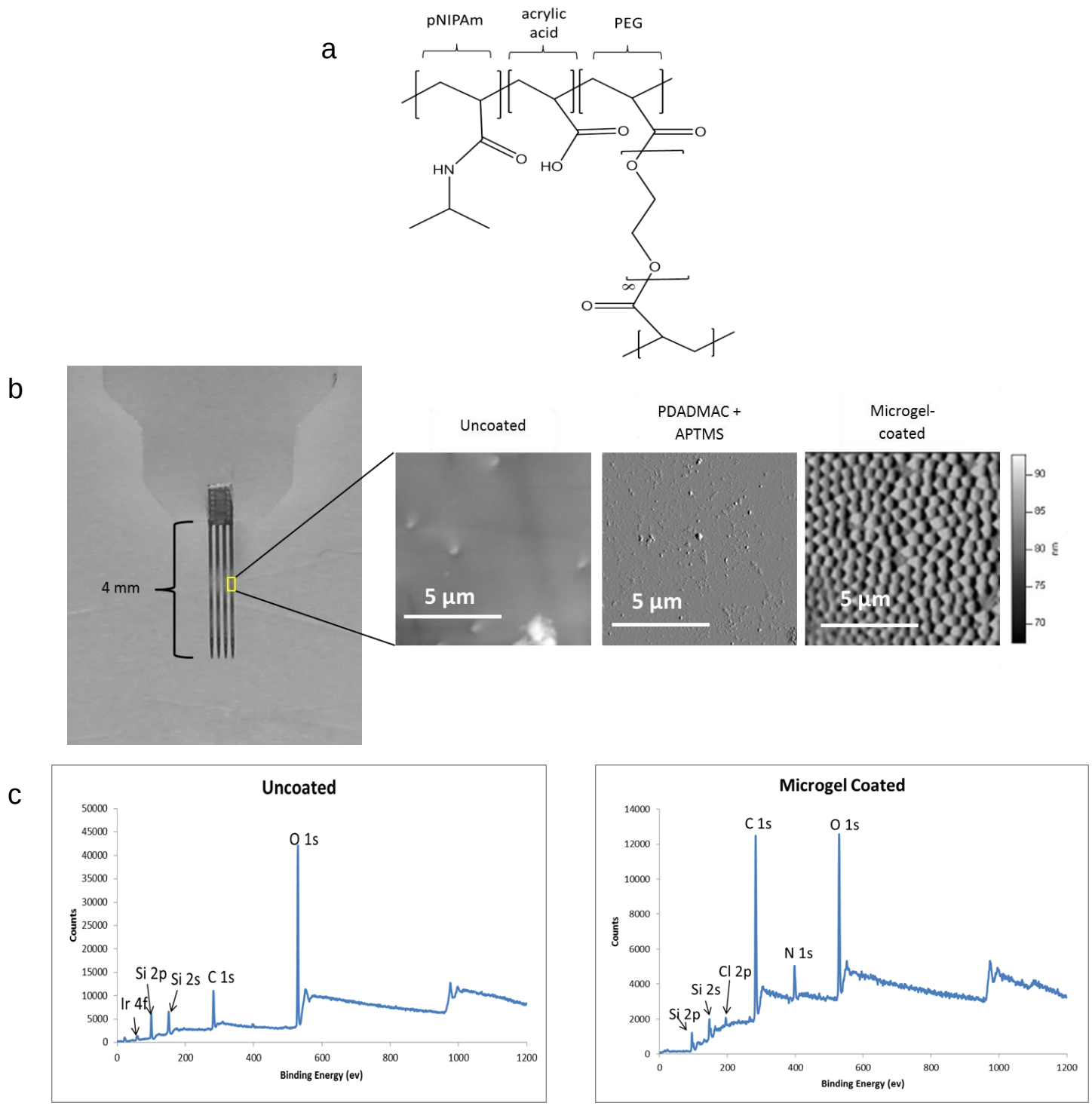

Figure 3.1: Microgel coatings applied to the surface of the neural electrode. (a) Chemical structure of the microgel contains pNIPAm, PEG, and acrylic acid. (b) Photo of the neural electrode (left) with AFM scans for uncoated, PDADMAC+APTMS only, and multi-layer microgel-coated surfaces. The microgel coating application was further verified using X-ray electron spectroscopy to verify differences between the uncoated and microgel-coated (c) surfaces with the absence of iridium 4f peak and prominent C1s and N1s peaks on the microgel-coated sample.

In Vitro Cell Adhesion

Uncoated and microgel-coated electrodes were seeded with mixed glial cells (astrocytes + microglia) to evaluate adhesion to these materials. Analysis of results from the *in vitro* experiment indicates the effectiveness of the microgel coating for reducing cell adhesion on the surface of electrodes as well as high viability (>99%) of plated cells. Similar cell density and cell spreading were observed on the glass coverslip beneath each sample, indicating continuity of cell seeding and spreading between samples (Figure 3.2a). There was significantly reduced cell adhesion and cell spreading on the microgel-coated electrode surface as compared to the uncoated control (Fig. 3.2b). Each of these representative images shows significantly higher cell adhesion and spreading on the uncoated electrodes whereas the microgel-coated images indicate very few cells attached to the surface and reduced cell spreading. The total cell spreading was analyzed by taking a series of images along the length of the electrode and averaging total cell spread area per electrode. Cell spread area was quantified (Fig. 3.2c) by determining the area of the cells present on the electrode surface using ImageJ area measurement tool. There was a significant difference in cell spread area between the samples, with approximately 60 times lower cell adhesion on microgel-coated samples compared to uncoated controls.

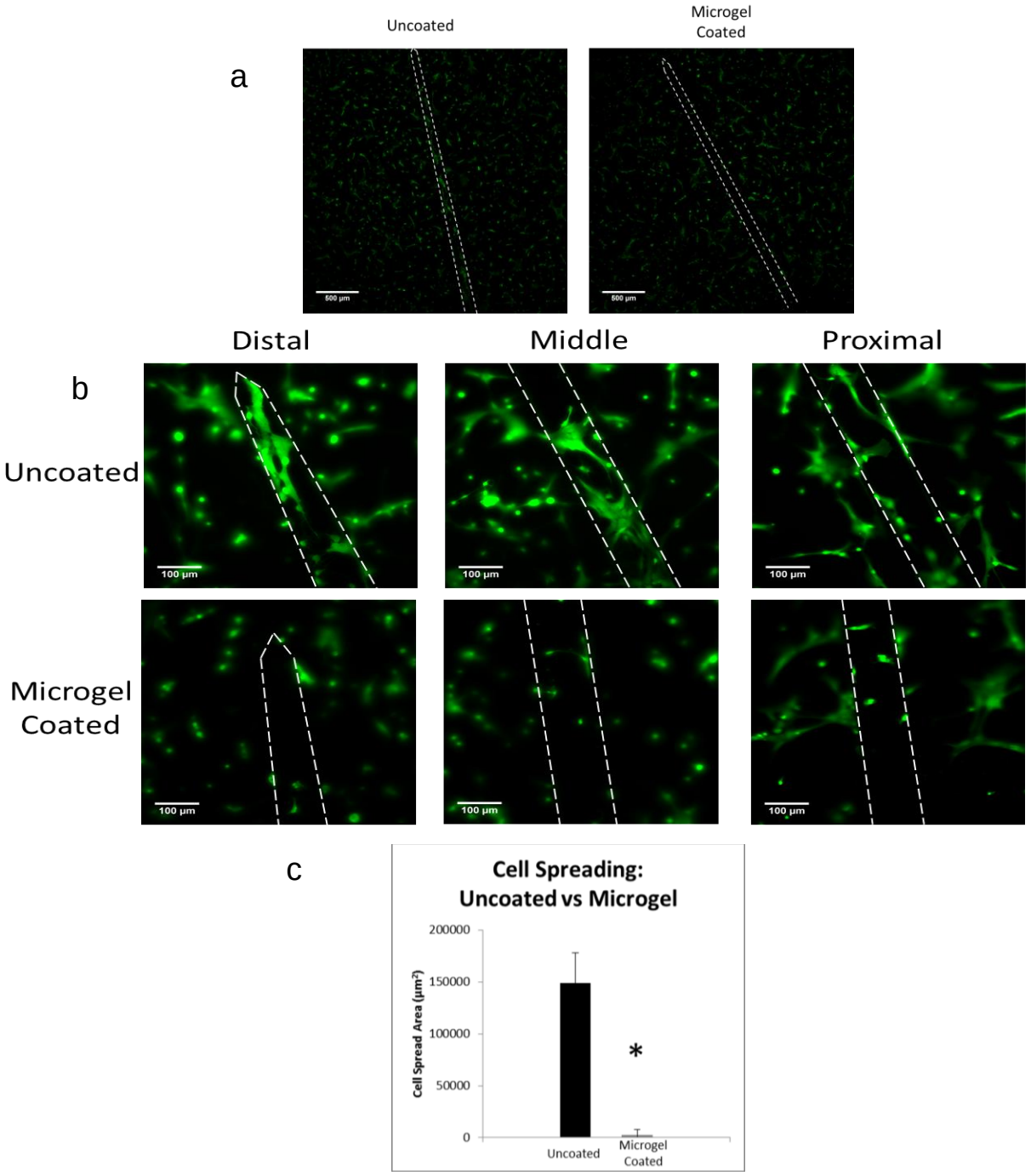

Figure 3.2: Electrodes were plated with mixed glial cells (astrocytes and microglia) and cultured for 24 hours. (a) Representative images of the *in vitro* assay showing cell adhesion on the uncoated (left) and microgel-coated (right) electrodes and underlying coverslips, indicating continuity of cell density and cell spreading on the coverslip beneath each electrode. (b) Microgel coatings reduce *in vitro* mixed glial cell adhesion on electrodes. Samples were stained using LIVE/DEAD stain (Invitrogen) and imaged using fluorescence microscopy. (c) Cell spreading area was analyzed using ImageJ to determine the amount of cell spread area for each group. Microgel coatings reduced cell adhesion on the electrode surface compared to uncoated controls ($p<0.01$). Data is presented as mean ± standard error of the mean, n=3 electrodes. Scale bars = 100µm.

Host Response of Electrodes Implanted in the Brain

Microgel-coated electrodes and uncoated controls were implanted into the rat cortex. Tissue responses in the vicinity of the electrode were analyzed at three time points: 1 week, 4 weeks, and 24 weeks using immunostaining of cryosectioned samples. Image analysis was implemented to quantify levels of markers associated with neuroinflammation and neuronal cell survival (Fig. 3.3). Markers associated with neuroinflammation comprised GFAP (astrocytes), OX42/CD11b (resident macrophages), and ED1/CD68 (activated macrophages). Each of these markers was used to stain sections from all animals. Images from each sample were analyzed and staining intensities for each marker over a distance of 500 μm perpendicular from the edge of the electrode injury were evaluated. These intensity profiles were then fit using non-linear regression to Equation 1. In this equation, the initial set of parameters, $intensity_1$ and $decay_1$, correspond to the initial steep descent of the intensity curve and represent the host response in area closest to the electrode surface at distances ≤100 μm. The second set of parameters, $intensity_2$ and $decay_2$, correspond to the second phase of the curve with gradual descent of the intensity, indicating cell response in the area farther from the electrode at distances >100 μm.

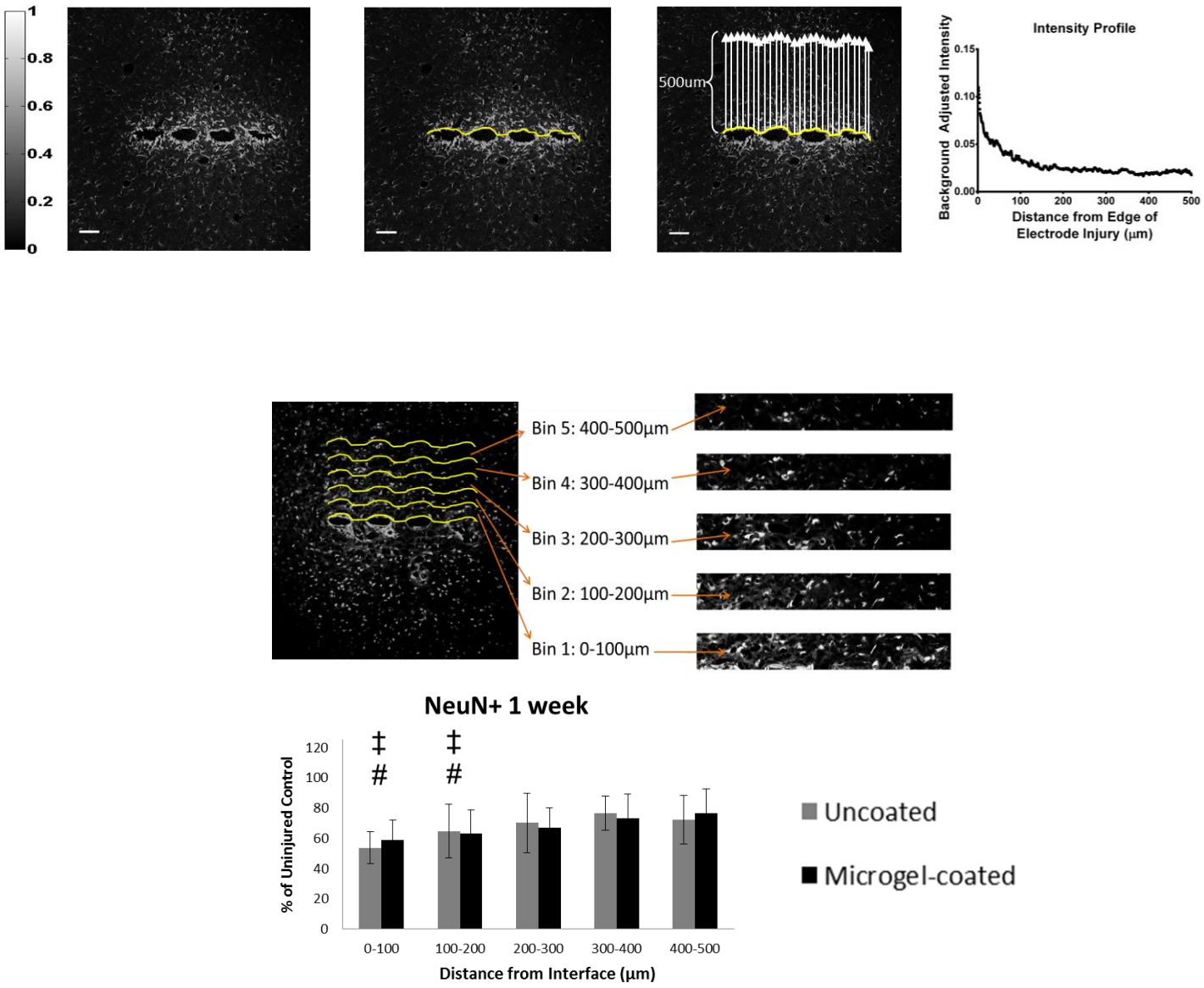

Figure 3.3: Analysis of immunostaining was performed using a custom MATLAB program. (a) The IHC images for each sample of GFAP, OX42, or ED1 stained sections were displayed and a curve generated along the edge of the scar formed by the electrode. A scale bar (left) indicates the intensity values of the staining from 0 (black) to 1 (white). The program determines the average of the intensity along the curve from 0-500μm away from the scar and generates an intensity curve as a function of distance. Sample intensity curve is shown from an uncoated electrode at 24 weeks for GFAP stain (a, right). This curve is fit with Equation 1 and parameters for each curve are compared between groups. (b) Image processing for NeuN stained samples involves dividing the 500 μm image into 5 equal-sized bins of 100 μm and counting NeuN positive cells in each bin. These NeuN+ cell counts are compared to the uninjured control from the contralateral hemisphere. Scale bar = 100 μm.

Representative images of immunostaining for GFAP (astrocytes, Fig. 3.4a) show the progression of astrocytic scar formation as well as representative intensity curves (Fig. 3.4b, Fig. 3.7) at 1 week, 4 weeks, and 24 weeks. Plots of the curve fit parameters for intensity (Fig. 3.4c) indicate changes in the parameters over time. At 1 week, the microgel-coated samples had higher staining for $intensity_1$, $decay_1$, and $intensity_2$ parameters while $decay_2$ was lower compared to uncoated electrodes. There were also significant increases for $intensity_1$ and $decay_1$ for both uncoated and microgel-coated samples from 1 to 4 weeks, while the $decay_2$ parameter decreased for uncoated samples. At 4 weeks, staining for $intensity_1$, $decay_1$, and $decay_2$ parameters were higher for microgel-coated samples while $intensity_2$ was higher for uncoated samples. From 4 to 24 weeks $intensity_1$ and $decay_1$ decreased for microgel-coated electrodes. At 24 weeks, all parameters were higher for uncoated electrodes than microgel-coated electrodes.

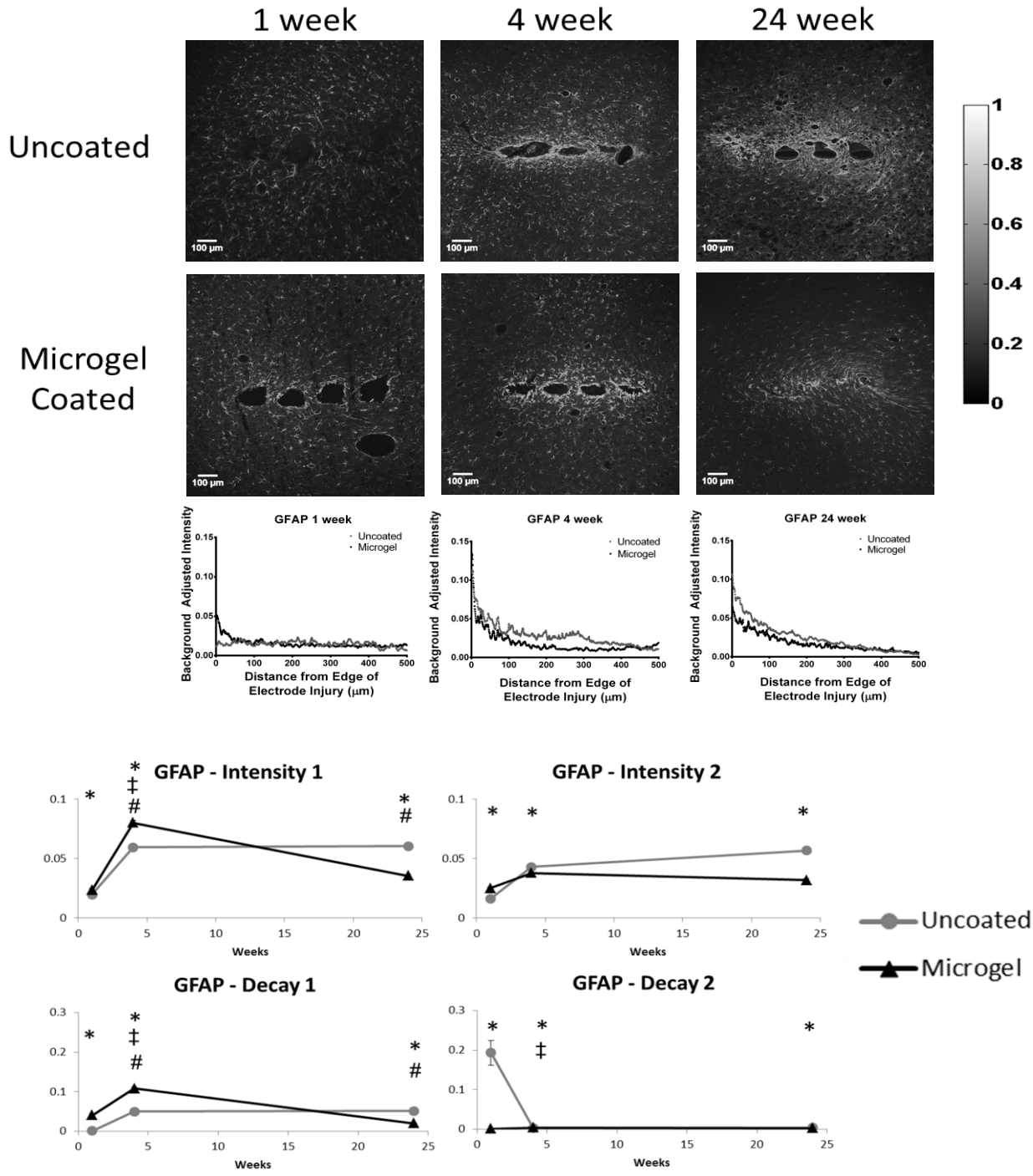

Figure 3.4: Immunofluorescence images and corresponding intensity scale (a) from each time point and group of samples stained with glial fibrillary acidic protein (GFAP), a marker for astrocytes (n=4 animals for all groups except n=3 for uncoated at 24 weeks). Curve fits on each intensity curve are completed using Equation 1. Representative intensity curves from background-corrected images (b) are located below the representative immunostaining images for each time point. Parameter curves (c) indicate changes in parameter values over time for the experimental groups. Symbols indicate: ***** significant differences between the groups at one time point, ‡ significant differences over time between the indicated and preceding time-point for uncoated samples, # significant differences over time between the indicated and preceding time-point for microgel-coated samples.

OX42 staining (resident microglia, Fig. 3.5a) and representative intensity curves (Fig. 3.5b, Fig. 3.7) were analyzed in a similar manner to GFAP, with curve fit parameters represented in Fig. 3.5c. At 1 week, $intensity_1$ and $decay_2$ were higher for uncoated samples while $intensity_2$ and $decay_1$ were higher for microgel-coated samples. From 1 to 4 weeks, $decay_1$ increased for microgel-coated samples whereas $decay_2$ decreased for uncoated electrodes. At 4 weeks, all parameters were higher for microgel-coated electrodes compared to uncoated controls. From 4 to 24 weeks $decay_1$ decreased for microgel-coated samples. At 24 weeks, uncoated samples had higher $intensity_1$ and $decay_1$ and lower $intensity_2$ parameter values than microgel-coated samples.

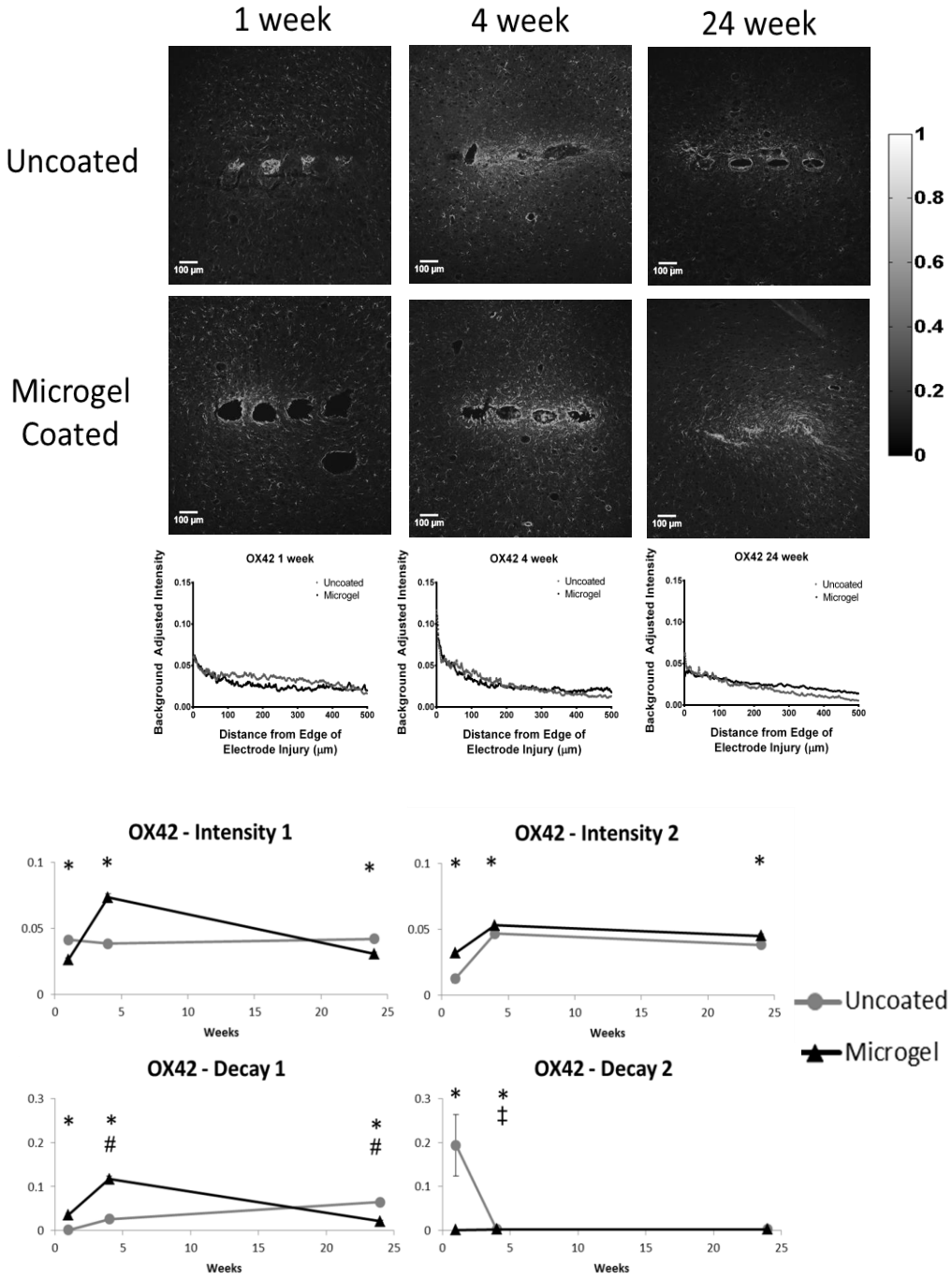

Figure 3.5: Immunofluorescence images and corresponding intensity scale (a) from each time point and group of samples stained with OX42 (CD11b), a marker for microglia. Representative intensity curves from background-corrected images (b) are located below the representative immunostaining images for each time point. Parameter curves (c) were generated in a similar manner to those for GFAP and indicate changes in intensity and decay values over time for the experimental groups. Symbols indicate: ***** significant differences between the groups at one time point, ‡ significant differences over time between the indicated and preceding time-point for uncoated samples, # significant differences over time between the indicated and preceding time-point for microgel-coated samples.

Results for ED1 staining (activated microglia, Fig. 3.6a) and representative intensity curves (Fig. 3.6b, Fig. 3.7) indicated the changes in parameters over time (Fig. 3.6c). At 1 week, $intensity_1$ and $intensity_2$ were higher for uncoated electrodes compared to microgel-coated electrodes. From 1 to 4 weeks, $decay_1$ and $intensity_2$ parameters decreased for uncoated electrodes while $decay_1$ increased for microgel-coated samples. At 4 weeks $intensity_1$, $intensity_2$, and $decay_2$ were all higher for uncoated samples while $decay_1$ was lower than that for microgel-coated samples. From 4 to 24 weeks, parameters for uncoated electrodes increased for $intensity_1$ and $decay_1$ while $decay_1$ decreased for microgel-coated samples. At 24 weeks, $intensity_1$, $decay_1$, and $intensity_2$ were higher and $decay_2$ was lower for uncoated electrodes compared to microgel-coated electrodes.

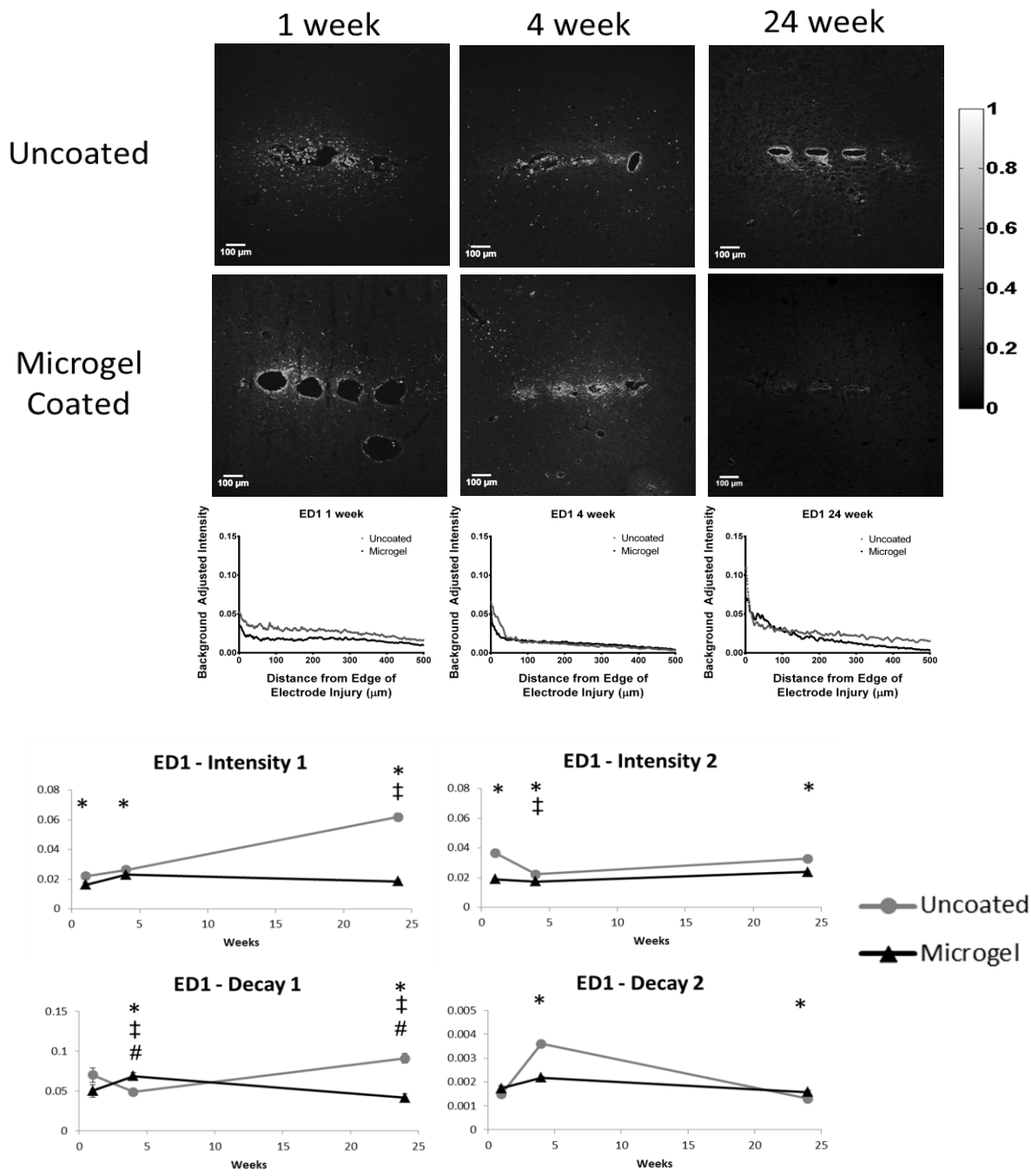

Figure 3.6: Immunofluorescence images and corresponding intensity scale (a) from each time point and group of samples stained with ED1 (CD68), a marker for activated microglia. Representative intensity curves from background-corrected images (b) are located below the representative immunostaining images for each time point. Parameter curves (c) were generated in a similar manner to those for GFAP and indicate changes in parameter values over time for the experimental groups. Symbols indicate: ***** significant differences between the groups at one time point, ‡ significant differences over time between the indicated and preceding time-point for uncoated samples, # significant differences over time between the indicated and preceding time-point for microgel-coated samples.

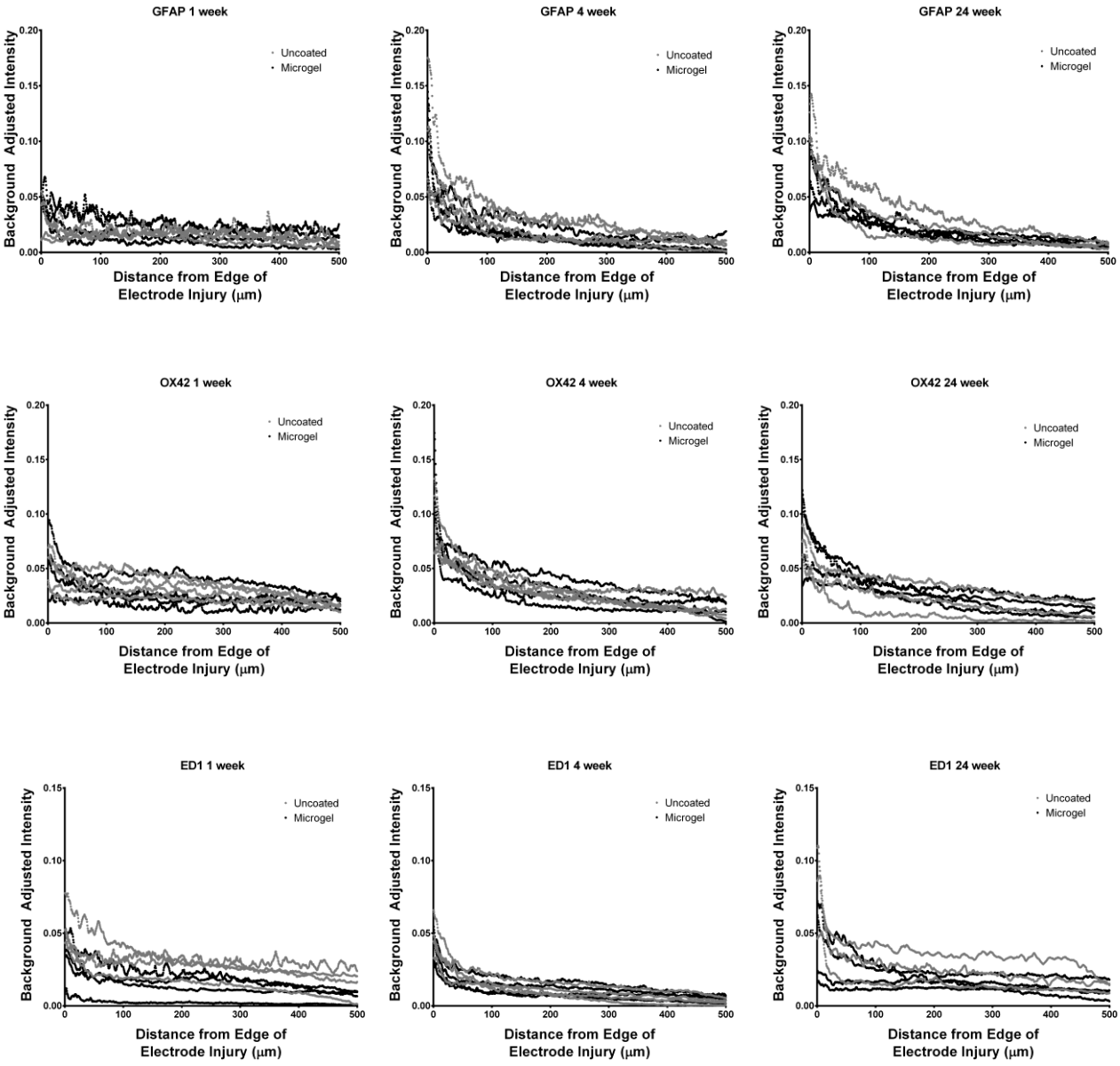

Figure 3.7: Intensity curves for each time point showing the staining intensity for each individual sample using GFAP (top row), OX42 (middle row), and ED1 (bottom row) at 1 week (left column), 4 weeks (middle column), and 24 weeks (right column).

Data obtained from NeuN (neuronal nuclei) staining was analyzed such that each image was divided into five 100 µm bins, allowing for each NeuN+ cell to be counted and normalized to the uninjured contralateral side (Fig. 3.3b). Each image was plotted with the first bin starting at the edge of the implant. The number of NeuN+ cells per bin were plotted to determine changes in neuronal density for each group. Representative images of NeuN staining (Fig. 3.8a) indicated the presence of neuronal nuclei in each sample group, as quantified in Fig. 3.8b. At 1 week the uncoated and micorgel-coated samples were significantly lower than the contralateral (control) samples at 0-100 µm and 100-200 µm bins for both groups. At 4 weeks, NeuN+ staining around uncoated samples was significantly lower than microgel-coated samples at 0-100 µm, and both groups were significantly lower than the contralateral control at the same distance. Additionally, the uncoated samples were significantly lower than the contralateral control at 200-300 µm. At 24 weeks, the microgel-coated samples had significantly lower neuronal density than the contralateral control at 0-100 µm and 100-200 µm, as well as significantly lower neuronal density compared to the 4 week time point in the 400-500 µm bin.

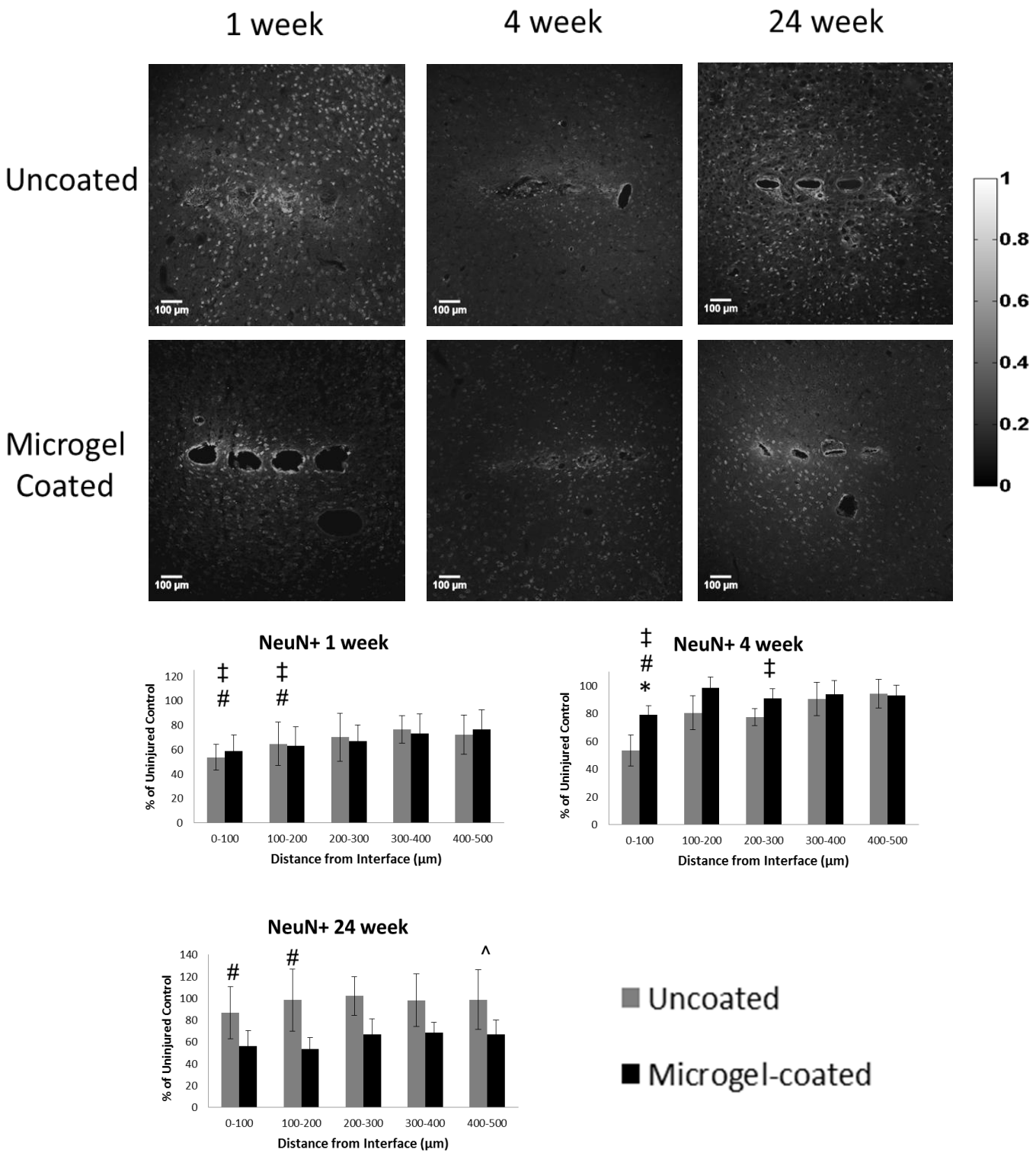

Figure 3.8: Immunofluorescence images (a) from each time point and experimental group stained with NeuN, a marker for neuronal. Graphs for each time point (b) indicate the average number of neuronal nuclei in each 100µm bin for uncoated and microgel-coated samples as a percentage of the cells found in the contralateral uninjured control. Symbols indicate: ***** significant differences between uncoated and microgel-coated samples, ‡ significant differences between uncoated and contralateral samples, # significant differences between microgel-coated and contralateral samples, ^ significant differences between the indicated and preceding time-point for microgel-coated samples.

Discussion

We have engineered a microgel coating for neural electrodes consisting of poly(NIPAm-*co*-AAc-PEG(575)-DA) particles that is applied to the surface of the electrodes using crosslinking chemistry and cationic "glue". Previous work from our lab has shown success with the monolayer microgel coatings for reducing cell adhesion and protein adsorption [101, 107], as well as significantly reducing acute and chronic inflammatory responses [102]. We have also observed moderate effects in reducing fibrous capsule formation in chronic implantation [103]. The multilayer coating used in this study performed well *in vitro* with cell adhesion experiments with mixed astrocyte and microglia cultures showing a significant reduction in the number of adherent cells and amount of cell spreading on microgel-coated electrodes compared to uncoated controls. However, the *in vivo* data obtained from chronic implantation of the electrode into the rat cortex indicated only modest improvements in the cellular responses around the implanted electrode including variable cell response over time and persistence of inflammation and scar formation at chronic time points. At 24 weeks of implantation, microgel-coated electrodes exhibited reduced astrocytic and activated macrophage staining in the vicinity of the electrode. However, neuronal density close to the electrode was reduced for microgel-coated electrodes.

Cell adhesion studies were performed to compare mixed glial attachment between the uncoated and microgel-coated electrode surfaces. The mixed glial cells were chosen due to the presence of astrocytes and microglia, two of the main cell types involved in inflammation and scar formation. Microglial attachment studies have been performed by

others [57] to observe differences in cell attachment to electrode surfaces. Monolayer microgel coatings have shown reduced protein adsorption [107, 108] and reduced cell adhesion in other applications [101-103]. Quantification of *in vitro* data of multilayer coatings cultured with mixed glial cells showed promising results with significantly reduced cell adhesion on the electrode surface when coated with microgel particles. The significant reduction in cell spread area suggested the potential of the microgel coating for reducing cell adhesion in the early stages of cell-electrode interaction.

The *in vivo* data gathered from histological samples indicated a time-dependent tissue response surrounding neural electrodes. Staining for GFAP (astrocytes) around implanted electrodes at 1 week indicated the $intensity_1$, $decay_1$, and $intensity_2$ parameters were higher for microgel-coated samples, indicating increased astrocyte presence around the microgel-coated samples initially after implantation. From 1 week to 4 weeks the astrocyte staining parameters for uncoated samples increased for $intensity_1$ and $decay_1$ while decreasing for $decay_2$ while the microgel-coated sample parameters increased for $intensity_1$ and $decay_1$. This increase is a well-known response to chronically implanted electrodes and has been observed in multiple studies [12, 15, 17] as it is indicative of the scar formation that occurs over time around implanted electrodes. The 4 week time point showed increased staining for $intensity_1$, $decay_1$, and $decay_2$ parameters on microgel-coated samples while $intensity_2$ was higher for uncoated samples. These data indicate that astrocyte staining corresponding to the area closest to the electrode, was higher in the microgel-coated sample while the higher $intensity_2$ value for uncoated samples indicated increased astrocyte staining farther from the electrode at distances >100 μm. From 4 to 24 weeks microgel-coated sample parameters $intensity_1$ and $decay_1$ parameters decreased.

All parameters for uncoated samples were higher than microgel-coated samples at 24 weeks. The change in parameters over time as well as at the 24 week time point indicated a reduction in astrocyte presence in response to the microgel-coated electrode, showing an improvement in one of the major constituents of the scar formation that occurs *in vivo*. Overall, the data indicate that GFAP staining increases initially and is maintained chronically as the intensity values indicate persistence of higher GFAP staining around the implanted electrode. These results are consistent with other studies reporting increasing astrocyte recruitment over time [12, 15, 64] as well as variation at different time points [17, 30] indicating the variable nature of tissue response to implanted electrodes.

Staining for resident microglia using OX42 / CD11b showed variability over time in tissue response to chronically implanted electrodes. At the 1 week time point, uncoated samples had higher $intensity_1$ and $decay_2$ parameters while $decay_1$ and $intensity_2$ were higher for microgel-coated samples. The data indicated higher resident microglial staining around uncoated electrodes in first phase of the decay equation corresponding to the 0-100 μm distance from the electrode surface as well as faster decay of staining intensity in the second phase of the decay equation corresponding to the 100-500 μm distance from the implantation site. Conversely, higher microglial staining at the 100-500 μm distance indicates increased microglial presence away from the electrode site as well as faster decay of microglial staining intensity closest to the electrode surface around microgel-coated samples. The $decay_1$ parameter for microgel-coated samples increased from 1 to 4 weeks, indicating a faster decay in resident microglial presence at short time points close to the electrode surface. For the same time frame, uncoated sample $decay_2$

decreased indicating a slower decline in the resident microglial staining at distances 100-500 μm from the electrode surface. By 4 weeks all parameters for microgel-coated samples were higher than uncoated samples indicating increased microglial presence around microgel-coated samples. From 4 to 24 weeks $decay_1$ decreased for microgel-coated samples, and at 24 weeks uncoated electrode parameters were higher than microgel-coated electrode parameters for $intensity_1$ and $decay_1$ and lower for $intensity_2$. The changes at later time points indicate higher microglial staining around uncoated samples at distances close to the electrode surface while microgel-coated samples had higher staining at distances farther from the electrode surface at 100-500 μm from the implant. Overall, the variations in tissue response over time are similar to results observed in other studies of microglial response with an initial increase after implantation followed by fluctuations over time [30] as the tissue is constantly changing around the implant.

Response of activated microglia to the implanted electrodes also showed temporal changes in the reactivity of astrocytes in surrounding tissue. Activated microglia (ED1 / CD68) staining parameters showed higher $intensity_1$ and $intensity_2$ for uncoated samples at 1 week, indicating higher microglial activation after initial implantation. From 1 to 4 weeks, the microgel-coated $decay_1$ parameter increased while uncoated $decay_1$ and $intensity_2$ decreased, resulting in higher $intensity_1$, $intensity_2$, and $decay_2$ and lower $decay_1$ for uncoated samples compared to microgel-coated samples at 4 weeks. These data indicate the increased presence of activated microglia around uncoated electrodes with parameters associated with both phases of the decay equation, which corresponds to distance both close to (0-100 μm) and farther (100-500 μm) from the electrode surface

and is consistent with previously reported results [12]. The lower $decay_1$ parameter also indicates a slower decay around uncoated samples in the area closest to the electrode. From 4 to 24 weeks, parameters for uncoated electrodes increased for $intensity_1$ and $decay_1$, while $decay_1$ decreased for microgel-coated samples. At 24 weeks $intensity_1$, $decay_1$, and $intensity_2$ were higher and $decay_2$ was lower for uncoated samples. These data indicate maintenance of microglial activation around uncoated samples across the 500 μm analysis area, but also indicate a faster decay rate in staining close to the implanted electrode and slower decay rate farther from the electrode surface. The variation in ED1 activity over time is consistent with observations in the literature [30] as long-term studies have observed a similar response. As with the GFAP and OX42 markers, each cell response is variable over time with parameters that change between time points.

NeuN stain was used to identify neuronal nuclei in the area around implanted electrodes. At 1 week there were significant differences between the uncoated and contralateral (uninjured control) NeuN+ counts, as well as between the microgel-coated and contralateral samples at 0-100 μm and 100-200 μm for both groups. This indicates a decrease in neuronal density close to the electrode surface soon after implantation, and this trend is similar to what has been observed in literature [12, 17]. At 4 weeks, the neuronal density around uncoated samples was significantly lower than microgel-coated samples at 0-100μm, and both groups were significantly lower than the contralateral control at the same distance. Additionally, the uncoated samples were significantly lower than the contralateral control at 200-300 μm. These data indicate the continued effect of the electrode presence in reducing neuronal cell density near the electrode surface, as

constant presence of the electrode in the tissue continues to affect neuronal survival [12]. At 24 weeks, the microgel-coated samples had significantly lower neuronal density than the contralateral control at 0-100 μm and 100-200 μm, as well as significantly lower neuronal density compared to the 4 week time point in the 400-500 μm bin. This result was unexpected as we had hypothesized that the microgel-coating would improve the long-term cell response. We do not know the exact cause for the lower neuronal density around microgel-coated samples at 24 weeks. Overall, the data show lower neuronal staining levels near the implant, which increase as you move away from the injury. This behavior indicates the effect of the environment around the injury, likely a combination of physical injury from implantation as well as the resulting inflammatory response and cytokine release, which causes neuronal loss near the implant site. This is a significant problem for neural electrode function as neurons must be present near the site of the electrode for the implant to be functional in receiving neuronal signals.

Future work with microgel coatings can improve upon the material to make it more suitable for chronic neural electrode implantation. Several polymer coatings have been developed that demonstrate reduced protein adsorption and astrocytic recruitment around the implant [58, 69], and others with reduced impedance and other improvements in conductive polymers to improve neuronal signal propagation [109, 110]. One the of major responses that occurs after implantation of any material is the formation of scar-like tissue around the implant as the body tries to separate the implant from the tissue. The astrocytes and microglia in the brain contribute to this scar formation and it is believed that increased inflammation contributes to the activation of these cell types. Further modification of the microgel coatings with immunomodulators to control

inflammation may contribute to greater improvements for tissue response to implanted electrodes. Release of anti-inflammatory agents can help to mediate the tissue response to a greater extent if the inflammation is controlled effectively. Many groups have attempted to modulate this inflammatory response with both passive and active release of anti-inflammatory factors. Zhong et al. developed a polymer coating with passive release of dexamethasone that showed a reduction in GFAP staining intensity, ED1 staining, and neuronal loss at 1 week and 4 weeks post-implantation [64]. Mercanzini et al. also demonstrated effectiveness of dexamethasone in a short term study to reduce astrocyte and microglial recruitment at 3 weeks [67]. Taub et al. showed the effectiveness of coatings containing IL-1Ra compared to laminin coatings, demonstrating reductions in GFAP staining with the IL-1Ra coating [82]. Others have tried to increase neuronal survival and attachment *in vitro* [55, 100] however these coatings also improve cell attachment for unwanted cell types such as astrocytes. Additionally, the studies showing improvement in multiple cell types (astrocytes, microglia, and neurons) were only performed for short time points ~4 weeks. A recent study has investigated long-term effects of Parylene-C coating for reducing cell adhesion on implanted silicon electrodes [60]. Although the results demonstrated reduced cell adhesion on the Parylene-C coated electrode, the inflammatory response persisted through the 12-week time point. We hypothesized that the composition of our microgel coating, containing temperature responsive pNIPAm combined with the "gold-standard" poly(ethylene glycol) for reducing cell adhesion, would provide a suitable alternative for reducing cell adhesion. Although both the Parylene-C coating presented by Winslow et al and the microgel coating presented in this study had reduced cell adhesion *in vitro*, the long-term *in vivo*

observations indicated maintenance of long-term inflammatory response. Together, these studies indicate that the problem with chronically implanted electrodes goes beyond the need for a non-adhesive surface alone, but likely requires additional modification including inflammation attenuation. While many of these coatings showed some improvement there is no coating that solves all long-term tissue response problems, underscoring the need for further research. Our study indicated some improvement on certain parameters of GFAP, OX42, and ED1 staining with the microgel coating, similar to many of the studies listed above. However, maintaining long-term improvement for chronic time points is a difficult task which requires more investigation.

There are many areas for improvement in the area of neural electrode implantation. The response of the tissue surrounding the electrode is variable depending on the implant and the time point and continues to change over time. This variable environment provides a significant challenge for improving long-term electrode function, but we believe further modification of the electrode surface can provide options. Several labs have investigated the effects of modified electrode design geometry on the tissue response surrounding the electrode. Some groups have shown that while minimizing damage using smaller electrodes may provide some positive effects [44], the persistence of the electrode in the tissue remains a significant problem [1]. Modification of electrode design geometry [39, 111] and insertion techniques [112] to minimize tissue injury and blood-brain-barrier disruption [41] may also provide better options. Another area of for potential improvement is the choice of electrode materials to improve upon the mechanical mismatch [48] that exists between stiff electrodes and soft neural tissue. Several groups have shown potential for improvement in tissue response when using

materials that adapt after implantation with a resulting electrode that is softer and more mechanically similar to the brain tissue than stiff electrodes using computational [113] and experimentally validated models [50, 114]. Using electrodes that are untethered has also indicated positive results compared to electrodes that are attached to the skull [44]. Adding neuron-specific survival and attractant factors [53] may also improve upon the recording potential, but these factors must also avoid recruitment of other cell types such as astrocytes which contribute to problematic scar formation.

Conclusion

The findings from many of these studies reiterate the importance of addressing the inflammatory response as inflammation is a factor that persists as part of the host response to implanted electrodes [21]. Long-term inflammation and microglial activation contribute to the foreign body response and failure of electrodes implanted for chronic time points [111]. Reduction of the inflammatory response can be achieved by releasing anti-inflammatory agents at the most beneficial time point, where specific drugs are targeted to be released at a time when the corresponding target molecule is at its peak in the inflammatory cascade. The multi-faceted problem of improving long-term electrode functionality is a complicated task that will likely involve a combination of targets including reducing unwanted cell adhesion from astrocytes and microglia, maintaining neuronal survival and presence around the electrode, and reducing inflammation in the surrounding tissue. Modification of microgel-coated electrodes with anti-inflammatory agents to modulate inflammation around electrodes may provide an effective method for maintaining functionality of chronically implanted neural electrodes.

Acknowledgements

This work was supported by National Institutes of Health Grants: F31NS073358 (SMG) and T32EB006343-01A2 (RVB); GAANN Fellowship for Drug Design, Development, and Delivery: US Department of Education P200A090099; Georgia Tech/Emory Center for the Engineering of Living Tissues and the Atlanta Clinical and Translational Science Institute under PHS Grant UL RR025008 from the Clinical and Translational Science Award Program. XPS analysis was performed by the National ESCA and Surface Analysis Center for Biomedical Problems (NESAC/BIO): NIH EB-002027. We also thank Emily Herman from the Lyon lab for help with AFM imaging.

CHAPTER 4

ENGINEERING A PROTEASE-DEGRADABLE PEG-MALEIMIDE COATING WITH ON-DEMAND RELEASE OF IL-1RA TO IMPROVE TISSUE RESPONSE TO NEURAL ELECTRODES

Introduction

Knowledge gained from the studies in Aim 1 contributed to a more thorough understanding of the necessity for improved coatings on neural electrodes. While the microgel coating was not successful in improving the long-term tissue response to implanted neural electrodes as measured by cellular stains for microglia and astrocytes, the information gained from the study indicated a need to develop a coating with more than just a passive non-fouling surface modification. Rather, it is important to engineer a coating that will possess a combination of non-fouling properties in addition to an immunomodulatory aspect. As discussed in the literature review, there have been studies that developed coatings with incorporated anti-inflammatory agents with mixed results. Collectively, these results indicate the need to engineer a better coating to improve the tissue response to the implanted electrodes. We hypothesized that a coating comprising a protein adsorption/cell adhesion-resistant layer with controlled on-demand release of the anti-inflammatory agent IL-1Ra would improve the tissue response and neuronal survival near the implant-tissue interface.

First, we started with a material that has been characterized for use as a non-fouling surface. Poly(ethylene glycol) (PEG) is a synthetic polymer that is used as a biocompatible material for implantable devices [115]. PEG has been widely characterized

as a non-fouling material because of the reduced protein adsorption and reduced cell adhesion on the PEG surface [116-118]. Additionally, PEG-based coatings have been applied to neural electrodes with promising results *in vitro* including reduced cell adhesion and protein adsorption [59, 119]. Finally, PEG-based materials have been successfully used for delivery of cells and bioactive molecules including dexamethasone [120], proteins [121], fibroblasts [93], VEGF and pancreatic islets [98], among others.

Another important factor in choosing a material for coating is the ability to engineer an on-demand response to inflammatory stimuli. Protease degradable hydrogels are a promising option as the inflammatory cascade causes up-regulation of many proteases including MMPs [83, 84]. Specifically, PEG hydrogels that degrade in response to proteases such as MMP-1 and MMP-2 are of interest for this work [93, 122], especially because these MMPs have been implicated as an important part of the inflammatory cascade in the brain [85, 89]. Recent work by Patterson and Hubbell provided thorough characterization of protease-degradable peptide sequences, including cleavage by MMPs, that can be used as crosslinkers for PEG macromers in PEG hydrogels [122]. As part of this characterization, the study analyzed over two dozen peptide sequences for use with protease-degradable hydrogels. Based on this paper, we chose two protease-sensitive, crosslinking peptides for use in this engineered hydrogel coating: GCRDGDQGIAGFDRCG (GDQ) and GCRDVPMSMRGGDRCG (VPM). GDQ has very slow degradation kinetics (k_{cat} = 0.79 s^{-1} for MMP-1 and no observable degradation for MMP-2), whereas VPM has fast degradation kinetics (k_{cat} = 5.25 s^{-1} for MMP-1 and 4.82 s^{-1} for MMP-2) in response to MMP challenge. Importantly, these peptides contain cysteines at both end of the molecule; the free thiol in these residues

reacts rapidly with the maleimide group in the PEG macromers to produce a crosslinked hydrogel. These PEG-mal hydrogels and crosslinking peptides have been previously characterized and used successfully by our lab for other drug and cell delivery applications [97, 98].

Finally, we chose to incorporate IL-1 receptor antagonist (IL-1Ra) as the anti-inflammatory agent to be released. IL-1 is up-regulated in brain injury [73, 77, 79], and IL-1Ra has been shown to be an effective molecule to improve neuronal survival in addition to reducing inflammation in the brain [81]. Additionally, IL-1Ra has been used in humans to treat several diseases involving inflammation and has a good record of safety [80].

Combining all of these important considerations, we have engineered a novel coating with three essential components:

1) a protein adsorption- and cell adhesion-resistant PEG hydrogel;

2) incorporated anti-inflammatory IL-1Ra, known to reduce inflammation in brain injury models;

3) protease-sensitive crosslinkers for on-demand release of IL-1Ra in response to proteases which are up-regulated during inflammation.

Materials and Methods

PEG-maleimide Coating of Electrodes

Electrodes were purchased from NeuroNexus Technologies (CM16 A4x4-4mm-200-200-1250) and consist of a silicon substrate with iridium wires and active sites. Each electrode is 4-mm long with four active sites on each of four prongs, and each active site has an area of 1250 mm^2. Electrodes were cleaned to remove contaminants remaining after manufacture using serial 5-min incubations in trichloroethylene (JT Baker), acetone (Sigma-Aldrich), and methanol (Sigma-Aldrich). Electrodes were then rinsed with absolute ethanol (Decon Labs). The surface was functionalized using a silane-based adhesion layer that is grafted onto the silicon oxide layer of the electrode. Briefly, the electrodes were incubated for 2 hours in 2.5% silane-PEG-maleimide (Nanocs Inc.) in DMSO, then rinsed with absolute ethanol and PBS. Multi-treatment PEG-mal coatings were deposited using a dip-coating technique developed for this project. Electrodes were incubated in solution with crosslinking peptide, either GDQ or VPM, for 2 minutes, rinsed with PBS, incubated for 2 minutes in 4-arm, 20 kDa PEG-maleimide, and rinsed with PBS. Alternating incubations in crosslinking peptide followed by PEG were repeated to achieve the desired number of treatments per coating, with each set of peptide and PEG considered as one complete treatment. For samples presenting only the PEG hydrogel (designated as PEG), the samples were coated with six treatments of PEG-mal and GDQ, whereas the coatings containing IL-1Ra (PEG + IL-1Ra) were coated with two treatments of PEG-mal and GDQ followed by four treatments of PEG-mal/IL-1Ra and VPM. Coating deposition was verified by X-ray photoelectron spectroscopy (XPS).

While the coatings do incorporate different crosslinkers, this hydrogel system with both crosslinkers has been extensively characterized by our lab and there are minimal differences in hydrogel structure. Silicon wafers were used as a surrogate for the Si substrate of the electrodes, and coating thickness was analyzed by wet-cell ellipsometry of coatings on Si wafers by Dr. Yang Wei and Dr. Robert Latour at Clemson University. Ellipsometry measurements were performed using Sopra GES5 variable angle spectroscopic ellipsometer (Sopra Inc., Palo Alto, CA) and the accompanying GESPack software package. Briefly, a total of six spectra for at least two test points on each sample in deionized water were scanned from 350 nm to 800 nm at 10 nm intervals using an incident angle of 70°. The thickness of the test substrate was estimated from a model and determined using the regression method in Sopra's Winelli (ver. 4.08) software.

***In Vitro* Analysis of Cell Adhesion**

Either uncoated or PEG-coated silicon wafers were placed in individual wells of a 96-well plate. The samples (n = 4 per group) were washed three times with 70% ethanol followed by three washes with sterile PBS. Mixed astrocyte and microglial cells were added to each well at a density of 50,000 cells/cm^2. The samples were cultured in DMEM/F12 (Invitrogen) and 10% FBS (Invitrogen) at 37ºC and 5% CO_2 for 24 h. Samples were stained with LIVE/DEAD stain (Invitrogen) and imaged with a 20X Apo Nikon objective (0.75 NA). Cell spread area on the electrode surface was measured using ImageJ software (NIH).

Cytokine Release Analysis

Si wafers were coated as described above with 6 treatments of PEG-mal and GDQ for PEG samples and 2 treatments of PEG-mal and GDQ followed by 4 treatments of

PEG-mal + IL-1Ra and VPM for the PEG + IL-1Ra samples. The samples (n = 4 per group) were placed in a 96-well plate and washed three times with 70% ethanol followed by three times with sterile PBS. Cells were seeded at a density of 30,000 cells/well in DMEM + N2 supplement (Life Technologies) in an ultra-low attachment cell culture plate. Cells were incubated overnight at 37ºC and 5% CO_2 before rinsing the samples and transferring the samples to a new well to avoid detecting cytokine release from distressed cells that remained in suspension. The samples were stimulated with 10 ng/ml granulocyte macrophage colony stimulating factor (GM-CSF) to promote cytokine secretion [57] and incubated for 48 hours. Levels of IL-1β and TNF-α were analyzed using ELISA (R&D Systems).

IL-1Ra Release Characterization

Si wafer samples (n = 4 per group) were coated as described above with two treatments of PEG-mal with GDQ crosslinker followed by 4 treatments of PEG-mal + IL-1Ra with VPM crosslinker. The samples were placed in a 96-well plate and washed three times with 70% ethanol followed by three washes with sterile PBS. The samples were incubated with supernatant from LPS-stimulated mixed glia cultures or naive media and supernatant samples were collected at specified time points for analysis using an ELISA (R&D Systems).

Electrode Implantation

NIH guidelines for the care and use of laboratory animals (NIH Publication #85-23 Rev. 1985) were observed. All surgical procedures were approved by the Institutional Animal Care and Use Committee at the Georgia Institute of Technology. Male Sprague-Dawley rats (Charles River Laboratories) weighing 200-300g were anesthetized with

isofluorane (n = 8 per group). The surgical site was shaved and hair removed with Nair, then cleaned with isopropyl alcohol and chlorohexaderm before mounting the animal onto a stereotactic frame. Marcaine (0.15 mL of 0.5%) was injected subcutaneously at the site of incision. A midline incision 2-3 cm long was made in the scalp and the periosteum retracted to expose the cranium. Three 1 mm-diameter pilot holes were made around the skull, two posterior to bregma on either side of the midline and one anterior and right of bregma. A 4.7 mm stainless steel bone screw (Fine Science Tools 19010-00) was inserted into each of the pilot holes, with each screw penetrating the skull but leaving about 1-2 mm of each screw head remaining out of the skull to serve as an attachment point for the headcap. The craniotomy for electrode insertion was made anterior to and left of bregma using a 2.7 mm trephine bit (Fine Science Tools 18004-27). The dura was resected and folded away from the insertion site. The electrode was held in the stereotactic frame above the 2.7 mm hole and slowly lowered into the cortex, careful to avoid any large vasculature in the surgical area. Agarose gel (1.5% w/v, SeaKem) was filled into the opening around the electrode and dental acrylic (OrthoJet) was used to anchor the electrode assembly to the skull. The scalp incision was closed and triple-antibiotic ointment was applied to the wound. Each animal was given an injection of 0.03 mg/kg sustained release buprenorphine for pain relief allowed to recover from anesthesia under a heat lamp. All animals were fully ambulatory post recovery and no complications were observed.

At 4 weeks the animal was anesthetized with ketamine/xylazine/acepromazine (50, 10, and 1.67 mg/kg body weight respectively). For samples used for histological sections (n = 8 per group), the animal underwent transcardial perfusion with 200 mL

0.4% papaverine HCl in 0.9% NaCl, followed by 50 mL of 0.9% NaCl, and 200 mL of 4% paraformaldehyde in phosphate buffer. After perfusion, the rat was decapitated and excess tissue removed from the skull before placing the intact skull into 4% paraformaldehyde overnight. The following day, the intact skull was moved to 30% sucrose in PBS. After one day in 30% sucrose, the skull cavity was opened and the brain was carefully removed. Any electrodes remaining in the brain were removed from the tissue before placing the whole brain into a 50 mL conical tube with 30% sucrose overnight until the brain sank to the bottom of the tube. The purpose of the sucrose solution was to serve as a cryoprotectant for the brain during immunostaining analyses. Following sinking to the bottom of the 50 mL conical tube, samples were embedded in OCT and frozen using isopentane in liquid nitrogen. For samples to be used for qRT-PCR analysis (n = 7 per group), the animal was anesthetized with ketamine/xylazine/acepromazine prior to transcardial perfusion with 100 mL cold PBS followed by 100 mL 30% sucrose in PBS. Upon finishing the perfusion, the rat was decapitated and the brain promptly removed from the skull. A 2-mm biopsy punch was used to remove brain samples which were immediately placed in RNAlater (Life Technologies) and stored at -20ºC until analysis by qRT-PCR.

Histological Evaluation

Samples were sectioned in 16-mm thick sections using a cryostat and stained for various cell markers as indicated in Table 4.1. All primary antibodies were visualized with Alexa-Fluor 488 secondary antibody (Invitrogen) and counterstained with DAPI for cell nuclei recognition. Upon completion of staining, all slides were imaged using a 10X Nikon objective (0.30 NA) and SPOT Advanced software (Diagnostic Instruments).

Analysis of inflammatory and neuronal markers was conducted in a similar manner to Aim 1.

Table 4.1: Antibodies used for immunofluorescence analysis

Antibody	Supplier	Cell / Tissue Identified
Glial fibrillary acidic protein (GFAP)	Abcam ab7260	Astrocytes
NeuN	Millipore MAB377	Neuronal nuclei
OX42 / CD11b	Chemicon CBL1512	Resident microglia
ED1 / CD68	AbD Serotec MCA341R	Activated microglia
Alexa Fluor - Rat IgG	Life Technologies A11006	Blood brain barrier breach
CS56	Sigma C8035	Chondroitin sulfate

Quantitative Reverse Transcriptase – Polymerase Chain Reaction (qRT-PCR)

Samples for qRT-PCR were stored in RNAlater buffer (Qiagen) until processing. Individual biopsy punch (2 mm diameter) samples from the electrode implantation site and the uninjured contralateral hemisphere were collected from each animal. Samples were placed in Qiazol (Qiagen) and homogenized using a Lab Gen 7 tissue homogenizer (Cole Palmer) for ~1 minute. Tissue homogenate was placed in a QIAshredder column followed by total RNA extraction with the RNEasy MinElute Cleanup Kit (Qiagen). All RNA samples were tested for quality using a Nanodrop and had a 260/280 value of 2 or higher. Subsequent cDNA conversion was completed using the RT^2 First Strand Kit (Qiagen). Total cDNA, corresponding to mRNA expression, was analyzed using the Fluidigm BioMark system. 16 gene targets (Table 4.2) were analyzed to observe changes in inflammation as well as neural cell markers, GAPDH was used as a housekeeping gene. The Ct values were normalized using ΔΔCt method, normalizing to the contralateral uninjured hemisphere and the housekeeping gene. Results are presented as fold change in gene expression compared to the uninjured contralateral hemisphere per group.

Table 4.2: Gene Targets for qRT-PCR Analysis

IL-1α	Interleukin - 1α	MMP-2	Matrix metalloproteinase – 2, 3, 9, 13
IL-1β	Interleukin - 1β	MMP-3	
IL-1Ra	Interleukin -1 receptor	MMP-9	
IL-6	Interleukin - 6	MMP-13	
IL-10	Interleukin - 10	NGF	Nerve growth factor
MCP-1	Monocyte chemoattractant protein - 1	BDNF	Brain derived neurotrophic factor
TNF-α	Tumor necrosis factor - α	CNTF	Ciliary neurotrophic factor
IFN-γ	Interferon-γ	GFAP	Glial fibrillary acidic protein

Statistical Analysis

Data presented are mean +/- standard error. All analyses were performed using GraphPad Prism 6.0. Statistical analyses for differences between thickness of multiple treatments of PEG hydrogel, *in vitro* cell adhesion, and cytokine release were performed using one-way ANOVA with Tukey's multiple comparison test. Statistical analysis of differences between PEG and PEG + IL-1Ra coating thickness was analyzed using an unpaired t-test. Curve fit parameters for immunostaining intensity curves were analyzed for normal distribution using the D'Agostino & Pearson normality test. As these parameters were found be not normally distributed, the curve-fit parameters were analyzed using a Kruskal-Wallis test with Bonferroni-Dunn's multiple comparison test to test for differences among groups. Analysis of NeuN data was performed using a 2-way repeated measures ANOVA with Tukey's multiple comparison test. PCR data was analyzed using a one-way ANOVA with Tukey's multiple comparison to test for differences between groups. A p-value <0.05 was considered significant.

Results

Characterization of PEG Hydrogel Coatings

Silicon surfaces (electrode or Si wafer) were coated with the PEG-mal hydrogel coating. Figure 4.1a shows a diagram of the predicted structure of the coating consisting of silane-PEG-mal, a protease degradable crosslinker, and PEG-maleimide molecules. Figure 4.1b shows XPS survey spectra for uncoated and 6-treatment PEG hydrogel-coated surfaces. As seen in the narrow band scans in Figure 4.1c, clear shifts in the C1s peak demonstrate PEG-coated samples having a higher portion of C-C, H bonds as a result of coating deposition. The thickness of the coatings was analyzed by wet-cell ellipsometry. Figure 4.2a show that the thickness of the PEG coating increases with increasing treatment deposition, and a 6-treatment coating is approximately 30 nm thick, a reasonable measurement given the size of the coating components. Figure 4.2b shows the difference in thickness between a 6-treatment coating of PEG and a 6-treatment coating with 2 treatments PEG and 4 treatments PEG + IL-1Ra, with the latter being thicker. The increased thickness for the PEG + IL-1Ra is not surprising given the incorporation of the anti-inflammatory protein (17 kDa, corresponding to a 3 nm diameter sphere [123]).

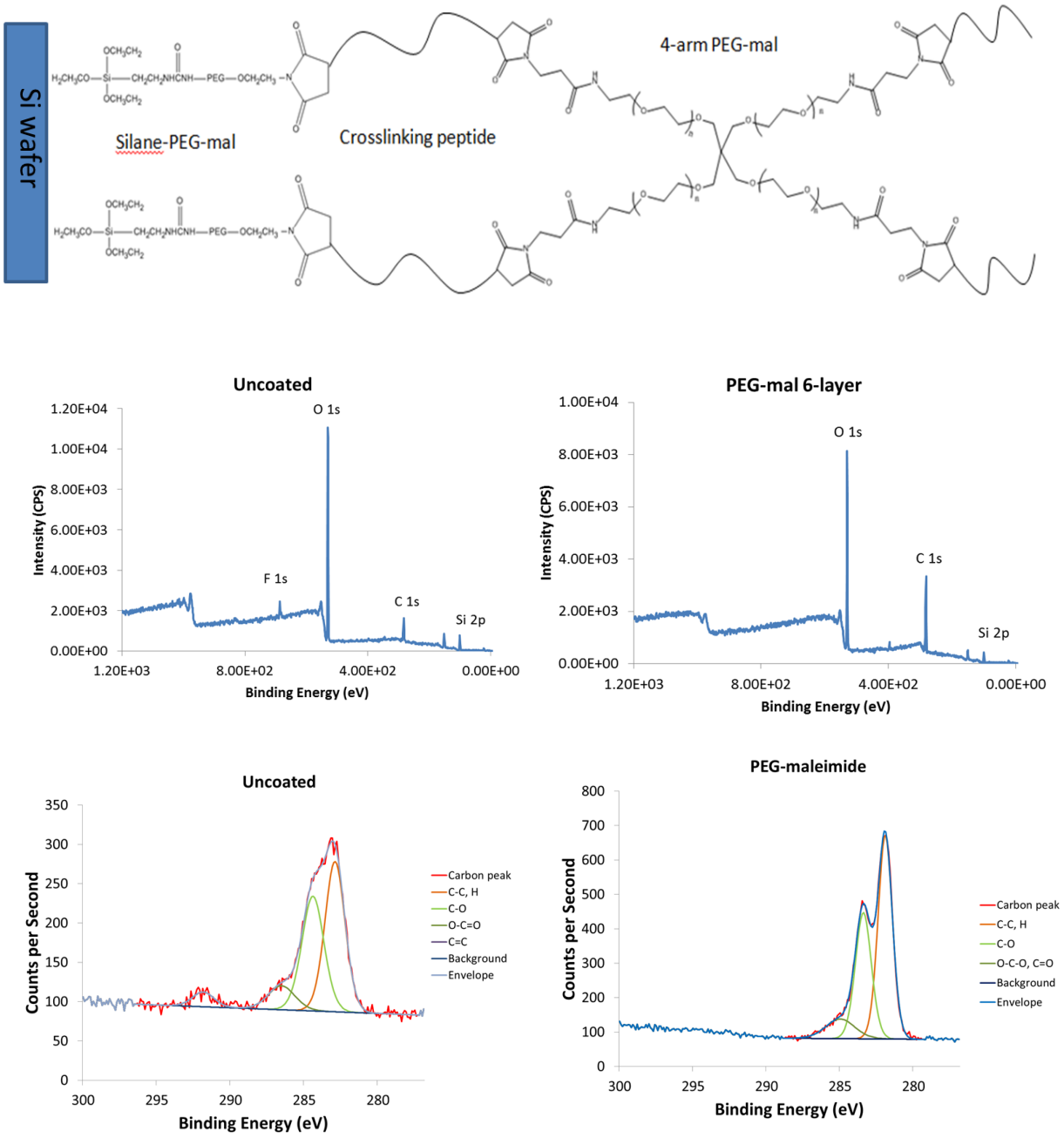

Figure 4.1: PEG coatings applied to the surface of electrodes. (a) Chemical structure of the PEG coating applied to the surface of the silicon substrate. (b) XPS spectra of uncoated (left) and PEG coated (right) electrodes. (c) Detailed carbon shifts of the uncoated (left) and PEG-coated (right) surfaces.

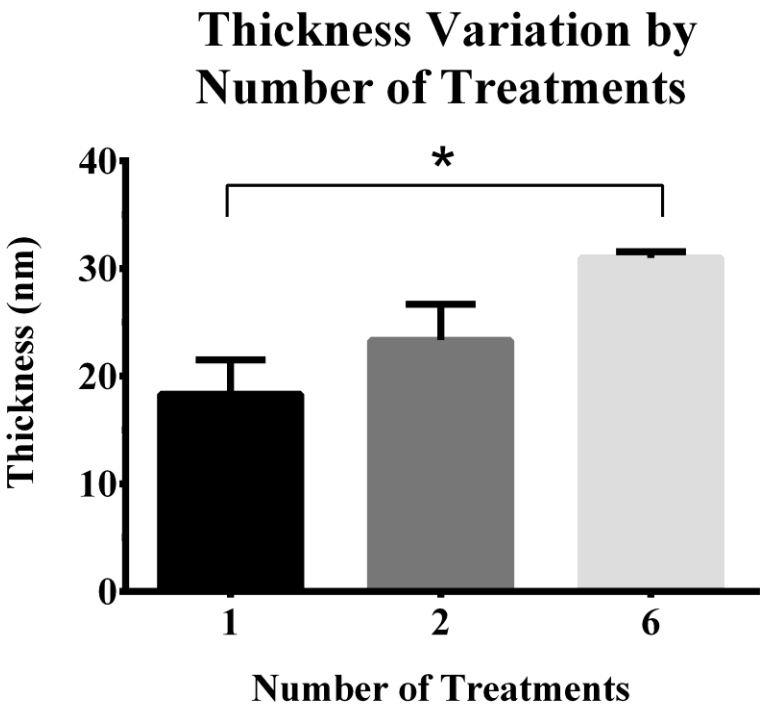

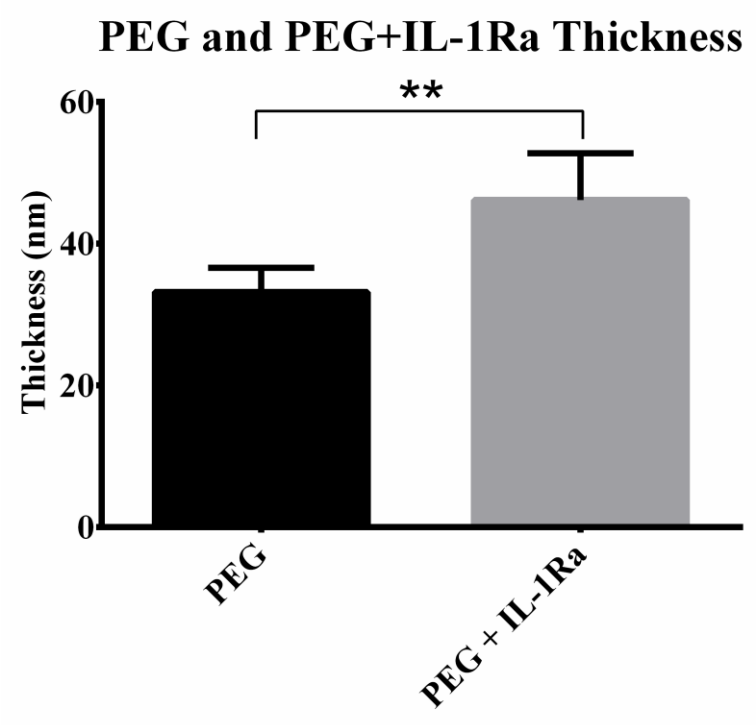

Figure 4.2: PEG coating thickness analyses. (a) Thickness of the coating increases with increasing number of treatments applied to the surface. (b) Incorporating IL-1Ra yields a thicker coating than with the PEG alone. * = $p<0.05$, ** = $p<0.01$.

In Vitro Cell Adhesion

Silicon wafer samples were coated with one, two, or six treatments of PEG hydrogel using GDQ as the crosslinking peptide. Uncoated and PEG-coated surfaces were seeded with mixed glial cells (astrocytes + microglia) to evaluate cell adhesion to the coating. Cells were stained with Live/Dead stain with >90% live cells on the surfaces. Analysis of these results indicated that the PEG hydrogel reduces cell attachment and spreading compared to uncoated controls (Figure 4.3a). The PEG coated samples had significantly reduced cell adhesion and cell spreading when analyzed by total number of attached cells (Figure 4.3b), total area per attached cell (Figure 4.3c), and total area covered by attached cells (Figure 4.3d). The results indicated that the 6-treatment coating yielded the best reduction of cell adhesion and cell spreading. Additionally, the 2-treatment coating provided sufficient non-fouling behavior so that a 2-treatment non-degradable PEG coating can be used as a "base" coating for the additional 4-treatment PEG + IL-1Ra coating to yield a total of 6 treatments.

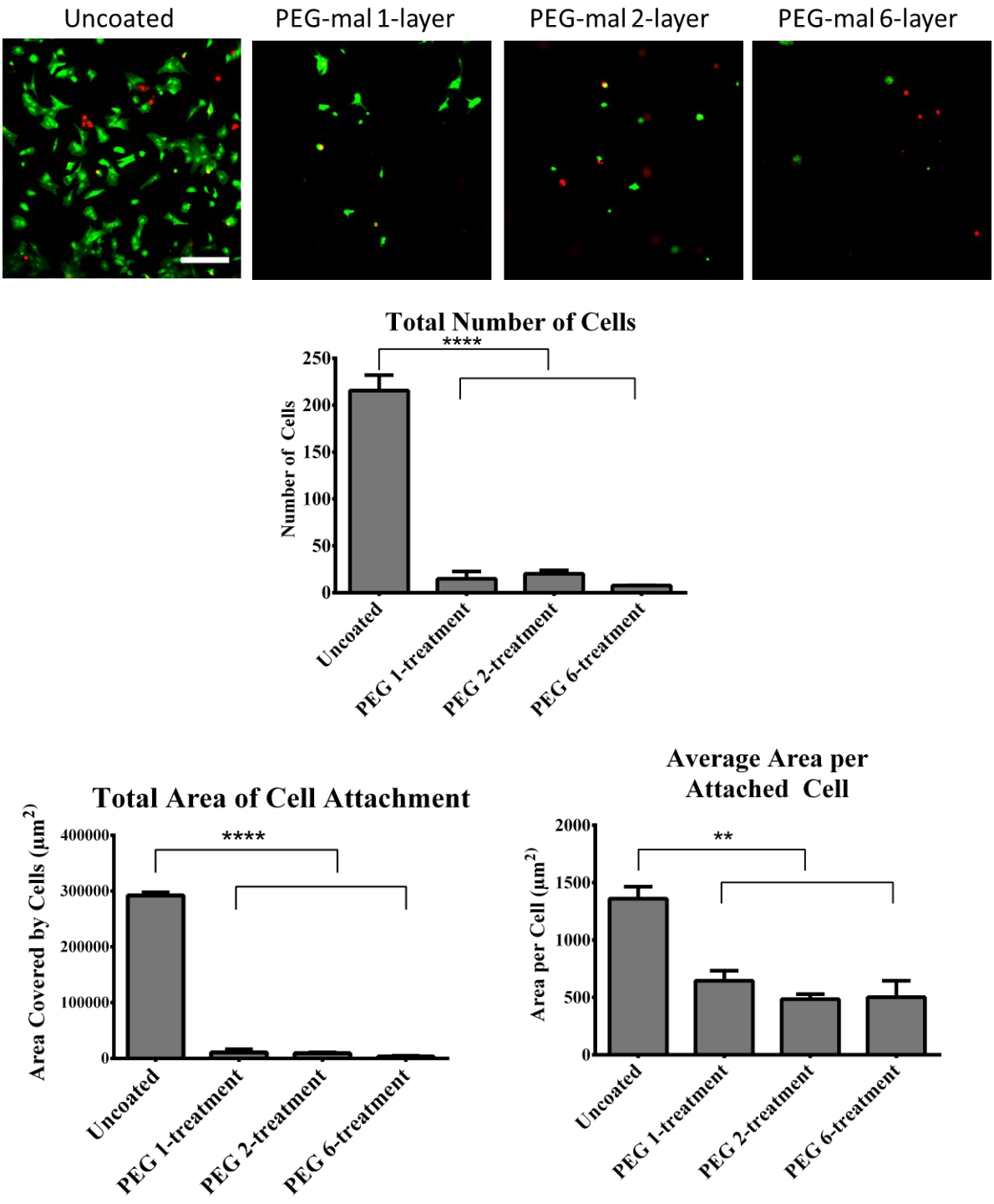

Figure 4.3: Cell adhesion on varying PEG layers. (a) Live/Dead stain of cell adhesion on uncoated and PEG coated surfaces with 1, 2, or 6 treatment cycles. Scale bar = 250 μm. (b) Total number of cells adhered, (c) area per attached cell, and (d) total area covered by adhered cells on the surface is significantly lower on PEG coated surfaces than uncoated surfaces. ** = $p<0.01$, **** = $p<0.0001$.

In Vitro Inflammatory Cytokine Release

Untreated and coated surfaces were tested to evaluate the release of cytokines, specifically IL-1β (Figure 4.4a) and TNF-α (Figure 4.4b), from mixed glial cells in response to stimulation with GM-CSF for 48 hours. These results indicated that levels of IL-1β were significantly higher on uncoated surfaces than those coated with PEG or PEG + IL-1Ra (detection limit = 5 pg/ml). TNF-α levels on the uncoated surface were significantly higher while levels for the coated surfaces were below the detection limit (detection limit = 5 pg/ml). These results indicate that the PEG and PEG + IL-1Ra coatings reduce the release of inflammatory cytokines compared to uncoated surfaces.

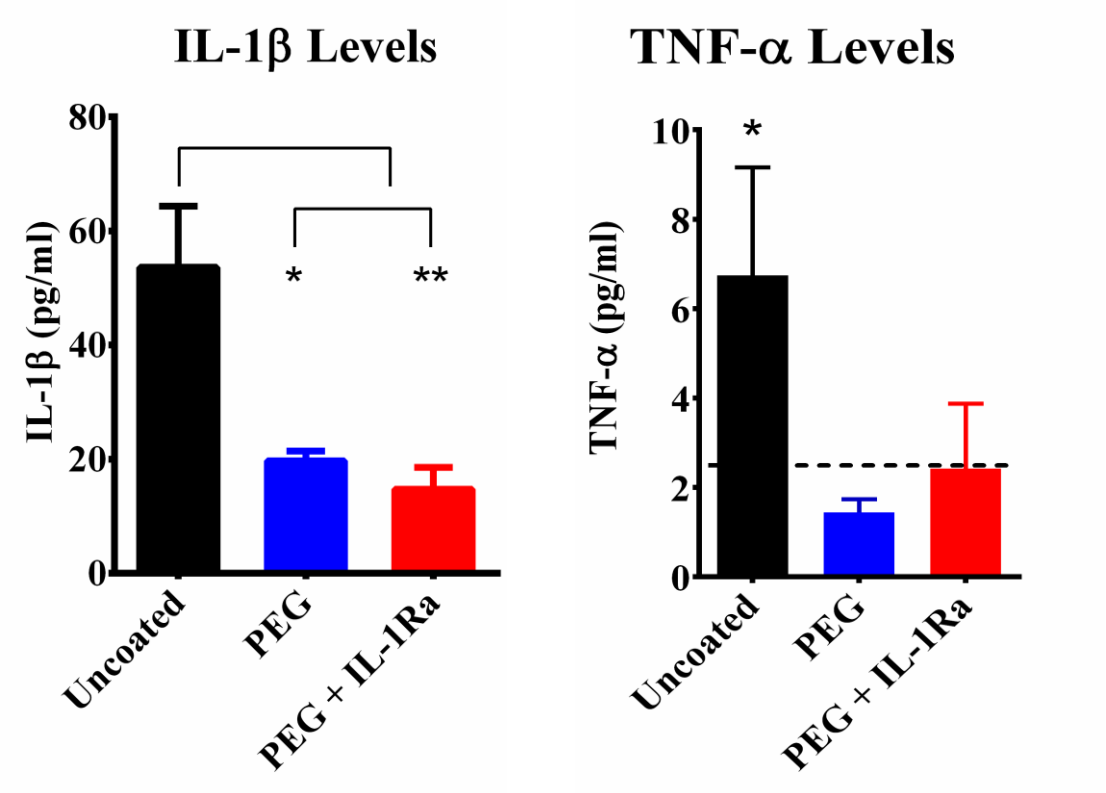

Figure 4.4: Cytokine release on uncoated, PEG, and PEG+ IL-1Ra coated surfaces in response to GM-CSF stimulation. (a) IL-1β was significantly higher on uncoated surfaces. (b) TNF-α was significantly higher on the uncoated surface, and levels on coated surfaces were below detection limits. * = $p<0.05$, ** = $p<0.01$.

IL-1Ra Release

In order to assess the stimulus-responsive release of IL-1Ra, we examined the release of IL-1Ra over time using an ELISA (Figure 4.5). Samples were placed in conditioned media from cells stimulated with LPS (to release proteases) or naïve media. The release curve showed that samples incubated with the LPS-stimulated cell culture media had an increasing release over time following a simple hyperbolic curve. Samples incubated in naive media had a basal level of release, probably due to gel swelling.

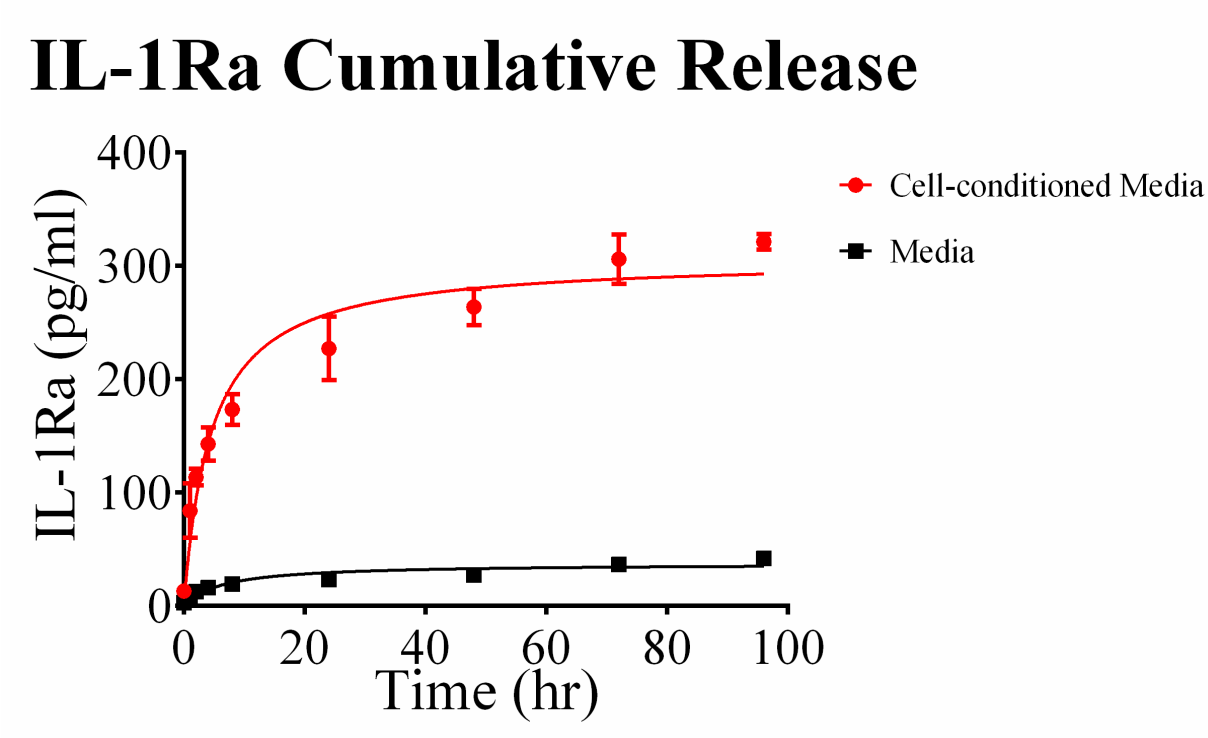

Figure 4.5: IL-1Ra release curve shows that IL-1Ra release is higher with LPS-stimulated cell media compared to media alone.

Inflammatory Marker Expression *In Vivo*

Histological sections for each experimental condition (n = 8 per group) were analyzed using the markers described in Table 4.1 and intensity profiles were analyzed using the curve fit approached described in Aim 1. A pilot study demonstrated no gross differences in inflammatory markers along the mid-shaft of the electrode, so all analyses were performed using sections at approximately 500 μm from the cortex surface. It is also important to note that there is considerable animal-to-animal variability in these experiments, an issue which must be considered when analyzing the data for implanted electrodes.

Resident microglia were stained with OX42/CD11b (Figure 4.6). There were no significant differences among groups for $Intensity_1$, $Intensity_2$, and $Decay_{slow}$. However, the $Decay_{fast}$ parameter was significantly higher for PEG + IL-1Ra compared to PEG coatings, indicating that the intensity of resident microglial staining near the implant interface (0-100 μm) decays at a faster rate for PEG+IL-1Ra samples compared to other conditions. This is an important finding because it indicates that presence of resident microglial cells decreases at a faster rate close to the electrode surface for the PEG + IL-1Ra group.

Activated microglia were stained with ED1/CD68 (Figure 4.7) and astrocytes were stained with GFAP for glial fibrillary acidic protein (Figure 4.8). These stains showed no significant differences among groups for any parameters. This result indicates that neither the PEG coating nor the coating releasing IL-1Ra altered the distribution of these cell types in the vicinity of the implanted electrode.

Chondroitin sulfate antibody (CS56) was used to stain for glycosaminoglycans (GAG, Figure 4.9), which are a major extracellular matrix component of the astroglial scar. The $Decay_{slow}$ parameter was significantly lower for the PEG + IL-1Ra group compared to uncoated samples indicating that the amount of GAG staining decreases at a slow rate at distances far from the electrode surface (>100 μm).

Rat IgG was used as a marker for blood-brain barrier (BBB) breach (Figure 4.10), as this molecule permeates into brain tissue from comprised vasculature. The $Intensity_1$ parameter was significantly lower for PEG + IL-1Ra compared to uncoated surfaces, while the $Intensity_2$ parameter significantly lower for PEG + IL-1Ra compared to PEG alone. These differences indicate that the amount of IgG staining is lower around PEG + IL-1Ra coated electrodes, indicating a lower level of BBB breach. There were no differences between the decay parameters.

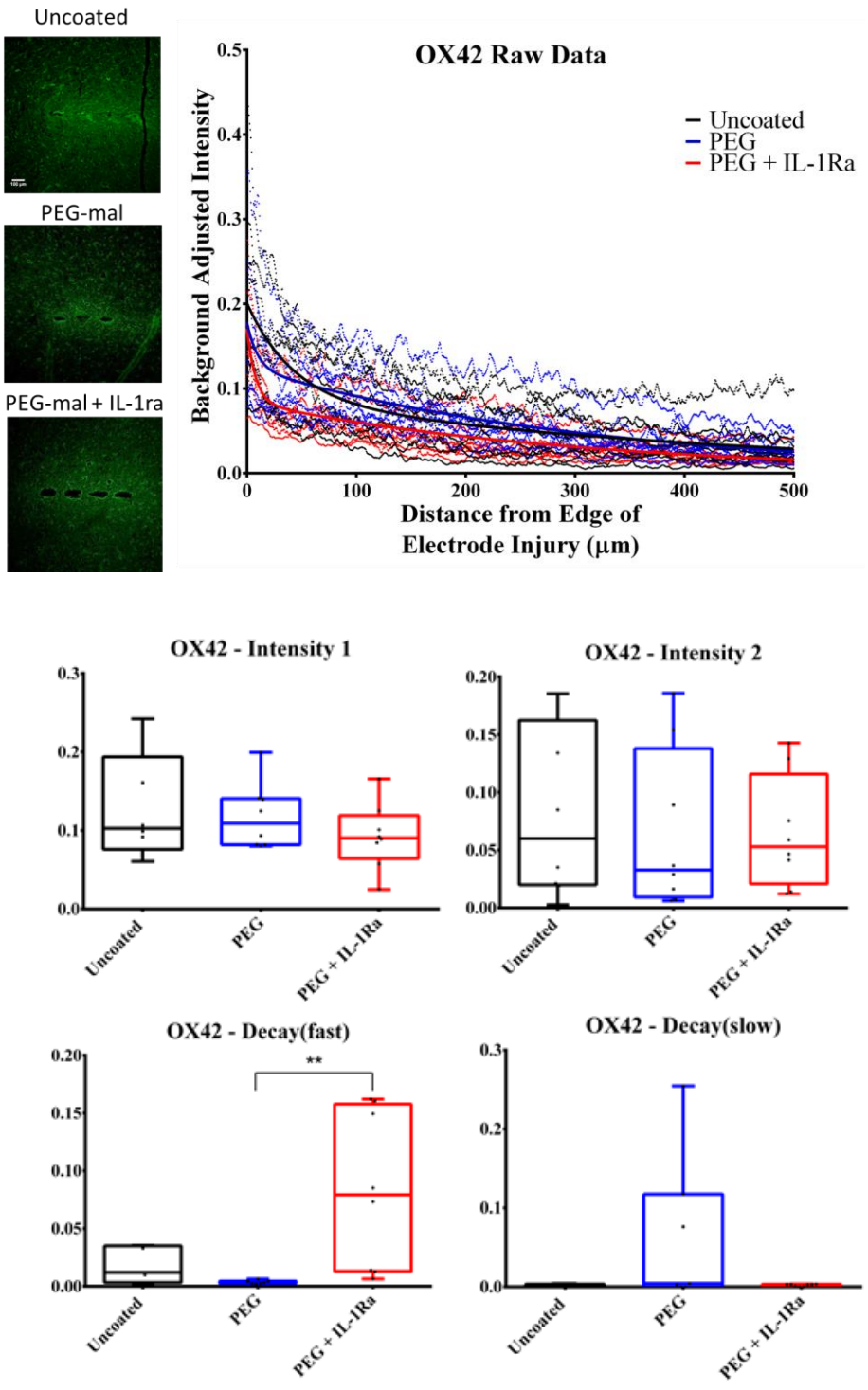

Figure 4.6: Immunofluorescence analysis of resident microglia (OX42). (a) Immunofluorescence images (left) and corresponding intensity scale (right) for uncoated, PEG, and PEG + IL-1Ra (n=8 per group). (b) Parameter plots indicate differences in each parameter of Equation 1 for each experimental group. The initial decay parameter is significantly higher for PEG + IL-1Ra compared to PEG alone. ** = $p<0.01$.

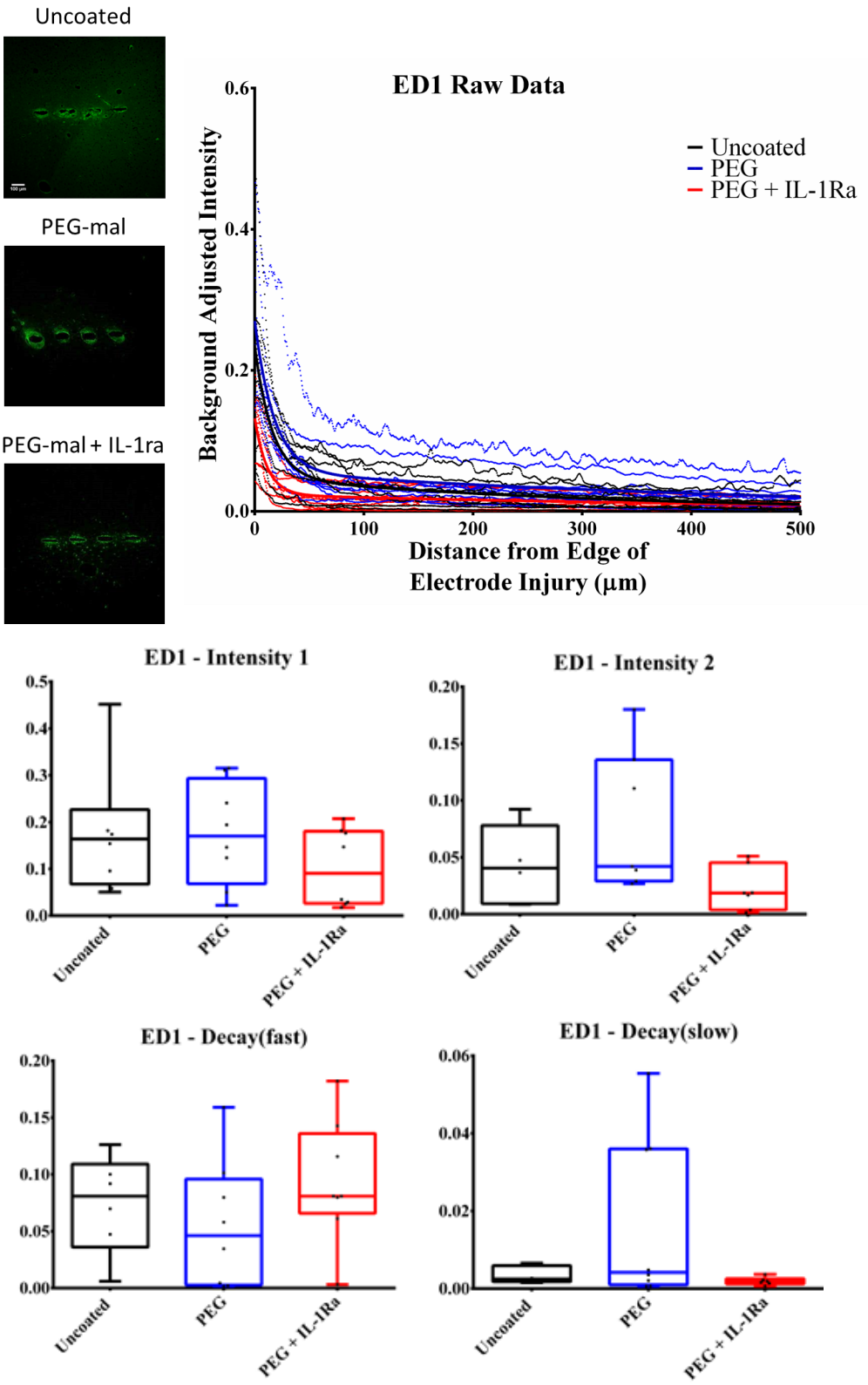

Figure 4.7: Immunofluorescence analysis of activated microglia (ED1). (a) Immunofluorescence images (left) and corresponding intensity scale (right) for uncoated, PEG, and PEG + IL-1Ra (n=8 per group). (b) Parameter plots indicate differences in each parameter of Equation 1 for each experimental group.

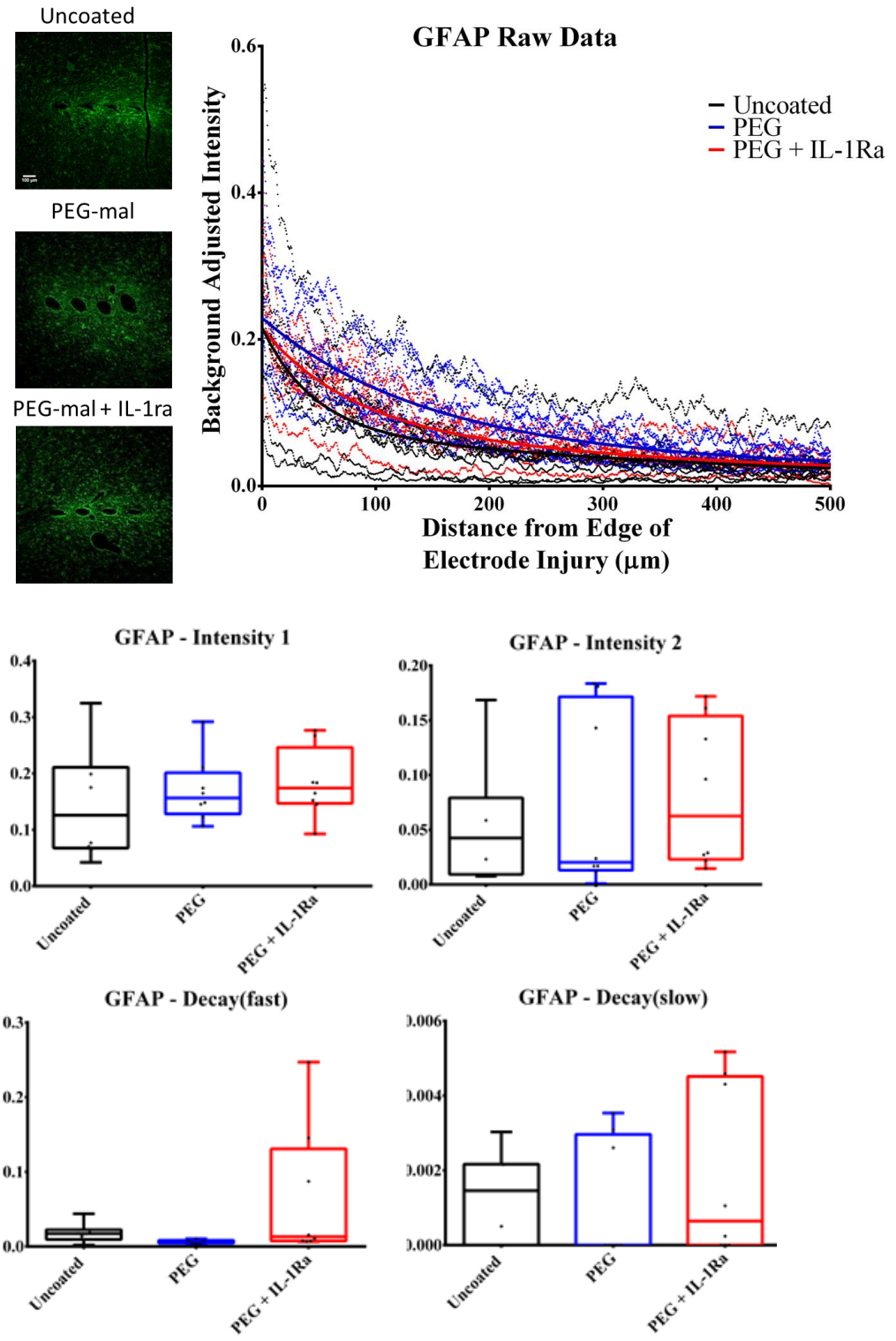

Figure 4.8: Immunofluorescence analysis of glial fibrillary acidic protein (GFAP) for astrocytes. (a) Immunofluorescence images (left) and corresponding intensity scale (right) for uncoated, PEG, and PEG + IL-1Ra (n=8 per group). (b) Parameter plots indicate differences in each parameter of Equation 1 for each experimental group.

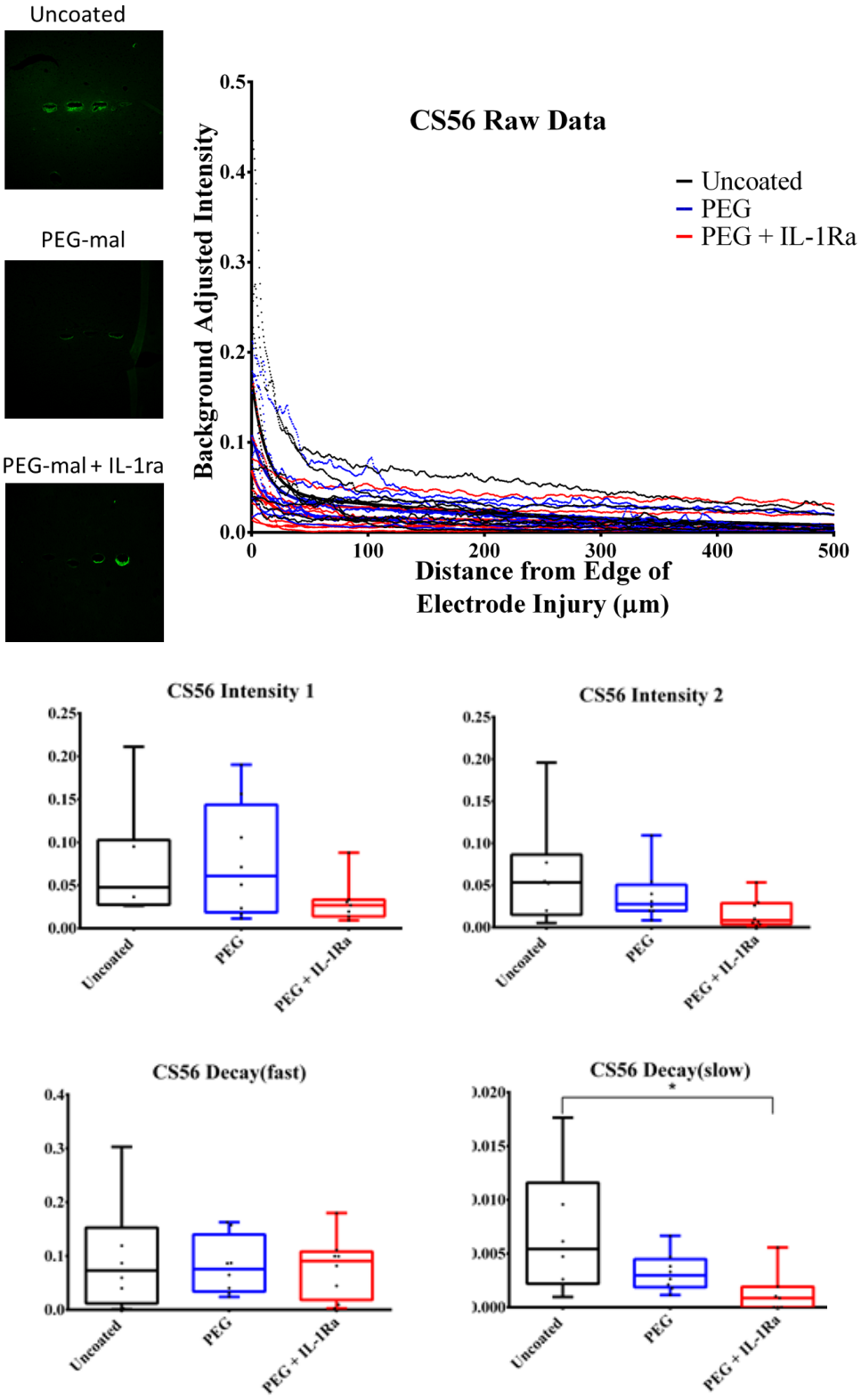

Figure 4.9: Immunofluorescence analysis of chondroitin sulfate (CS56) to observe glycosaminoglycans at the injury site. The $Decay_{slow}$ parameter was significantly lower for PEG + IL-1ra compared to uncoated samples. Other parameters were not significantly different. * = $p < 0.05$.

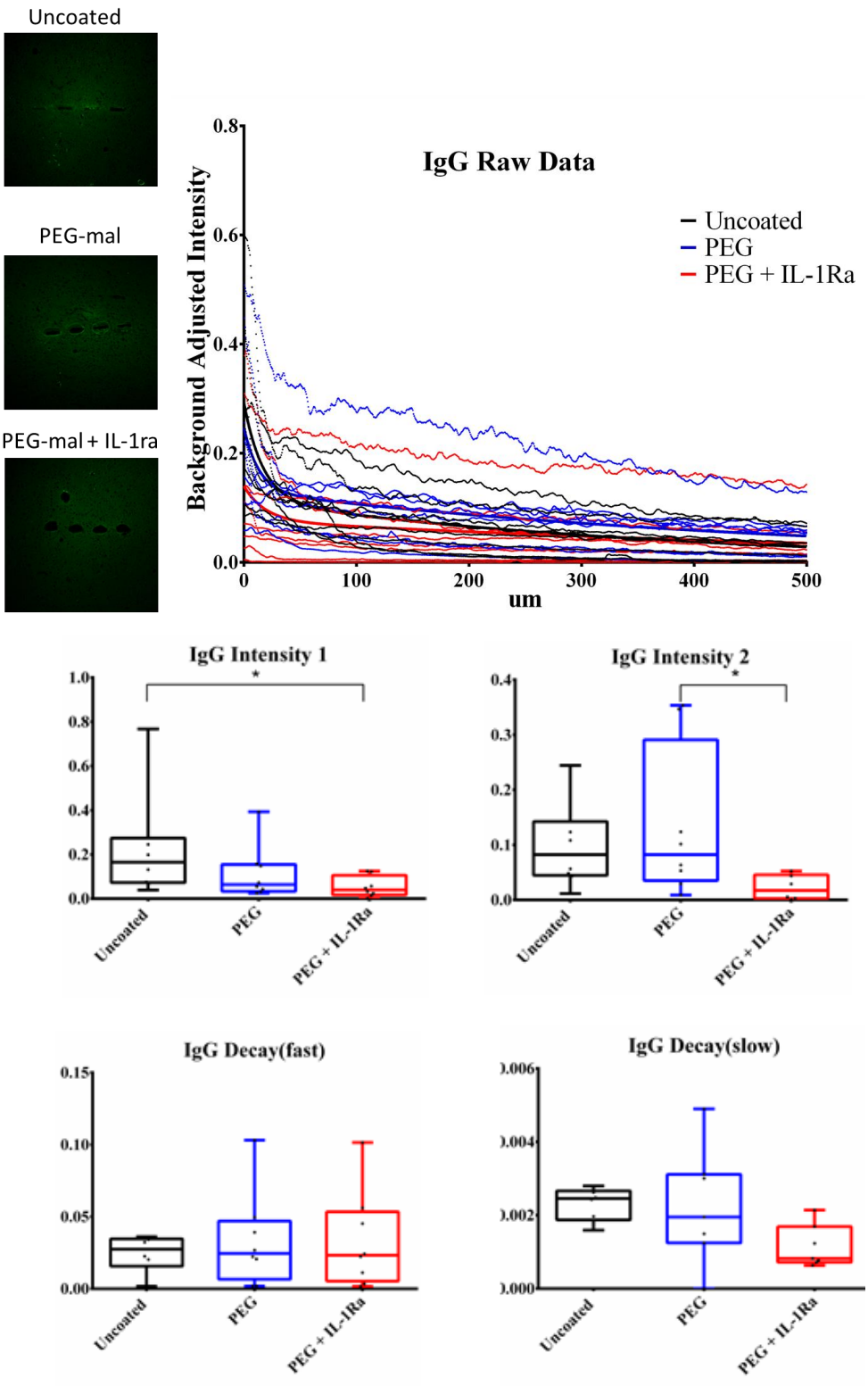

Figure 4.10: Immunofluorescence analysis of rat IgG for blood brain barrier breach. For both stains, the $Decay_{slow}$ parameter was significantly lower for PEG + IL-1ra compared to uncoated samples. $Intensity_2$ was also significantly lower for PEG + IL-1Ra compared to uncoated electrodes. Other parameters were not significantly different. * = $p < 0.05$.

Neuronal Survival

To analyze neuronal survival, the number cells positive for NeuN (neuronal nuclei) were counted per specified 50- or 100- μm bin at a distance of 0 – 500 μm from the implant insertion site (Figure 4.11). Neuronal survival increased for both PEG and PEG + IL-1Ra coated electrodes compared to uncoated controls. For the 0-50 μm bin, the number of NeuN+ cells in the PEG + IL-1Ra group was not significantly different from the uninjured contralateral control. In the 50-100 μm bin, both PEG and PEG + IL-1Ra were not significantly different from the uninjured control. At distances 100+ μm from the interface, all three groups were not significantly different from the uninjured control. This data indicates increased neuronal survival around the electrode within the first 100 μm from the implant interface for the coated electrodes. This location is most critical for maintaining electrode functionality because the neurons closest to the electrode will provide the electrical signals that will be received by the electrode.

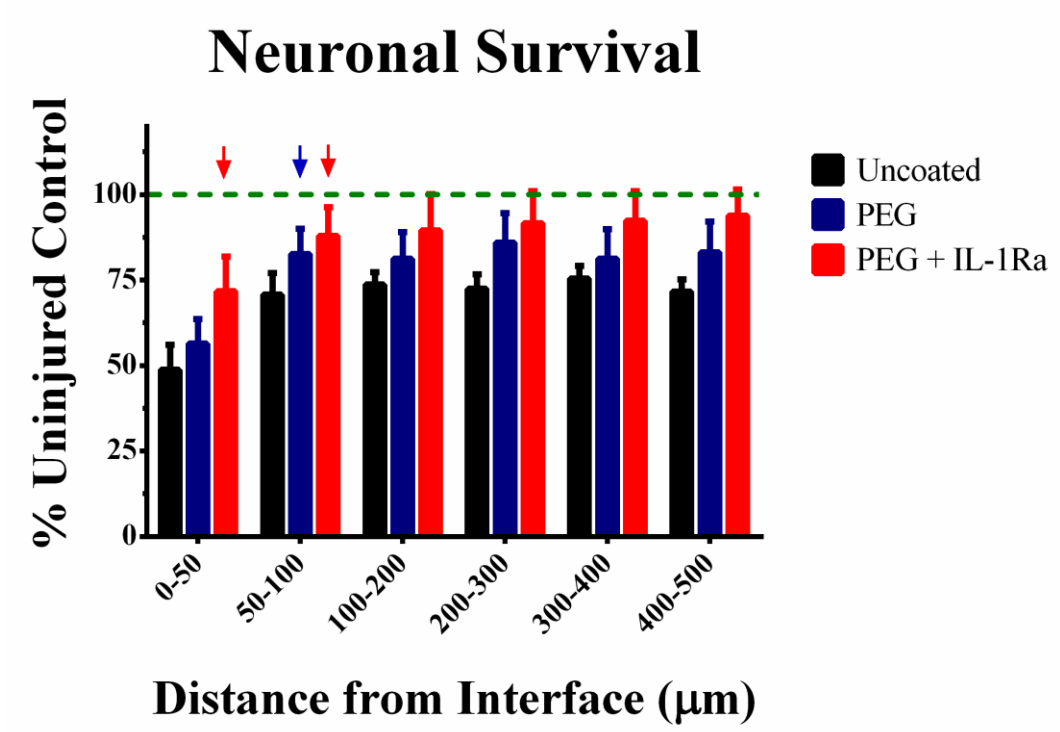

Figure 4.11: Neuronal survival around the electrode. Uninjured control is indicated by the green dotted line. PEG + IL-1Ra was not significantly different from the uninjured control for any distance analyzed as indicated by the red arrows. At 50 – 100 μm from the tissue/implant interface, PEG and PEG + IL-1Ra groups were not significantly different from the uninjured control as indicated by the blue and red arrows, respectively. All groups were not significantly different from the uninjured control at distances greater than 100 μm from the implant.

Quantitative RT-PCR Analysis

Quantitative RT-PCR was used to compare gene expression from brains (n = 7 per group) implanted with uncoated, PEG, or PEG + IL-1Ra electrodes, as well as the contralateral uninjured control. Gene expression analysis was conducted for the following gene targets: IL-1α, IL-1β, IL-1Ra, IL-6, IL-10, TNF-α, IFN-γ, MCP-1, MMP-2, MMP-3, MMP-9, MMP-13, NGF, GFAP, BDNF, and CNTF. The heat map generated by the Fluidigm software is seen in Figure 4.12. The fold change differences between the genes can be seen in Figure 4.13, with the genes showing significant differences between groups outlined in green.

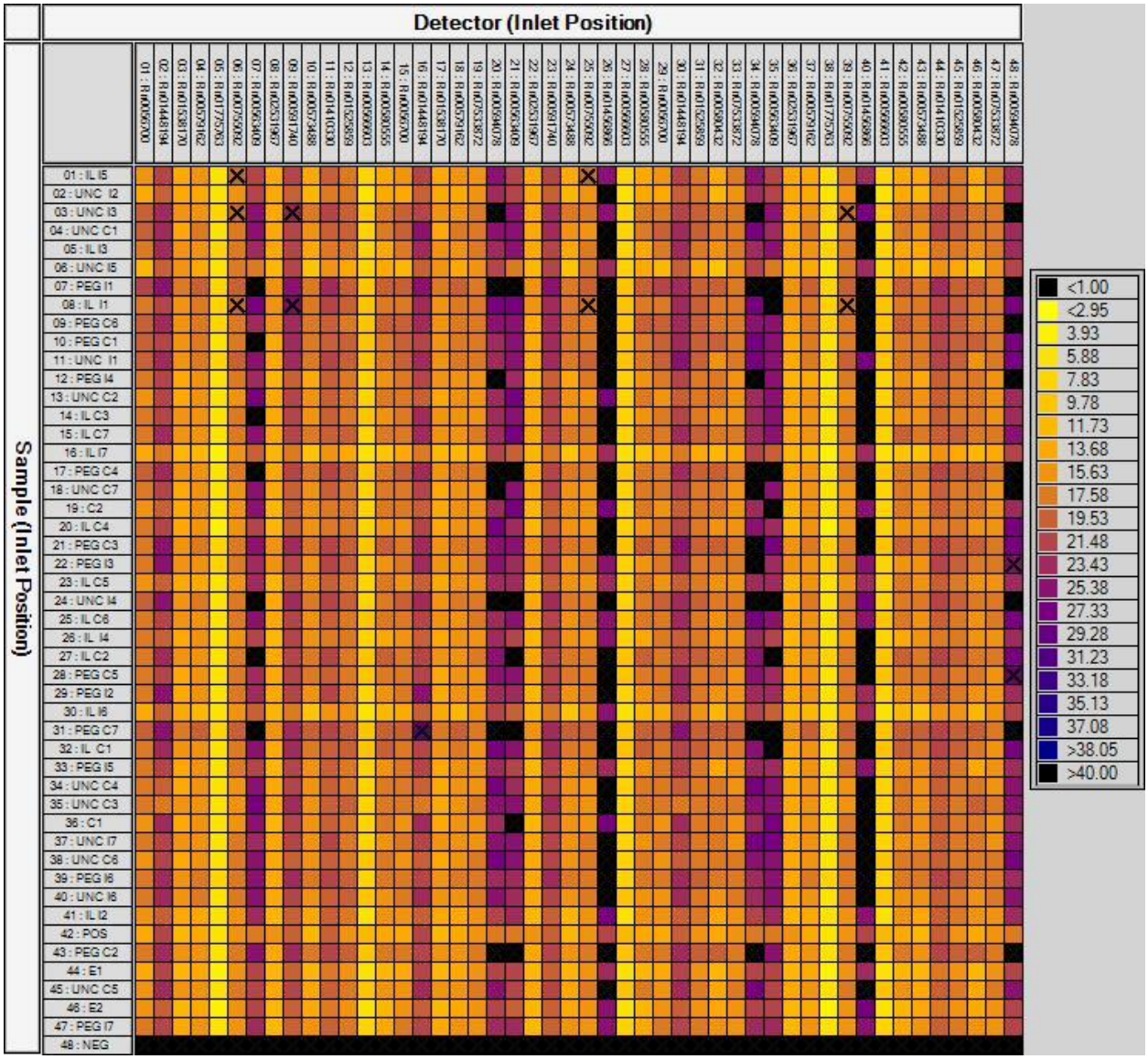

Figure 4.12: Heat map of the Ct values generated by the Fluidigm BioMark system.

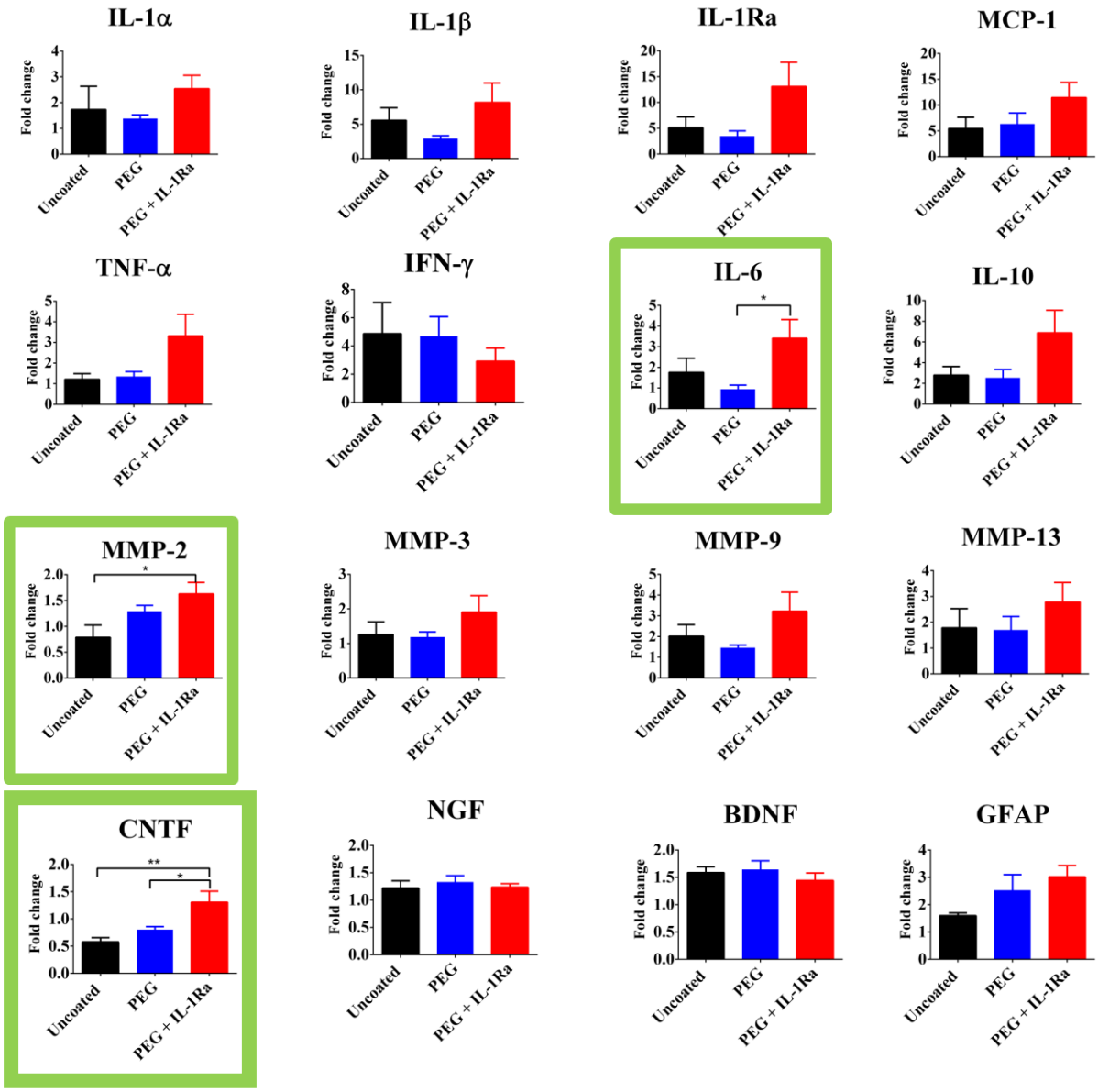

Figure 4.13: Fold change values for the 16 gene targets analyzed with qRT-PCR. Genes with significant differences are outlined in green. * = $p<0.05$, ** = $p < 0.01$.

Discussion

We have engineered a polymer coating for neural electrodes that consists of a non-fouling coating made of poly(ethylene glycol) that contains a protease-degradable crosslinker and an anti-inflammatory agent, IL-1Ra, that is released on-demand in response to proteases associated with the inflammatory response. The conclusions from Aim 1 showed that a non-fouling coating alone does not yield significant improvement to the tissue and inflammatory response to implanted neural electrodes [124]. This result indicated a need to incorporate an anti-inflammatory agent into the coating in an attempt to reduce the inflammatory response to implanted neural electrodes.

In the present study, we coated the surface of the electrodes with a multi-layer PEG-maleimide coating. The coating was characterized using XPS and wet-cell ellipsometry to verify presence of the coating on the surface as well as increasing coating thickness corresponding with increasing treatment deposition, respectively. We characterized resistance to cell-adhesion by coating silicon wafer samples and plating them with mixed glial cells for 24 hours. This *in vitro* analysis indicated that PEG coated surfaces with one, two, or six treatments were resistant to cell adhesion. The total number of attached cells, average area per attached cell, and total cell attached area on each sample were all significantly lower on coated samples compared to uncoated samples. Additional *in vitro* characterization was completed to observe differences in cytokine release from mixed glial cells plated on the uncoated, PEG, and PEG + IL-1Ra surfaces. After plating the cells and stimulating the cells with GM-CSF for 48 hours, the cytokine levels were analyzed using ELISA. Cells plated on uncoated surfaces released significantly more IL-1β and TNF-α than PEG or PEG + IL-1Ra coated surfaces. These

data indicate that the PEG-coated surfaces reduce inflammatory cytokine release from mixed glial cells. This result is likely due to the fact that the coated surfaces have less cell adhesion than uncoated surfaces, thereby containing fewer cells to release cytokine in response to the GM-CSF stimulus. This result is consistent with previous work with non-fouling/cell adhesion-resistant coatings [57]. We also characterized the release of IL-1Ra from coated samples using ELISA. PEG + IL-1Ra samples were plated with media from LPS-stimulated mixed glial cells or PBS. Stimulation of mixed glial cells with LPS stimulates release of cytokines and proteases which cause cleavage of the protease-degradable crosslinking peptides in the PEG hydrogel, releasing IL-1Ra. The coatings incubated in conditioned media from LPS-treated cultures released significantly more IL-1Ra over time than the samples incubated in PBS, indicating the protease-dependent release of IL-1Ra from the degradable coating. Incubating samples in naïve media (not exposed to cells) showed similar release results compared to PBS. Collectively, the *in vitro* results indicated a promising cell adhesion-resistant and anti-inflammatory coating to be used for *in vivo* analysis.

For the *in vivo* portion of this study, uncoated, PEG, and PEG+IL-1Ra coated electrodes were implanted in the brain of rats for 4 weeks to evaluate the *in vivo* response of the brain to implanted electrodes. Samples were collected, cryosectioned, and stained for markers to indicate cell response to the implanted electrode as well as blood brain barrier breach. The samples for OX42, ED1, GFAP, CS56, and IgG were analyzed using similar methods to Aim 1 where the intensity curve for each sample was fit with a curve using Equation 1. Samples stained with OX42 / CD11b for resident microglia had no differences in $Intensity_1$, $Intensity_2$, and $Decay_{slow}$ parameters between the groups.

However, the $Decay_{fast}$ parameter was significantly higher for PEG + IL-1Ra compared to PEG coatings, indicating that the intensity of resident microglial staining near the implant interface (0-100 μm) decays at a faster rate for PEG+IL-1Ra samples. This difference in the OX42 $Decay_{fast}$ parameter indicates that the IL-1Ra has an effect on microglial recruitment to the electrode / tissue interface. While the initial intensity does not vary, the reduction in microglial staining at 0 – 100 μm from the implant shows an improvement in the cell response and microglial recruitment to the area around the electrode.

Data for ED1/CD11b and GFAP staining, indicating activated microglia and astrocytes, respectively, showed no significant differences for any of the parameters among the groups. We hypothesized that the anti-inflammatory factor incorporated into the PEG-coating would reduce the inflammatory response in the surrounding tissue. However, persistence of activated microglia around the implant for all experimental groups indicates that the IL-1Ra does not prevent microglial activation. Since microglial activation is an important part of the inflammatory cascade, it is apparent that inflammation persists in the tissue. Additionally, we hypothesized that the non-fouling PEG surface would reduce astrocyte recruitment and subsequent scar formation; however, this did not occur in the rat model. This is an important finding because it indicates a need for better *in vitro* evaluation techniques. The 2D cell culture system is a good starting point, but further evaluation with more complex *in vitro* systems is necessary to determine if a particular coating can perform well *in vivo.*

CS56 staining for chondroitin sulfate indicates the presence of glycosaminoglycans, and IgG shows areas of blood brain barrier breach around the injury site. The $Decay_{slow}$ parameter was significantly higher for uncoated samples compared to

PEG+IL-1Ra for CS56, indicating a faster decrease of CS56 staining at areas >100μm from the injury site. The lack of differences among the groups for CS56 staining is consistent with results from other studies [64]. For the IgG stain, the lower $Intenisty_1$ and $Intensity_2$ parameters for PEG + IL-1Ra compared to uncoated and PEG coated electrodes, respectively, indicates that the amount of BBB breach around the PEG + IL-1Ra coated electrodes is significantly reduced compared to the uncoated and PEG electrodes. This is an important finding because literature indicates that the persistence of the electrode in the tissue and the subsequent continued BBB breach is correlated with persistence of inflammation in the brain [18], and reducing the effect of BBB breach may reduce inflammatory responses in the long term. At this point, it is not known if the reduction in IgG staining / BBB breach is due to a reduction of the initial inflammatory response, faster healing response over time, or a combination of the two in the presence of the IL-1Ra, but this would be an interesting aspect to explore in future studies. Notably, Bellamkonda and colleagues recently demonstrated that reduced BBB breach correlates with improved electrode recording function [18]. Whether the PEG coatings and IL-1Ra release improve electrode function will need to be examined in future studies.

Finally, NeuN staining for neuronal nuclei showed differences in neuronal survival among the three groups. We observed increased neuronal survival for the PEG + IL-1Ra group at 0 - 50 μm as well as increased survival for PEG and PEG+IL-1Ra at 50 - 100 μm. The neuronal survival for all groups was not significantly different from the uninjured control at distances greater than 100 μm from the electrode surface. This is an important finding because neurons are necessary for electrode functionality. If the neurons surrounding the implant do not survive after electrode insertion, then the

electrode cannot receive any electrical signals from the surrounding tissue, rendering the device useless. Increasing neuronal survival is essential to maintaining long-term electrode function. The ideal response of the brain would result in no neuronal death upon implantation of a neural electrode. However, improvement within the first 100 μm is a promising finding as electrodes can record neuronal activity to a radius of ~100 microns or more from the electrode surface [125].

Analysis of gene expression in the brain around the electrode implantation site yielded important insights into the tissue responses to implanted electrodes. Of the 16 genes that were analyzed, only three had significant differences among groups. For IL-6, the fold change gene expression was significantly higher in the PEG + IL-1Ra group compared to the PEG group. While IL-6 is traditionally identified as a pro-inflammatory cytokine [79], there is evidence to suggest that it plays a role in activation of downstream cell-survival and anti-apoptotic factors [78]. The up-regulation of MMP-2 in the PEG + IL-1Ra group compared to the uncoated group is an interesting finding. MMP-2 is found in activated astrocytes [126], which is consistent with the presence of recruited astrocytes around the implanted electrode. It is unknown why the MMP-2 levels are up-regulated in the PEG + IL-1Ra group but not in the PEG or uncoated, considering the inflammatory markers for astrocytes and activated microglia showed no differences between the groups. The increase in MMP-2 in the PEG + IL-1Ra group is also contradictory to some extent, as MMP-2 is implicated in promoting BBB breach [126], but the IgG staining intensity was significantly lower for PEG + IL-1Ra samples. It is possible that the release of MMP-2 is occurring as part of a redundant system in response to down-regulation of a different inflammatory cytokine, as there are many redundant signaling pathways in the

cell biology. Alternatively, MMP-2 up-regulation may reflect the activation of tissue repair mechanisms. Regardless, the presence of MMP in the injury site validates the use of this protease-degradable coating as the MMPs will cause desired degradation of the coating and release of the anti-inflammatory therapeutic.

Gene expression of neural-specific markers showed significantly higher expression of cilliary neurotrophic factor (CNTF) in PEG + IL-1Ra group compared to PEG and uncoated groups. CNTF is important for neuronal survival and neurite outgrowth [127]. Interestingly, research has shown that IL-1β is required for the production of CNTF [128], indicating that inflammatory cytokines can play a role in both pro-inflammatory activation as well as anti-inflammatory cytokine activation downstream. The lack of differences in NGF and BDNF were surprising given the increased neuronal survival found in the PEG + IL-1Ra group, however this may also indicate that other factors such as CNTF or others not investigated here may play a more significant role in neuronal survival. Overall, the results from the gene expression studies are generally consistent with the findings from the immunofluorescence analysis, showing persistence of inflammation and increased expression of a neuronal survival gene. These results indicate possible targets for future research into inflammation and neuronal survival in the brain.

The findings from this study lead to several important conclusions about neural electrode research. First, the coating presented here had promising *in vitro* results with regards to reduced cell adhesion and reduced cytokine release on PEG-coated samples. However, these results did not translate well with regards to inflammatory cell recruitment *in vivo*. Astrocyte and activated microglial recruitment did not vary between

groups and the resident microglial recruitment analysis showed only slight improvement for PEG+IL-1Ra over the PEG coating alone or uncoated electrodes. Also, the CS56 staining showed no improvement with the PEG coatings compared to uncoated samples. IgG staining, a surrogate for BBB breach, showed reduced BBB breach around PEG + IL-1Ra electrodes at all distances analyzed (0-500 μm). The gene expression analysis yielded interesting results that were consistent with the overall findings from the immunofluorescence analysis, and also provide information that may lead to a better understanding of targets for future therapies. Additionally, this study also showed promising results with regards to improving neuronal survival on coated surfaces which is an important finding for improving long-term electrode functionality.

It is important to note the lack of translation between *in vitro* and *in vivo* success. The *in vitro* screening used here is similar to other studies [57, 69, 119, 129] using 2D cell culture methods to demonstrate the non-fouling characteristics of the coating. However, the lack of translation between *in vitro* and *in vivo* success indicates the need for a better screening system prior to implantation. The 2D *in vitro* system does not emulate the complex systems that exist in the brain. While 3D culture systems do exist [130-133], there is still a lack of vasculature and the associated problems that arise with blood-brain barrier breach as well as limited inflammatory stimuli due to the lack of BBB breach and surrounding full tissue injury. The data from this study indicates a need to develop better *in vitro* validation methods that better emulate the complex tissue response for future studies.

Additionally, it is important to consider the options for analyzing the tissue response to implanted neural electrodes. The use of immunostaining markers to stain

tissue sections and then evaluation at variations of staining intensity is a very coarse measurement of the tissue response. While it is important to understand the cell response around the electrode, there must also be other methods used to gain a complete picture of the tissue response. Finally, this work indicates the need for a multi-component coating. The PEG+IL-1Ra had better results overall than PEG alone, with both coatings performing better than the uncoated electrodes with respect to neuronal survival. The tissue response to implanted electrodes is a complicated problem that will likely need a complex solution including non-fouling coatings in addition to bioactive molecules including anti-inflammatory agents as well as others to support neuronal survival to yield the best response. Overall, it is important to consider the multi-faceted problems that exist with implanting neural electrodes in the brain when trying to develop a suitable solution.

Acknowledgements

This work was supported by National Institutes of Health Grants: F31NS073358 (SMG) and T32EB006343-01A2 (RVB); GAANN Fellowship for Drug Design, Development, and Delivery: US Department of Education P200A090099; Georgia Tech/Emory Center for the Engineering of Living Tissues and the Atlanta Clinical and Translational Science Institute under PHS Grant UL RR025008 from the Clinical and Translational Science Award Program. XPS analysis was performed by the National ESCA and Surface Analysis Center for Biomedical Problems (NESAC/BIO): NIH EB-002027. Wet-cell ellipsometry measurements were performed by Dr. Peter Latour and Dr. Yang Wei from Clemson University. We would also like to thank Dr. Michelle LaPlaca and JT Shoemaker for supplying primary mixed glial cells.

CHAPTER 5

SUMMARY OF CONCLUSIONS

There are several important conclusions that can be drawn from this work to add to the knowledge in the field. First, the thermo-responsive microgel coating performed well *in vitro* with reduced cell adhesion on the surface of coated electrodes compared to uncoated controls. Although the *in vitro* results were promising, the long-term tissue response to microgel coated electrodes implanted in the brain indicated a lack of effective reduction in inflammation *in vivo*. Based on these results, we hypothesized that future studies would need to incorporate a bioactive factor.

Using the information we learned from the microgel study, we decided to move forward with the PEG-maleimide coating with protease-degradable crosslinker to release an incorporated IL-1Ra anti-inflammatory agent. This coating also performed well *in vitro* with studies to analyze cell attachment, inflammatory cytokine release, and IL-1Ra release from coated samples. Subsequent *in vivo* studies indicated only minor improvement in one parameter of the inflammatory cytokine markers. However, IgG staining, a surrogate for BBB breach, was reduced for PEG + IL-1Ra coatings compared to uncoated electrodes, suggesting that this anti-inflammatory agent improves some inflammatory outcomes. Consistent with this observation, neuronal survival was significant and maintained in response to coated electrodes, with the best improvement observed for the PEG + IL-1Ra group. This is an important finding because neuronal survival is essential to long-term functionality of the electrode since the neuronal electrical signals are the signals that need to be received at the electrode surface.

Additionally, results from the gene expression analysis study indicate potential targets for future therapies which may be useful in producing better modifications to improve the tissue response to implanted electrodes.

One important aspect of this research that must be considered moving forward is the concept of biological significance vs. statistical significance. While a statistically significant result may pass a mathematical evaluation of differences from a control or untreated sample, it is important to analyze these results in the context of what will actually be useful to patients. Will a statistically significant change of $p<0.05$ provide enough modification to improve an implanted device in a patient? The only way to determine such statistical vs. biological significance is with live, functional testing to see if modified devices do indeed work longer and better than their unmodified counterparts. It is also important to consider how the intervention itself will affect the recording functionality. In the case of this coating, there is only a finite amount of IL-1Ra available on the device. Once the coating is degraded and all IL-1Ra has been released, the system may require further intervention in order to maintain the improved tissue response. There are options such as implantable pumps and systemic drug dosing, but these interventions will run into issues of increased clinical visits, systemic side effects from drugs, and problems with patient compliance. The ideal coating or modification would make the implant "invisible" to the body, such that it could exist in the tissue without provoking an immune response. Until we find that "magic bullet," however, it is important to continue to research promising options.

An additional important finding from this research is the necessity for better *in vitro* methods of analysis. The microgel-coated and PEG-coated surfaces performed well

in cell adhesion tests showing less cell adhesion on coated surfaces, indicating the non-fouling nature of the coatings. Additionally, the cytokine analysis of the PEG surfaces further indicated the effectiveness of this coating to reduce the inflammatory response. However, these results did not translate to effective reduction of inflammatory cell markers in the brain, leading to the need to develop a better option for *in vitro* analysis option.

Overall, this work contributes to the knowledge of the field because it describes, in detail, two different coatings that were used to try to improve the tissue response to implanted neural electrodes. Although the microgel coating was not successful, the PEG coating shows promise for future studies, especially with the increased neuronal survival observed when incorporating IL-1Ra. With further modification including other bioactive factors, we may be able to develop a coating that will lead to reduced inflammation as well as increased neuronal survival at the tissue – implant interface.

CHAPTER 6

FUTURE DIRECTIONS

First and foremost, it is important to understand that the tissue response to implanted materials in the brain is complicated and it is unlikely that the issue of maintaining long-term electrode functionality can be solved with a single approach. As with the rest of the body, the brain is a complex system with multiple cell types, incorporated vasculature, and immune and inflammatory response to foreign materials. The brain has the additional caveat of being an immuno-privileged site due to the mass transfer limitations of the blood brain barrier, leaving fewer options in terms of pharmacological intervention than would be available in the rest of the body. In order to maintain electrode functionality, it is important to mediate the recruitment of cells such as microglia and astrocytes to the implant site to reduce the inflammatory response and subsequent scar formation around the electrode. In addition to reducing inflammatory cell recruitment, it is also important to reduce neuronal cell death around the implant site. Finally, the blood-brain barrier breach is also an important factor than must be taken into consideration when analyzing the response to an implanted electrode.

Another important consideration of this research indicates the need for more thorough evaluation of the *in vitro* response to electrode coatings before moving forward with *in vivo* studies. While 2D and 3D culture systems have been used previously, they do not provide a complete picture of the response to electrode surfaces. It is difficult to recapitulate all aspects of brain response, including vasculature, BBB breach, subsequent

injury and inflammatory response, cytokine release, and cell recruitment. I believe the vasculature and associated BBB breach is an especially important aspect to address, although it is difficult to recapitulate in an *in vitro* model. It is difficult to know how a device will perform *in vivo* until you actually implant it in a living animal model, but more work towards developing a more complete *in vitro* system may provide an alternative for electrode evaluation.

In addition to developing new 3D cell culture based *in vitro* evaluation methods, there are also other potential alternatives that may serve to complement the knowledge gained from an *in vitro* cell system. Current methods already exist to evaluate gene expression in tissues, such as the analysis presented in this thesis. By analyzing gene expression in conjunction with the functionality of implanted electrodes in animals, it may be possible to determine specific genes that are up- or down-regulated in the animals with the best functional outcome. These genes can then be used as targets for future screening tools. With recent advances in gene expression analysis, it is possible to analyze large sample sets using small quantities of starting material to analyze gene expression from small samples as small as single-cell replicates. High throughput screening of future electrode modifications using an *in vitro* assay to measure gene expression may provide an additional level of understanding when analyzing cell response and looking at the response of specific gene targets that are found to be significant for improved electrode functionality. Combining the analysis of these gene targets with other *in vitro* evaluation methods may yield a better overall picture of the potential for the electrode to be successful in an animal model.

In addition to new screening methods, it is important to further investigate the on-demand release aspect for bioactive factors. In a system such as the one used for this research, the coating is degraded to release the anti-inflammatory agent in response to inflammation in the brain. This is an important characteristic because the bioactive factor is being release on an as-needed basis, and not just as a bolus response at initial implantation. By incorporating several bioactive factors with different stimuli as triggers for degradation, it may be possible to control the responsiveness of the coating based on the different cytokines that are released in different phases of the inflammatory cascade.

Finally, it is important to realize that the complex problems surrounding the use of cortical electrodes may be solved by looking into completely different methods of analyzing neuronal activity in the brain. Techniques using voltage sensitive dyes or gene therapy may provide a less-invasive method for analyzing the brain's response to a particular stimulus. Other non-invasive methods such as electroencephalogram (EEG) may one day be able to pinpoint activity in a specific region of the brain, allowing for a non-invasive measure of neuronal firing in the area of interest for cortical electrodes. While the current electrode technology does have the potential to be useful in future BMI developments, it is important to analyze all existing technologies to determine which one will provide the best overall outcome for patients, even if that means moving to a new technology altogether.

Overall, this problem will require a multi-component approach. This research shows the validity of non-fouling PEG coatings to improve neuronal survival compared to uncoated electrodes. Additionally, adding the anti-inflammatory agent IL-1Ra further increased the neuronal survival, indicating the importance for including bioactive factors

to mediate the inflammatory response. By developing new systems that can mediate the inflammatory response in a directed fashion, it is possible to improve the tissue response to implanted neural electrodes.

REFERENCES

1. Szarowski, D.H., et al., *Brain responses to micro-machined silicon devices.* Brain Res, 2003. **983**(1-2): p. 23-35.

2. Nicolelis, M.A. and S. Ribeiro, *Multielectrode recordings: the next steps.* Curr Opin Neurobiol, 2002. **12**(5): p. 602-6.

3. Schwartz, A.B., *Cortical neural prosthetics.* Annu Rev Neurosci, 2004. **27**: p. 487-507.

4. Schwartz, A.B., et al., *Brain-controlled interfaces: movement restoration with neural prosthetics.* Neuron, 2006. **52**(1): p. 205-20.

5. Birbaumer, N. and L.G. Cohen, *Brain-computer interfaces: communication and restoration of movement in paralysis.* J Physiol, 2007. **579**(Pt 3): p. 621-36.

6. Donoghue, J.P., *Connecting cortex to machines: recent advances in brain interfaces.* Nat Neurosci, 2002. **5 Suppl**: p. 1085-8.

7. Kennedy, P., et al., *Making the lifetime connection between brain and machine for restoring and enhancing function.* Prog Brain Res, 2011. **194**: p. 1-25.

8. Lebedev, M.A. and M.A. Nicolelis, *Brain-machine interfaces: past, present and future.* Trends Neurosci, 2006. **29**(9): p. 536-46.

9. Lebedev, M.A. and M.A. Nicolelis, *Toward a whole-body neuroprosthetic.* Prog Brain Res, 2011. **194**: p. 47-60.

10. Devivo, M.J., *Epidemiology of traumatic spinal cord injury: trends and future implications.* Spinal Cord, 2012. **50**(5): p. 365-72.

11. Ziegler-Graham, K., et al., *Estimating the prevalence of limb loss in the United States: 2005 to 2050.* Arch Phys Med Rehabil, 2008. **89**(3): p. 422-9.

12. Biran, R., D.C. Martin, and P.A. Tresco, *Neuronal cell loss accompanies the brain tissue response to chronically implanted silicon microelectrode arrays.* Exp Neurol, 2005. **195**(1): p. 115-26.

13. Anderson, J.M., A. Rodriguez, and D.T. Chang, *Foreign body reaction to biomaterials.* Semin Immunol, 2008. **20**(2): p. 86-100.

14. Avula, M.N., et al., *Modulation of the foreign body response to implanted sensor models through device-based delivery of the tyrosine kinase inhibitor, masitinib.* Biomaterials, 2013. **34**(38): p. 9737-46.

15. Polikov, V.S., P.A. Tresco, and W.M. Reichert, *Response of brain tissue to chronically implanted neural electrodes.* J Neurosci Methods, 2005. **148**(1): p. 1-18.

16. Fattahi, P., et al., *A Review of Organic and Inorganic Biomaterials for Neural Interfaces.* Adv Mater, 2014.

17. McConnell, G.C., et al., *Implanted neural electrodes cause chronic, local inflammation that is correlated with local neurodegeneration.* J Neural Eng, 2009. **6**(5): p. 056003.

18. Saxena, T., et al., *The impact of chronic blood-brain barrier breach on intracortical electrode function.* Biomaterials, 2013. **34**(20): p. 4703-13.

19. Allan, S.M. and N.J. Rothwell, *Inflammation in central nervous system injury.* Philos Trans R Soc Lond B Biol Sci, 2003. **358**(1438): p. 1669-77.

20. Graeber, M.B., W. Li, and M.L. Rodriguez, *Role of microglia in CNS inflammation.* FEBS Lett, 2011. **585**(23): p. 3798-805.

21. Winslow, B.D. and P.A. Tresco, *Quantitative analysis of the tissue response to chronically implanted microwire electrodes in rat cortex.* Biomaterials, 2010. **31**(7): p. 1558-67.

22. Anderson, J., *Biological Responses to Materials.* Annual Reviews Materials Research, 2001. **31**: p. 81-110.

23. Fawcett, J.W. and R.A. Asher, *The glial scar and central nervous system repair.* Brain Res Bull, 1999. **49**(6): p. 377-91.

24. Kim, Y.T., et al., *Chronic response of adult rat brain tissue to implants anchored to the skull.* Biomaterials, 2004. **25**(12): p. 2229-37.

25. Turner, J.N., et al., *Cerebral astrocyte response to micromachined silicon implants.* Exp Neurol, 1999. **156**(1): p. 33-49.

26. Tang, L. and J.W. Eaton, *Natural responses to unnatural materials: A molecular mechanism for foreign body reactions.* Mol Med, 1999. **5**(6): p. 351-8.

27. Jurgens, H.A. and R.W. Johnson, *Dysregulated neuronal-microglial cross-talk during aging, stress and inflammation.* Exp Neurol, 2012. **233**(1): p. 40-8.

28. Potter, K.A., et al., *The effect of resveratrol on neurodegeneration and blood brain barrier stability surrounding intracortical microelectrodes.* Biomaterials, 2013. **34**(29): p. 7001-15.

29. Hansson, E. and L. Ronnback, *Glial neuronal signaling in the central nervous system.* FASEB J, 2003. **17**(3): p. 341-8.

30. Potter, K.A., et al., *Stab injury and device implantation within the brain results in inversely multiphasic neuroinflammatory and neurodegenerative responses.* J Neural Eng, 2012. **9**(4): p. 046020.

31. Potter-Baker, K.A., et al., *A comparison of neuroinflammation to implanted microelectrodes in rat and mouse models.* Biomaterials, 2014.

32. Kipke, D.R., et al., *Silicon-substrate intracortical microelectrode arrays for long-term recording of neuronal spike activity in cerebral cortex.* IEEE Trans Neural Syst Rehabil Eng, 2003. **11**(2): p. 151-5.

33. Karumbaiah, L., et al., *Relationship between intracortical electrode design and chronic recording function.* Biomaterials, 2013. **34**(33): p. 8061-74.

34. Kozai, T.D., et al., *Ultrasmall implantable composite microelectrodes with bioactive surfaces for chronic neural interfaces.* Nat Mater, 2012. **11**(12): p. 1065-73.

35. Ludwig, K.A., et al., *Chronic neural recordings using silicon microelectrode arrays electrochemically deposited with a poly(3,4-ethylenedioxythiophene) (PEDOT) film.* J Neural Eng, 2006. **3**(1): p. 59-70.

36. Ollerenshaw, D.R., et al., *The adaptive trade-off between detection and discrimination in cortical representations and behavior.* Neuron, 2014. **81**(5): p. 1152-64.

37. Rousche, P.J. and R.A. Normann, *Chronic recording capability of the Utah Intracortical Electrode Array in cat sensory cortex.* J Neurosci Methods, 1998. **82**(1): p. 1-15.

38. Takeuchi, S., et al., *3D flexible multichannel neural probe array.* Journal of Micromechanics and Microengineering, 2004. **14**(1): p. 104-107.

39. Seymour, J.P. and D.R. Kipke, *Neural probe design for reduced tissue encapsulation in CNS.* Biomaterials, 2007. **28**(25): p. 3594-607.

40. Rennaker, R.L., et al., *A comparison of chronic multi-channel cortical implantation techniques: manual versus mechanical insertion.* J Neurosci Methods, 2005. **142**(2): p. 169-76.

41. Bjornsson, C.S., et al., *Effects of insertion conditions on tissue strain and vascular damage during neuroprosthetic device insertion.* J Neural Eng, 2006. **3**(3): p. 196-207.

42. Edell, D.J., et al., *Factors influencing the biocompatibility of insertable silicon microshafts in cerebral cortex.* IEEE Trans Biomed Eng, 1992. **39**(6): p. 635-43.

43. Ereifej, E.S., et al., *Nanopatterning effects on astrocyte reactivity.* J Biomed Mater Res A, 2013. **101**(6): p. 1743-57.

44. Thelin, J., et al., *Implant size and fixation mode strongly influence tissue reactions in the CNS.* PLoS One, 2011. **6**(1): p. e16267.

45. Cheung, K.C., *Implantable microscale neural interfaces.* Biomed Microdevices, 2007. **9**(6): p. 923-38.

46. Geddes, L.A. and R. Roeder, *Criteria for the selection of materials for implanted electrodes.* Ann Biomed Eng, 2003. **31**(7): p. 879-90.

47. Moshayedi, P., et al., *The relationship between glial cell mechanosensitivity and foreign body reactions in the central nervous system.* Biomaterials, 2014. **35**(13): p. 3919-25.

48. Lacour, S.P., et al., *Flexible and stretchable micro-electrodes for in vitro and in vivo neural interfaces.* Med Biol Eng Comput, 2010. **48**(10): p. 945-54.

49. Capadona, J.R., Tyler, Dustin J., Zorman, Christian A., Rowan, Stuart J., Weder, Christopher, *Mechanicaly Adaptive Nanocomposites for Neural Interfacing.* Materials Research Society, 2012. **37**: p. 581 - 589.

50. Harris, J.P., et al., *In vivo deployment of mechanically adaptive nanocomposites for intracortical microelectrodes.* J Neural Eng, 2011. **8**(4): p. 046010.

51. Cui, X., et al., *Surface modification of neural recording electrodes with conducting polymer/biomolecule blends.* J Biomed Mater Res, 2001. **56**(2): p. 261-72.

52. Cui, X. and D.C. Martin, *Electrochemical deposition and characterization of poly(3,4-ethylenedioxythiophene) on neural microelectrode arrays.* Sensors and Actuators B: Chemical, 2003. **89**(1-2): p. 92-102.

53. Cui, X., et al., *In vivo studies of polypyrrole/peptide coated neural probes.* Biomaterials, 2003. **24**(5): p. 777-87.

54. Green, R.A., et al., *Conducting polymers for neural interfaces: challenges in developing an effective long-term implant.* Biomaterials, 2008. **29**(24-25): p. 3393-9.

55. Azemi, E., G.T. Gobbel, and X.T. Cui, *Seeding neural progenitor cells on silicon-based neural probes.* J Neurosurg, 2010. **113**(3): p. 673-81.

56. Di, L., et al., *Protein adsorption and peroxidation of rat retinas under stimulation of a neural probe coated with polyaniline.* Acta Biomater, 2011. **7**(10): p. 3738-45.

57. Leung, B.K., et al., *Characterization of microglial attachment and cytokine release on biomaterials of differing surface chemistry.* Biomaterials, 2008. **29**(23): p. 3289-97.

58. Lu, Y., et al., *Poly(vinyl alcohol)/poly(acrylic acid) hydrogel coatings for improving electrode-neural tissue interface.* Biomaterials, 2009. **30**(25): p. 4143-51.

59. Rao, L., et al., *Polyethylene glycol-containing polyurethane hydrogel coatings for improving the biocompatibility of neural electrodes.* Acta Biomater, 2012. **8**(6): p. 2233-42.

60. Winslow, B.D., et al., *A comparison of the tissue response to chronically implanted Parylene-C-coated and uncoated planar silicon microelectrode arrays in rat cortex.* Biomaterials, 2010. **31**(35): p. 9163-72.

61. Dang, T.T., et al., *Spatiotemporal effects of a controlled-release anti-inflammatory drug on the cellular dynamics of host response.* Biomaterials, 2011. **32**(19): p. 4464-70.

62. Bezuidenhout, D., et al., *Covalent incorporation and controlled release of active dexamethasone from injectable polyethylene glycol hydrogels.* J Biomed Mater Res A, 2013. **101**(5): p. 1311-8.

63. Zhong, Y., McConnell, G.C., Ross, J.D. , DeWeerth, S.P., and Bellamkonda, R.V., *A Novel Dexamethasone-releasing, Antiinflammatory Coating for Neural Implants.* Proceedings of the 2 International IEEE EMBS, 2005(2nd International IEEE EMBS Conference on Neural Engineering): p. 522.

64. Zhong, Y. and R.V. Bellamkonda, *Dexamethasone-coated neural probes elicit attenuated inflammatory response and neuronal loss compared to uncoated neural probes.* Brain Res, 2007. **1148**: p. 15-27.

65. Kim, D.H. and D.C. Martin, *Sustained release of dexamethasone from hydrophilic matrices using PLGA nanoparticles for neural drug delivery.* Biomaterials, 2006. **27**(15): p. 3031-7.

66. Shain, W., et al., *Controlling cellular reactive responses around neural prosthetic devices using peripheral and local intervention strategies.* Ieee Transactions on Neural Systems and Rehabilitation Engineering, 2003. **11**(2): p. 186-188.

67. Mercanzini, A., et al., *Controlled release nanoparticle-embedded coatings reduce the tissue reaction to neuroprostheses.* J Control Release, 2010. **145**(3): p. 196-202.

68. Zhong, Y. and R.V. Bellamkonda, *Controlled release of anti-inflammatory agent alpha-MSH from neural implants.* J Control Release, 2005. **106**(3): p. 309-18.

69. Klaver, C.L. and M.R. Caplan, *Bioactive surface for neural electrodes: decreasing astrocyte proliferation via transforming growth factor-beta1.* J Biomed Mater Res A, 2007. **81**(4): p. 1011-6.

70. Abidian, M.R., Martin, David C., *Multifunctional Nanobiomaterials for Neural Interfaces.* Advanced Functional Materials, 2009. **19**: p. 573-585.

71. Wadhwa, R., C.F. Lagenaur, and X.T. Cui, *Electrochemically controlled release of dexamethasone from conducting polymer polypyrrole coated electrode.* J Control Release, 2006. **110**(3): p. 531-41.

72. Potter, K.A., et al., *Curcumin-releasing mechanically adaptive intracortical implants improve the proximal neuronal density and blood-brain barrier stability.* Acta Biomater, 2014. **10**(5): p. 2209-22.

73. Arend, W.P., et al., *Interleukin-1 receptor antagonist: role in biology.* Annu Rev Immunol, 1998. **16**: p. 27-55.

74. Hanisch, U.K., *Microglia as a source and target of cytokines.* Glia, 2002. **40**(2): p. 140-55.

75. Jander, S., et al., *Cortical spreading depression induces proinflammatory cytokine gene expression in the rat brain.* J Cereb Blood Flow Metab, 2001. **21**(3): p. 218-25.

76. Karumbaiah, L., et al., *The upregulation of specific interleukin (IL) receptor antagonists and paradoxical enhancement of neuronal apoptosis due to electrode induced strain and brain micromotion.* Biomaterials, 2012. **33**(26): p. 5983-96.

77. Farooqui, A.A., L.A. Horrocks, and T. Farooqui, *Modulation of inflammation in brain: a matter of fat.* J Neurochem, 2007. **101**(3): p. 577-99.

78. Smith, J.A., et al., *Role of pro-inflammatory cytokines released from microglia in neurodegenerative diseases.* Brain Res Bull, 2012. **87**(1): p. 10-20.

79. Steinman, L., *Inflammatory cytokines at the summits of pathological signal cascades in brain diseases.* Sci Signal, 2013. **6**(258): p. pe3.

80. Arend, W.P., *The balance between IL-1 and IL-1Ra in disease.* Cytokine Growth Factor Rev, 2002. **13**(4-5): p. 323-40.

81. Pinteaux, E., N.J. Rothwell, and H. Boutin, *Neuroprotective actions of endogenous interleukin-1 receptor antagonist (IL-1ra) are mediated by glia.* Glia, 2006. **53**(5): p. 551-6.

82. Taub, A.H., et al., *Bioactive anti-inflammatory coating for chronic neural electrodes.* J Biomed Mater Res A, 2012. **100**(7): p. 1854-8.

83. Malemud, C.J., *Matrix metalloproteinases (MMPs) in health and disease: an overview.* Front Biosci, 2006. **11**: p. 1696-701.

84. Manicone, A.M. and J.K. McGuire, *Matrix metalloproteinases as modulators of inflammation.* Semin Cell Dev Biol, 2008. **19**(1): p. 34-41.

85. Rosenberg, G.A., *Matrix metalloproteinases and their multiple roles in neurodegenerative diseases.* Lancet Neurol, 2009. **8**(2): p. 205-16.

86. Ferguson, T.A. and D. Muir, *MMP-2 and MMP-9 increase the neurite-promoting potential of schwann cell basal laminae and are upregulated in degenerated nerve.* Mol Cell Neurosci, 2000. **16**(2): p. 157-67.

87. Goussev, S., et al., *Differential temporal expression of matrix metalloproteinases after spinal cord injury: relationship to revascularization and wound healing.* J Neurosurg, 2003. **99**(2 Suppl): p. 188-97.

88. Gursoy-Ozdemir, Y., et al., *Cortical spreading depression activates and upregulates MMP-9.* J Clin Invest, 2004. **113**(10): p. 1447-55.

89. Rosenberg, G.A., *Matrix metalloproteinases in brain injury.* J Neurotrauma, 1995. **12**(5): p. 833-42.

90. Lo, E.H., X. Wang, and M.L. Cuzner, *Extracellular proteolysis in brain injury and inflammation: role for plasminogen activators and matrix metalloproteinases.* J Neurosci Res, 2002. **69**(1): p. 1-9.

91. Tian, W. and T.R. Kyriakides, *Matrix metalloproteinase-9 deficiency leads to prolonged foreign body response in the brain associated with increased IL-1beta levels and leakage of the blood-brain barrier.* Matrix Biol, 2009. **28**(3): p. 148-59.

92. Anderson, S.B., et al., *The performance of human mesenchymal stem cells encapsulated in cell-degradable polymer-peptide hydrogels.* Biomaterials, 2011. **32**(14): p. 3564-74.

93. Patterson, J. and J.A. Hubbell, *Enhanced proteolytic degradation of molecularly engineered PEG hydrogels in response to MMP-1 and MMP-2.* Biomaterials, 2010. **31**(30): p. 7836-45.

94. Bott, K., et al., *The effect of matrix characteristics on fibroblast proliferation in 3D gels.* Biomaterials, 2010. **31**(32): p. 8454-64.

95. Bracher, M., et al., *Cell specific ingrowth hydrogels.* Biomaterials, 2013. **34**(28): p. 6797-803.

96. Tauro, J.R. and R.A. Gemeinhart, *Matrix metalloprotease triggered delivery of cancer chemotherapeutics from hydrogel matrixes.* Bioconjug Chem, 2005. **16**(5): p. 1133-9.

97. Phelps, E.A., et al., *Maleimide cross-linked bioactive PEG hydrogel exhibits improved reaction kinetics and cross-linking for cell encapsulation and in situ delivery.* Adv Mater, 2012. **24**(1): p. 64-70, 2.

98. Phelps, E.A., et al., *Vasculogenic bio-synthetic hydrogel for enhancement of pancreatic islet engraftment and function in type 1 diabetes.* Biomaterials, 2013. **34**(19): p. 4602-11.

99. Zisch, A.H., et al., *Cell-demanded release of VEGF from synthetic, biointeractive cell ingrowth matrices for vascularized tissue growth.* FASEB J, 2003. **17**(15): p. 2260-2.

100. Jun, S.B., et al., *Modulation of cultured neural networks using neurotrophin release from hydrogel-coated microelectrode arrays.* J Neural Eng, 2008. **5**(2): p. 203-13.

101. Singh, N., et al., *Covalent tethering of functional microgel films onto poly(ethylene terephthalate) surfaces.* Biomacromolecules, 2007. **8**(10): p. 3271-5.

102. Bridges, A.W., et al., *Reduced acute inflammatory responses to microgel conformal coatings.* Biomaterials, 2008. **29**(35): p. 4605-15.

103. Bridges, A.W., et al., *Chronic inflammatory responses to microgel-based implant coatings.* J Biomed Mater Res A, 2010. **94A**(1): p. 252-258.

104. Hermanson, G.T., *Bioconjugate techniques*. 1996, San Diego, CA: Academic Press.

105. McConnell, G.C., R.J. Butera, and R.V. Bellamkonda, *Bioimpedance modeling to monitor astrocytic response to chronically implanted electrodes.* J Neural Eng, 2009. **6**(5): p. 055005.

106. South, A.B., et al., *Centrifugal deposition of microgels for the rapid assembly of nonfouling thin films.* ACS Appl Mater Interfaces, 2009. **1**(12): p. 2747-54.

107. Nolan, C.M., et al., *Phase transition behavior, protein adsorption, and cell adhesion resistance of poly(ethylene glycol) cross-linked microgel particles.* Biomacromolecules, 2005. **6**(4): p. 2032-9.

108. Gan, D.J. and L.A. Lyon, *Synthesis and protein adsorption resistance of PEG-modified poly(N-isopropylacrylamide) core/shell microgels.* Macromolecules, 2002. **35**(26): p. 9634-9639.

109. Widge, A.S., et al., *Self-assembled monolayers of polythiophene conductive polymers improve biocompatibility and electrical impedance of neural electrodes.* Biosens Bioelectron, 2007. **22**(8): p. 1723-32.

110. Richardson-Burns, S.M., J.L. Hendricks, and D.C. Martin, *Electrochemical polymerization of conducting polymers in living neural tissue.* J Neural Eng, 2007. **4**(2): p. L6-L13.

111. Skousen, J.L., et al., *Reducing surface area while maintaining implant penetrating profile lowers the brain foreign body response to chronically implanted planar silicon microelectrode arrays.* Prog Brain Res, 2011. **194**: p. 167-80.

112. Nicolelis, M.A., et al., *Chronic, multisite, multielectrode recordings in macaque monkeys.* Proc Natl Acad Sci U S A, 2003. **100**(19): p. 11041-6.

113. Subbaroyan, J., D.C. Martin, and D.R. Kipke, *A finite-element model of the mechanical effects of implantable microelectrodes in the cerebral cortex.* J Neural Eng, 2005. **2**(4): p. 103-13.

114. Capadona, J.R., et al., *Mechanically adaptive nanocomposites for neural interfacing.* Mrs Bulletin, 2012. **37**(6): p. 581-589.

115. Hoffman, A.S., *Non-fouling surface technologies.* J Biomater Sci Polym Ed, 1999. **10**(10): p. 1011-1014.

116. Harbers, G.M., et al., *A functionalized poly(ethylene glycol)-based bioassay surface chemistry that facilitates bio-immobilization and inhibits non-specific protein, bacterial, and mammalian cell adhesion.* Chem Mater, 2007. **19**(18): p. 4405-4414.

117. Zhang, F., et al., *Surface modification of stainless steel by grafting of poly(ethylene glycol) for reduction in protein adsorption.* Biomaterials, 2001. **22**(12): p. 1541-8.

118. Zhang, M., T. Desai, and M. Ferrari, *Proteins and cells on PEG immobilized silicon surfaces.* Biomaterials, 1998. **19**(10): p. 953-60.

119. Sharma, S., R.W. Johnson, and T.A. Desai, *Evaluation of the stability of nonfouling ultrathin poly(ethylene glycol) films for silicon-based microdevices.* Langmuir, 2004. **20**(2): p. 348-56.

120. Nuttelman, C.R., M.C. Tripodi, and K.S. Anseth, *Dexamethasone-functionalized gels induce osteogenic differentiation of encapsulated hMSCs.* J Biomed Mater Res A, 2006. **76**(1): p. 183-95.

121. Bal, T., B. Kepsutlu, and S. Kizilel, *Characterization of protein release from poly(ethylene glycol) hydrogels with crosslink density gradients.* J Biomed Mater Res A, 2014. **102**(2): p. 487-95.

122. Patterson, J. and J.A. Hubbell, *SPARC-derived protease substrates to enhance the plasmin sensitivity of molecularly engineered PEG hydrogels.* Biomaterials, 2011. **32**(5): p. 1301-1310.

123. Erickson, H.P., *Size and shape of protein molecules at the nanometer level determined by sedimentation, gel filtration, and electron microscopy.* Biol Proced Online, 2009. **11**: p. 32-51.

124. Gutowski, S.M., et al., *Host response to microgel coatings on neural electrodes implanted in the brain.* J Biomed Mater Res A, 2014. **102**(5): p. 1486-99.

125. Buzsaki, G., *Large-scale recording of neuronal ensembles.* Nat Neurosci, 2004. **7**(5): p. 446-51.

126. Rosenberg, G.A., et al., *Immunohistochemistry of matrix metalloproteinases in reperfusion injury to rat brain: activation of MMP-9 linked to stromelysin-1 and microglia in cell cultures.* Brain Res, 2001. **893**(1-2): p. 104-12.

127. Ip, N.Y., et al., *Ciliary neurotrophic factor enhances neuronal survival in embryonic rat hippocampal cultures.* J Neurosci, 1991. **11**(10): p. 3124-34.

128. Herx, L.M., S. Rivest, and V.W. Yong, *Central nervous system-initiated inflammation and neurotrophism in trauma: IL-1 beta is required for the production of ciliary neurotrophic factor.* J Immunol, 2000. **165**(4): p. 2232-9.

129. Polikov, V.S., et al., *In vitro model of glial scarring around neuroelectrodes chronically implanted in the CNS.* Biomaterials, 2006. **27**(31): p. 5368-76.

130. Cullen, D.K., C.M. Simon, and M.C. LaPlaca, *Strain rate-dependent induction of reactive astrogliosis and cell death in three-dimensional neuronal-astrocytic co-cultures.* Brain Res, 2007. **1158**: p. 103-15.

131. Cullen, D.K., et al., *In vitro neural injury model for optimization of tissue-engineered constructs.* J Neurosci Res, 2007. **85**(16): p. 3642-51.

132. Cullen, D.K., et al., *High cell density three-dimensional neural co-cultures require continuous medium perfusion for survival.* Conf Proc IEEE Eng Med Biol Soc, 2006. **1**: p. 636-9.

133. Irons, H.R., et al., *Three-dimensional neural constructs: a novel platform for neurophysiological investigation.* J Neural Eng, 2008. **5**(3): p. 333-41.